

**STUDIES IN  
MOLECULAR RECOGNITION**

Thesis by

**MICHAEL A. PETTI**

In Partial Fulfillment of the Requirements  
for the Degree of  
Doctor of Philosophy

California Institute of Technology  
Pasadena, California

**1988**

(Submitted November 18, 1987)

To my wife, Toby

## ACKNOWLEDGEMENTS

It is a pleasure to acknowledge those who made my stay at Caltech enjoyable. First and foremost, I thank my advisor Dennis Dougherty for his support; his enthusiasm and motivation during the low points made them easier to deal with. I also want to thank him for teaching me about areas of chemistry I had no idea existed. He has taught me to be a scientist first, a molecule-maker second--a lesson for which I am very grateful.

Special thanks go to my wife, Toby, for her support and love; she put up with me during a stressful time yet always was there when I needed her.

I would like to thank the members of the Dougherty group. Whether in the laboratory or on the softball field, their support and enthusiasm are gratefully acknowledged. Certain events will be fondly remembered; others can only be described as the stuff that future embarrassing anecdotes are made of. The camaraderie of this group made working here all the easier. I can only hope that my future working environment is as much fun. I also thank others in the department, especially members of the Grubbs and Dervan groups for their support and friendship.

Finally, I thank Debbie Chester and Kathy Flanagan for their typing of this thesis. They both put up with me and numerous revisions far too often. I also thank Dave Stauffer for his invaluable proofreading of this thesis.

## ABSTRACT

A new class of water-soluble organic molecules containing hydrophobic binding sites is described. These host molecules, macrocycles assembled from 2,6-dihydroxy-9,10-dihydro-9,10-(1,2-dicarbomethoxy)-ethenoanthracene **8**, can possess a hydrophobic cavity having a grossly right- (or left-)handed sense of twist. We believe this dissymmetric helical cavity could provide a means for chiral discrimination between the enantiomers of a racemate in aqueous solution.

By varying the shape and size of the hydrophobic receptor site, such questions as the the roles of  $\pi$ -stacking, hydrophobicity and rigidity in molecular recognition are examined. The physical properties of these structures and their binding affinities for various guest molecules in aqueous solution are presented.

These molecules have an especially high affinity for the aliphatic guest adamantyltrimethylammonium iodide (ATMA). In addition, this guest is an elegant probe of host geometry in the binding event. Several lines of evidence indicate that ATMA associates with these hosts in different geometries. Variable-temperature binding studies indicate that the binding of ATMA to hosts **4CMESO** and **5CMESO** displays a "non-classical hydrophobic effect."

Further studies with other alkyltrimethylammonium salts explore the role of guest shape, size, rigidity and charge on  $K_a$ . Studies involving variations of host structure suggest that rigidity, hydrophobicity, charge

and donor-acceptor effects can significantly affect  $K_a$ .

Two hosts of very similar structure, a *p*-xylyl-linked macrocycle (**P-D**) and a *trans*-1,4-dimethylenecyclohexyl-linked macrocycle (**C6-L**) are compared. Evidence for a new host geometry, efficient at encapsulating flat aromatic molecules, similar in shape to a naphthalene, is presented. These hosts efficiently bind aromatic heterocyclic guests (e.g., indole, quinoline, isoquinoline) and the *N*-methyl analogues. In this study, **P-D** displays an added affinity for the cationic guests. This additional ion-dipole effect is worth at least 1 kcal/mol in binding free energy. The binding of aromatic heterocycles is shown to be driven by donor-acceptor  $\pi$ -stacking interactions and hydrophobic effects.

Thus, high binding affinities are achieved by a combination of forces without resorting to the use of highly lipophilic guests. These hosts maintain a clear separation of hydrophilic and hydrophobic groups, thereby eliminating the generally quite strong electrostatic interactions seen in other synthetic host systems.

Synthetic strategies to novel building blocks for new host structures are presented. These strategies could allow for the preparation of hosts having different solubility profiles, different aggregation properties and enhanced binding characteristics.

Table of Contents		page
<b>Acknowledgements</b>		iii
<b>Abstract</b>		iv
<b>List of Tables</b>		ix
<b>List of Figures</b>		xi
<b>List of Schemes</b>		xiii
<b>Chapter 1:</b>	<b>Introduction and Background</b>	<b>1</b>
	References for Chapter 1	18
<b>Chapter 2:</b>	<b>Design and Synthesis of a New Host System</b>	<b>21</b>
	Design	22
	Synthesis	25
	CMC Studies	33
	Experimental Section	38
	References for Chapter 2	48
<b>Chapter 3:</b>	<b>Physical Studies: The Case of Adamantyl-trimethylammonium Iodide</b>	<b>50</b>
	NMR Studies	51
	The Case of ATMA	55
	Variable Temperature Studies	59
	References for Chapter 3	69

<b>Chapter 4:</b>	<b>Physical Studies: Substituted Ammonium Ions and Aromatic Heterocyclic Guests</b>	72
	Introduction	73
	Synthesis	73
	CMC Studies	80
	Background	81
	Effect of Charge	83
	Cavity size: <b>5CMESO</b> vs. <b>PMESO</b>	89
	<b>5CDL</b>	95
	<b>C6-L</b>	98
	Donor-Acceptor $\pi$ -Stacking and Ion-Dipole Effects	101
	Conclusions	113
	Experimental Section	116
	References for Chapter 4	122
<b>Appendix A:</b>	<b>Calculated D Values for Host/Guest Complexes</b>	124
	<b>5CMESO</b>	125
	<b>PMESO</b>	128
	<b>5CDL</b>	132
	<b>C6-L</b>	139
<b>Chapter 5:</b>	<b>Design and Synthesis of Novel Building Blocks to New Host Structures</b>	145
	Solubilization at Neutral pH	146
	Macrobicyclic Host Systems	151

Linker Attachment Studies	153
Bridgehead Functionalization	160
Experimental Section	165
References for Chapter 5	176

	List of Tables	page
Table 1.1	Association constants for Diederich's host and various guests	15
Table 2.1	Yields of macrocycles from high-dilution ring-closure reactions	28
Table 2.2	Dimensions of the hydrophobic binding sites of the ethenoanthracene-based hosts	34
Table 3.1	$K_a$ and D values for Binding of ATMA to several hosts	58
Table 3.2	Temperature dependance of the association constant for ATMA with <b>4C</b> and <b>5CMESO</b> hosts	60
Table 3.3	Thermodynamic parameters ( $\Delta H$ and $\Delta S$ ) for the binding of aromatic guests to cyclodextrins	64
Table 3.4	Thermodynamic parameters ( $\Delta H$ and $\Delta S$ ) for the complex formation between cyclodextrins and adamantyl derivatives	66
Table 4.1	Grand table of association constants	74
Table 4.2	Effect of charge on $K_a$	86
Table 4.3	The "nitro effect"	90
Table 4.4	Cavity size data	93

Table 4.5	Association constants for <b>5CDL</b> and various guests	96
Table 4.6	Cyclohexyl versus benzyl comparison	97
Table 4.7	Association constants for <b>C6-L</b> and various guests	100
Table 4.8	Association constants for aromatic heterocyclic guests and Hosts <b>C6-L</b> and <b>P-D</b>	104
Table 4.9	Association Constants for <b>5CDL</b> and <b>C6-L</b> and aromatic heterocyclic guests	111

List of Figures		page
Figure 1.1	Tabushi's macrocyclic receptor molecule	4
Figure 1.2	Koga's macrocyclic receptor molecule	6
Figure 1.3	Variations of the linkers in the Koga system	8
Figure 1.4	Chiral Host designed by Koga	10
Figure 1.5	Diederich's first generation macrocyclic receptor molecule	11
Figure 1.6	Diederich's redesigned macrocyclic receptor molecule	13
Figure 2.1	General host design	23
Figure 2.2	<i>Meso</i> and <i>D,L</i> macrocycles	29
Figure 2.3	<b>3C</b> macrocycle decoupling experiment	31
Figure 2.4	CMC determination of <b>4CMESO</b> and <b>5CDL</b> by the NMR method	37
Figure 3.1	Three distinct domains that can occur when studying host-guest interactions by <sup>1</sup> H NMR spectroscopy	52
Figure 3.2	Adamantyltrimethylammonium iodide (ATMA), stick and CPK drawing	56
Figure 3.3	Variable temperature ATMA data	61

Figure 4.1	<i>P</i> -xylyl-linked hosts and half molecule control	76
Figure 4.2	D values (in ppm) for <i>p</i> - <i>tert</i> -butylphenyl-trimethylammonium and the hosts <b>5CDL</b> and <b>PMESO</b>	88
Figure 4.3	D values (in ppm) for benzyltrimethylammonium and <i>p</i> -nitrobenzyltrimethylammonium with various hosts	91
Figure 4.4	Rhomboid conformation of <b>C6-L</b> (carboxylates omitted for clarity)	106
Figure 4.5	D values (in ppm) of the methyl groups for complexes of <b>C6-L</b> and various isostructural methyl-substituted quinolines and isoquinolines	108
Figure 5.1	Novel building blocks	147
Figure 5.2	Two possible Topographies for Macrobicyclic Host Geometries	152
Figure 5.3	<sup>1</sup> H NMR spectra of amide diastereomers: A=higher R <sub>f</sub> diastereomer, B=lower R <sub>f</sub> diastereomer	157
Figure 5.4	CMC Determination of macrocyclic amide	159

	List of Schemes	page
Scheme 2.1	Synthetic Scheme to Ethenoanthracene based Hosts	26
Scheme 2.2	Introduction of water-solubilizing groups	32
Scheme 4.1	Synthetic scheme for cyclohexyl-linked host	77
Scheme 4.2	Hydrolysis of cyclohexyl-linked host	79
Scheme 5.1	Proposed Synthetic Route to Alkyltrimethyl-ammonium Ion-Based Macrocyclic Host System	148
Scheme 5.2	Synthetic Routes to Exocyclic Amines	150
Scheme 5.3	Synthesis of Chloroamide Building Block	154
Scheme 5.4	Macrocyclization of Chloroamide and Diphenol to form the two Amide Macrocycles	155
Scheme 5.5	Synthetic Route to the Triol Building Block	161
Scheme 5.6	Synthetic Route to the Asymmetric Anthrone	163
Scheme 5.7	Overall Synthetic Scheme for Macrobicycle Synthesis, starting from the Asymmetric Anthrone	164

**CHAPTER 1**  
**Introduction and Background**

The field of host-guest chemistry has been growing rapidly over the last decade.<sup>1</sup> The field is one involved with the more general phenomenon of molecular recognition. Molecular recognition, broadly defined, is the event in which two molecules come together and associate with one another to form a complex. A thermodynamic equilibrium constant defines this complex formation.

Molecular recognition is a fundamentally important biological process.<sup>2</sup> Whether it be the transport of a metal ion across a membrane by an ionophore, the recognition of a substrate by an enzyme, or the binding of protein to DNA, molecular recognition forms the basis of these key biological events. The understanding of the forces behind these events would be of great importance to the understanding of the specificity of these biological processes.

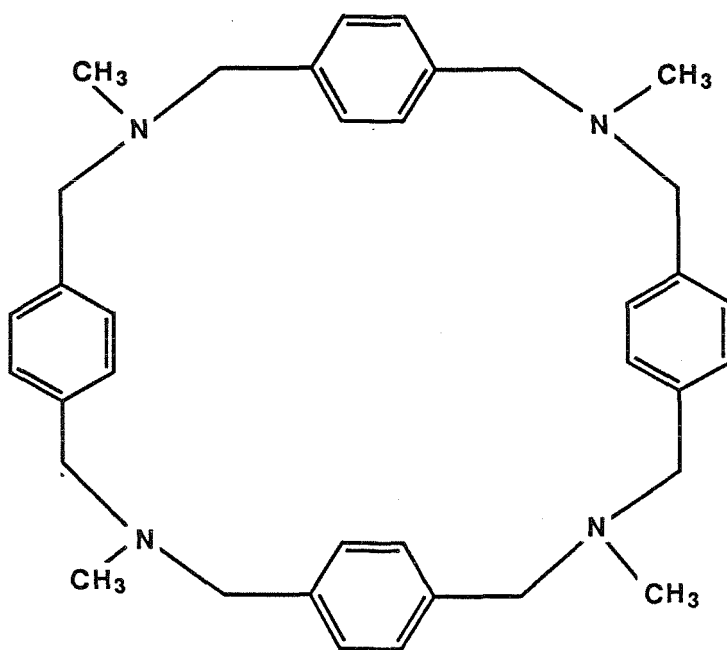
Cram<sup>3</sup> has pioneered the design of organic systems that mimic the ionophore function. He has shown that organic chemists can design systems that efficiently bind and transport metal ions into a lipophilic solvent. His molecules, the crown ethers, are essentially a ring of heteroatoms (typically oxygens) that point their lone-pair electrons towards the center of the cavity. These lone-pairs can then chelate an appropriately sized, positively charged ion. This field, through much research over the last ~ 20 years, is quite mature; it is now known how to achieve selectivity and specificity in the recognition of positively charged ions. Organic molecules can recognize and transport metal ions from an aqueous phase to an organic phase.<sup>3</sup>

Synthetic organic chemists have taken advantage of the properties of crown ethers to dissolve ionic species in organic solvents; typically insoluble ionic reagents can now be used in organic solvents.<sup>4</sup> These reagents, usually highly solvated and therefore not very reactive in aqueous solution, are quite

reactive in organic solvents and open up new reactivity for chemists to control. Examples include the strong oxidizing agent purple benzene<sup>5a</sup> (a solution of potassium permanganate in benzene) and 18-crown-6 mediated S<sub>N</sub>2 reactions.<sup>5b</sup>

The ability to recognize and bind an organic molecule in aqueous solution has become an area of current interest.<sup>6</sup> The best-known molecules that can bind organic molecules in aqueous solution are the cyclodextrins.<sup>7</sup> The cyclodextrins, cyclic oligomers of starch, are available in three sizes:  $\alpha$ ,  $\beta$ , and  $\gamma$  with  $\alpha$  having 6,  $\beta$  having 7 and  $\gamma$  having 8 glucose residues in the cyclic array. Cyclodextrins are water-soluble and do bind many molecules in their cavities, organic molecules among them. Considerable effort has been expended in the study of the properties of cyclodextrins as synthetic receptors. Cyclodextrins are fairly good at binding organic molecules, considering that the cavity of cyclodextrins is fairly polar. The oxygen atoms of the sugars point towards the center of the cavity, thereby reducing its hydrophobicity. Furthermore, the size of the cavity is restricted by what nature provides. If the molecule of interest does not fit within the cavity of the cyclodextrin, then it will not bind efficiently. To circumvent this size limitation, modified cyclodextrins with appended floors or walls have been prepared.<sup>8</sup> These modified cyclodextrins, while being a tremendous synthetic challenge, have been able to bind organic molecules better than their simple cyclodextrin precursors. Despite these limitations and the synthetic difficulties, cyclodextrins are still a very active area of current research.

To overcome some of the limitations of cyclodextrins, totally synthetic receptor molecules have been developed. Tabushi *et al.*<sup>9a</sup> designed a water-soluble cyclophane with a fairly hydrophobic cavity to study hydrophobic binding. His system, shown in Figure 1.1, is based on a xylylenediamine.



1

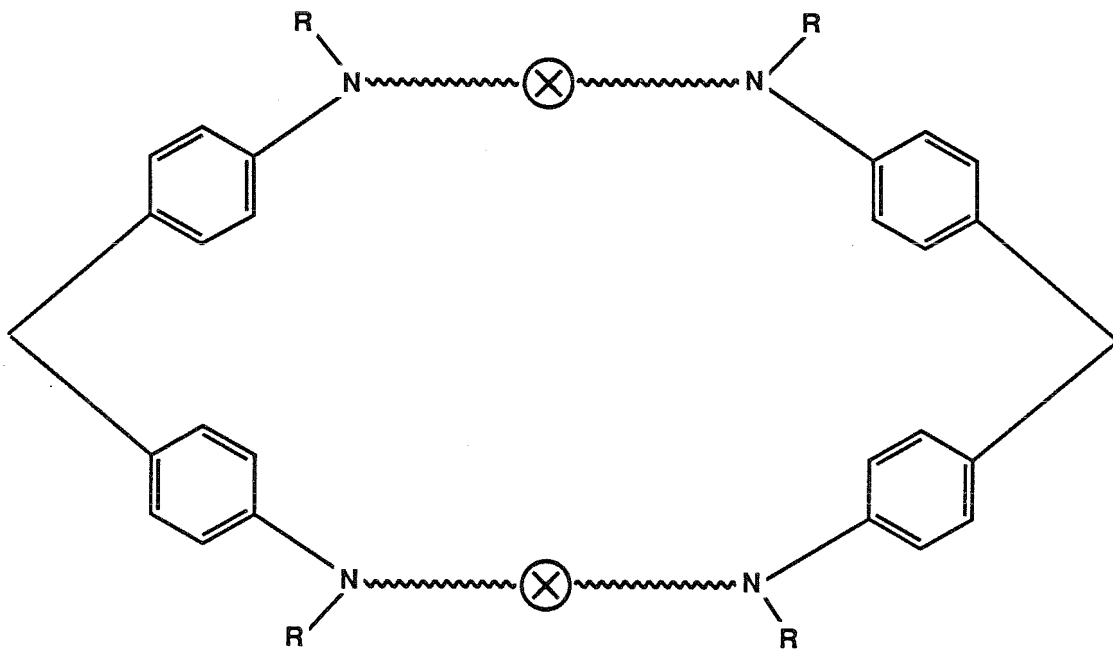
**FIGURE 1.1:** Tabushi's macrocyclic receptor molecule

The cavity is square with dimensions of  $5.5\text{\AA} \times 5.5\text{\AA}$ . The aromatic rings are in a face-to-face conformation as shown by NMR studies. Tabushi expected this host structure **1** to be capable of binding the phenyl or naphthyl ring of various structures. At  $\text{pH} = 4.2$ , **1** binds 1-anilino-8-naphthalenesulfonate (ANS) with an association constant  $K_a$  of  $380\text{ M}^{-1}$ . The same host, with water solubilization provided by quaternization of the amines by Meerwein's reagent, is also an enzyme mimic.<sup>9b,c</sup>

Shortly after Tabushi's finding, Koga *et al.*<sup>10a-d</sup> designed a new water-soluble host, **2** (Figure 1.2). This host, a cyclophane based on a diaminodiphenylmethane, is water-soluble below  $\text{pH} = 2$  (Figure 1.2). This molecule also binds ANS ( $K_a = 6300\text{ M}^{-1}$ ). Furthermore, this host selectively binds dihydroxynaphthalenes and various arenes. A crystal structure of the 1:1 complex of the host and durene (1,2,4,5-tetramethylbenzene) showed that the durene molecule was fully included within the host's cavity and was located at the center of symmetry of the molecule.<sup>10a</sup>

The conformation of **2** was also deduced from this x-ray structure. The four aromatic rings were in the face-to-face conformation similar to the result seen by Tabushi. The tetramethylene chain adopted the all *trans-anti* arrangement with the cavity having a boxlike shape. The corners of the box were provided by the diphenylmethane carbons and a *gauche* conformation around the aryl-N-CH<sub>2</sub> bonds. The cavity thus formed was roughly rectangular in shape and of the approximate dimensions  $3.5\text{\AA} \times 7.9\text{\AA}$ .

Koga realized that this receptor site could possibly distinguish among substituted naphthalenes because a naphthalene guest could adopt 4 inclusion geometries within the cavity of **2**.<sup>10b</sup> The axial geometry would have the long axis of the naphthalene ring perpendicular to the long axis of the rectangularly shaped receptor site. The equatorial geometry would have



2

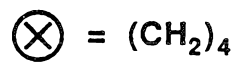


FIGURE 1.2: Koga's macrocyclic receptor molecule

the long axis of the naphthalene guest coincident with the long axis of the binding site. The pseudo-axial(pseudo-equatorial) geometry simply results from a rotation of the guest in the axial(equatorial) geometry, resulting in a complex where substituents in the 2,6-positions of the naphthalene would now point perpendicularly (parallel) to the long axis of the binding site. For 2,7-dihydroxynaphthalene, NMR studies<sup>10b</sup> indicated that the pseudo-axial geometry was the preferred geometry for the complex of this guest with **2**.

Koga has also varied the size, shape and hydrophobicity of the cavity to determine the effects of these parameters on the ability of these hosts to bind organic molecules (Figure 1.3).<sup>10c,d</sup> These hosts display remarkable differences in their ability to bind ANS. While most of the polymethylene-linked macrocycles showed little variation in their binding ability of ANS, an unsymmetrical host having a pentamethylene chain and a hexamethylene chain (CP56) was more effective at binding ANS by a factor of  $\approx 7$ . Koga suggests that the reason for the increased stability is the result of the better fit of ANS to the cavity of CP56.

While a host having a *para*-xylyl based linker surprisingly did not bind ANS, a host having a *trans*-1,4-dimethylenecyclohexyl based linker bound ANS more strongly by a factor of  $\approx 80$  relative to **2**. Based upon this evidence, Koga concluded that the hydrophobicity of the binding site was a major factor contributing to the strong binding of ANS. No further studies on the *para*-xylyl linked host have been published.

By studying a variety of naphthalene sulfonates, Koga probed the influence of host structure on binding selectivity. His studies<sup>10c</sup> showed that **2** was selective for  $\beta$ -substituted naphthalenes whereas CP56 was selective for  $\alpha$ -substituted naphthalenes. The *trans*-1,4-dimethylenecyclohexyl-linked macrocycle was more effective by a factor of 10 at binding the sulfonated

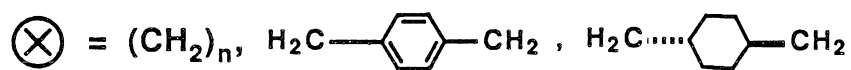
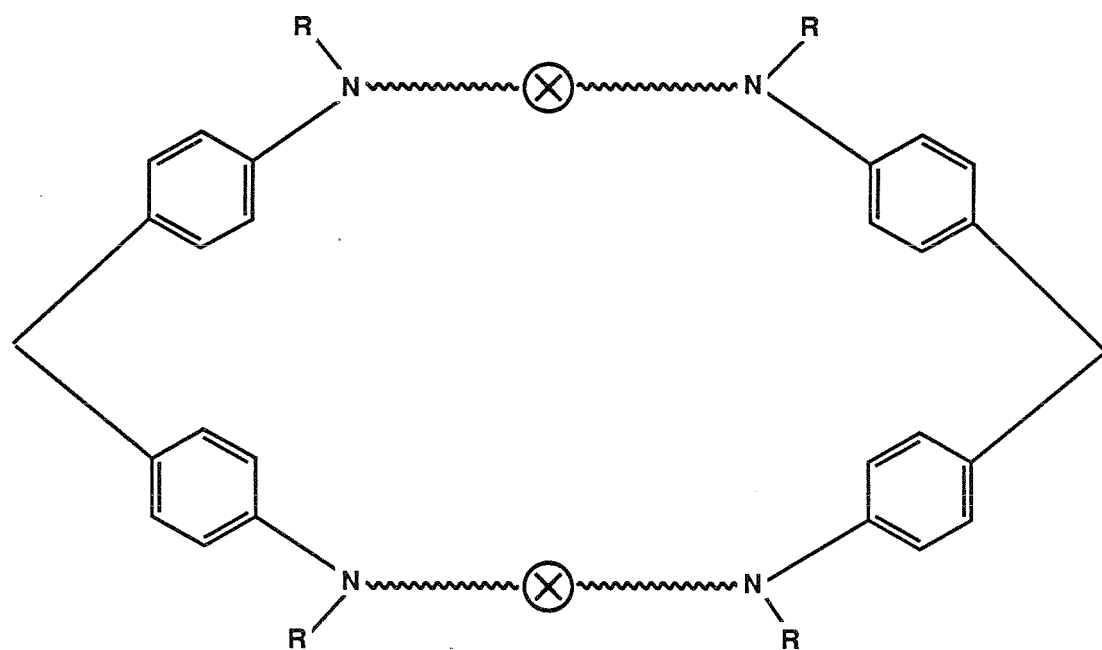


**FIGURE 1.3:** Variations of the linkers in the Koga system

naphthalenes and, like CP56, it was also selective for  $\alpha$ -substituted naphthalenes. Furthermore, for all the hosts studied, bisulfonates formed stronger complexes than monosulfonates. Koga concluded that "fitness of steric structure" and "electrostatic interaction" must both be maximized for strong complexation to occur between host and guest. The selectivities observed in the binding of the substituted naphthalenes were taken as evidence for a change in inclusion geometry from pseudo-axial for **2** to equatorial for the larger, more hydrophobic guests. CPK modeling studies supported this analysis.

Koga has also synthesized an optically active host, **3**, based on a tartrate-derived linker (Figure 1.4).<sup>10e</sup> Diastereomeric inclusion complexes were observed by <sup>1</sup>H NMR spectroscopy when the host was mixed with an aqueous solution of various racemic guests. However, neither association constants nor the enantiospecificities were reported.

Both Tabushi's and Koga's binding sites used nitrogen based groups to impart water solubility. However, these water-solubilizing groups were part of the hydrophobic cavity. This geometrical arrangement has two consequences: first, the cavity is reduced in hydrophobicity; second, electrostatics plays a large role in the observed binding constants. In an attempt to reduce the electrostatic effects and to study the binding by hydrophobic effects alone, Diederich's group designed a new type of host, **4** (Figure 1.5).<sup>11a-e</sup> Diederich also used ammonium ions for water solubilization but placed them well removed from the hydrophobic cavity to ensure separation of hydrophobic and hydrophilic groups.

One of the major insights into the properties of these molecules was made by Diederich. He reasoned that these molecules could aggregate as a function of concentration much as surfactants do. The molecule displayed a

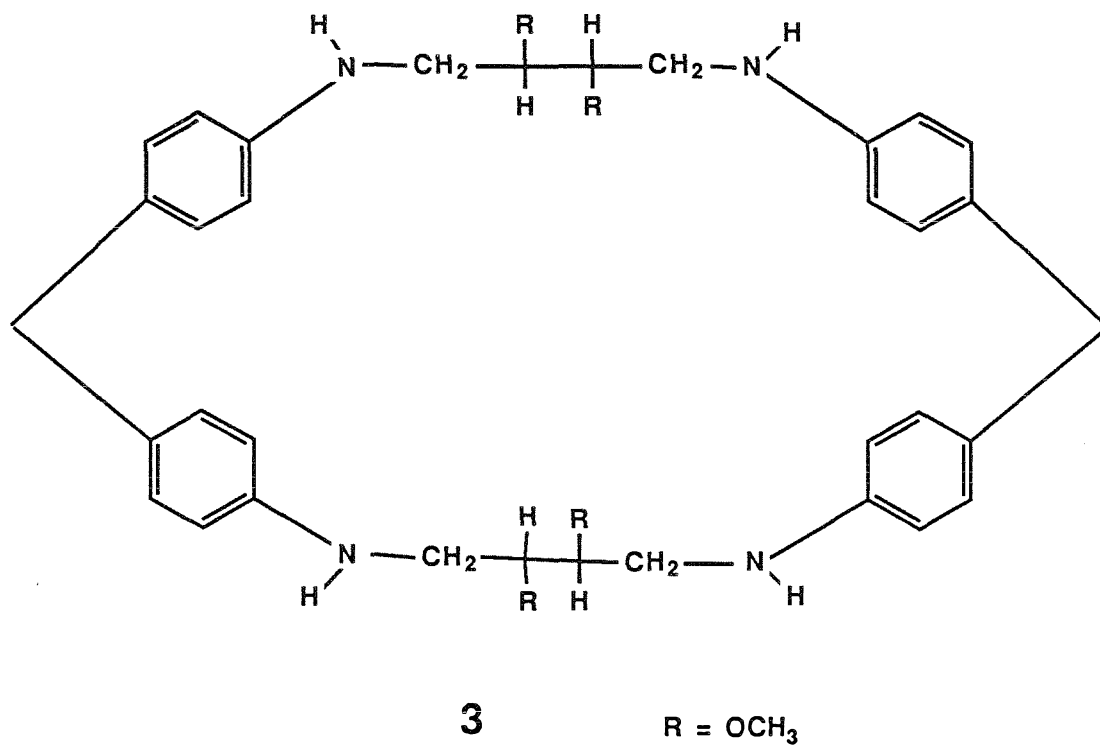
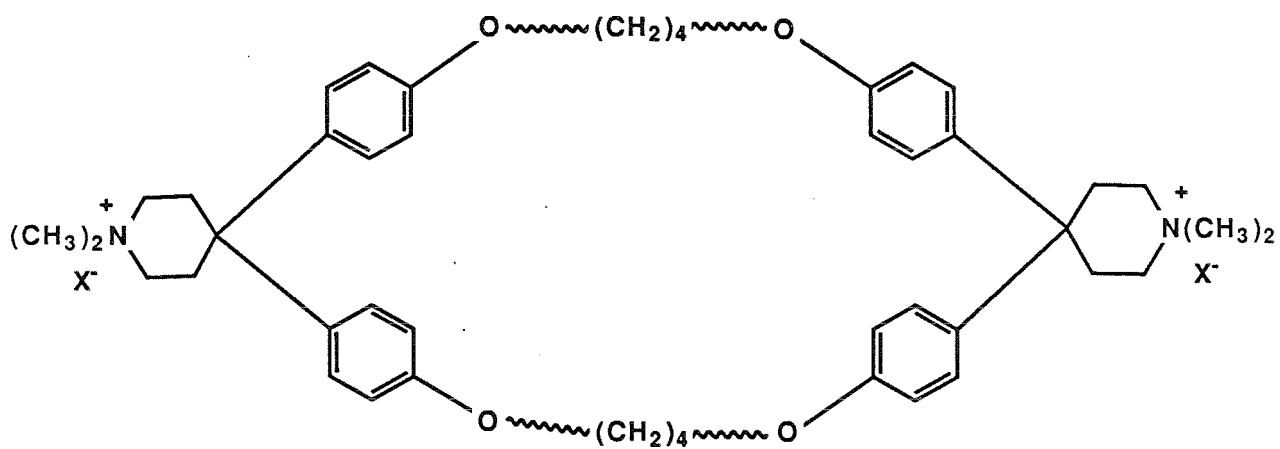


**FIGURE 1.4:** Chiral Host designed by Koga



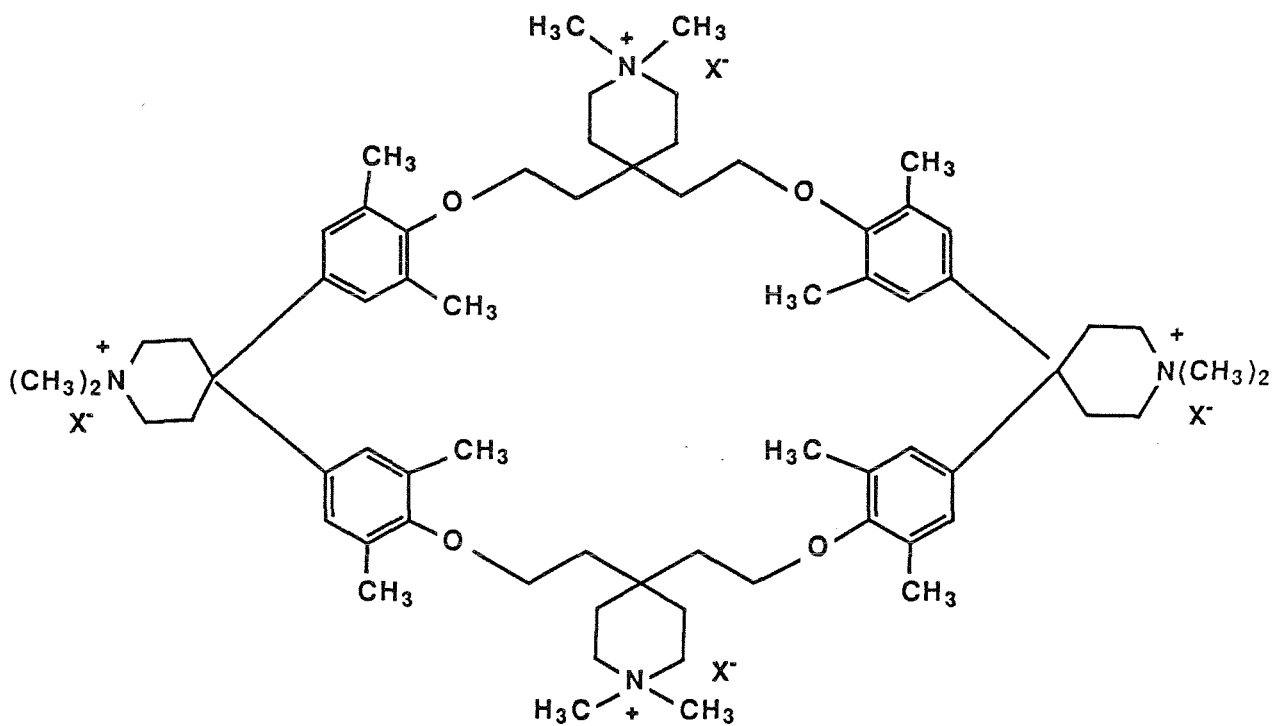
4

**FIGURE 1.5:** Diederich's first-generation macrocyclic receptor molecule

strongly concentration-dependent  $^1\text{H}$  NMR spectrum.<sup>11a</sup> The change of the chemical shifts with increasing concentration was accompanied by strong line-broadening of all the signals. Similar behavior has been noted for the  $^1\text{H}$  NMR spectrum of surfactants as a function of concentration; the determination of the concentration at which this aggregation begins (the CMC-critical micelle concentration) can be determined by a graphical procedure.<sup>12</sup> The determination of a CMC is now considered to be a must if the study of binding to an individual host molecule rather than to an aggregate is desired. The measurement of an association constant or any other physical study above the CMC of the host must be regarded with some skepticism, since the formation of an aggregate and its role in binding could cloud the monomeric binding issue.

The first generation host system designed by Diederich and Dick<sup>11a</sup> had a CMC of 160  $\mu\text{M}$ . **4** did bind ANS ( $K_a = 1500 \text{ M}^{-1}$ ); however, the low CMC of this host limited the binding studies to dilute solutions and excluded the use of  $^1\text{H}$  NMR spectroscopy as a tool for studying host-guest interactions. Therefore, a second generation of hosts was designed by Diederich *et al.* with some added improvements.<sup>11b-e</sup> Diederich desired a host with a higher CMC and a better binding capability. To achieve this he synthesized host **5**, shown in Figure 1.6. He reasoned that the extra added charge should reduce the ability of the host to aggregate; furthermore, he anticipated that adding eight methyl groups to the rim of the binding cavity should increase the hydrophobicity of the cavity and increase its ability to bind non-polar organic molecules. Both the design changes were successful and **5** has been extensively studied by the Diederich group.<sup>11b,c</sup>

Host **5** is monodisperse at concentrations below  $7.5 \times 10^{-3} \text{ M}$ . It efficiently binds ANS and its derivatives with association constants in the



5

**FIGURE 1.6:** Diederich's redesigned macrocyclic receptor molecule

range of  $10^5$ - $10^6$  M<sup>-1</sup>. Mono- and bisulfonates of naphthalene are also good guests for **5** with  $K_a$ s in the range of  $10^4$ - $10^6$  M<sup>-1</sup>; 2,6-naphthalenedisulfonate has a  $K_a > 10^6$  M<sup>-1</sup>. Diederich also studied neutral aromatic guests; Table 1.1 lists some of the interesting guests and their association constants.<sup>11b</sup> The near linear dependence of  $K_a$  on the inverse of the water solubility of these guests suggests that hydrophobicity is the major component of the observed binding. The only guest that did not bind well was a neutral aliphatic guest, adamantanol ( $K_a = 160$  M<sup>-1</sup>).

Diederich studied many of these host-guest interactions by <sup>1</sup>H NMR.<sup>11c</sup> Like Koga,<sup>10b</sup> Diederich observed axial and equatorial binding orientations of substituted naphthalenes within the cavity of **5**. However, for some of the guests, both geometries were observed. Significantly, the water-solubilizing spiropiperidinium groups on the methylene chains enhanced the binding of the naphthalene sulfonates to **5** via electrostatic interactions. When the aromatic guests were bound to **5**, the spiropiperidinium groups folded around the guest and brought the positively charged nitrogens close to the negatively charged sulfonates; this geometry was deduced from NMR studies indicating large upfield shifts of the methylene groups in the spiropiperidinium ring, an observation inconsistent with the binding of these guests to the open form of **5**. Nevertheless, strong complexation via electrostatic and hydrophobic interactions was achieved.

The force(s) behind the interaction of two organic molecules in aqueous solution are a combination of entropic and van der Waals-type forces. This effect has come to be known as the "hydrophobic effect," and numerous studies<sup>13</sup> aimed at the understanding of the phenomenon have been performed. Nevertheless, until the work of Tabushi and Koga, the use of a

**Table 1.1:** Association Constants for Diederich's host and various guests<sup>a</sup>

Guest	$K_a$ (M <sup>-1</sup> )
Perylene	$1.6 \times 10^7$
Pyrene	$1.5 \times 10^6$
Naphthalene	$1.3 \times 10^4$
Durene	$2.0 \times 10^3$
Azulene	$2.1 \times 10^4$
Biphenyl	$2.2 \times 10^4$

a) From reference 11b.

totally synthetic receptor molecule to recognize and bind another organic molecule was unknown.

The ability to design and synthesize an organic receptor molecule capable of binding other organic molecules selectively has opened up new avenues of research. The hydrophobic effect is at the crux of the binding event in aqueous solution, and chemists have long sought to harness this binding energy to do productive, useful, novel chemistry.<sup>14</sup>

One of the applications of the field of host-guest chemistry is the design of enzyme mimics.<sup>15,16</sup> Many molecules possessing hydrophobic binding sites have been modified so as to have enzyme-like properties. Modified cyclodextrins<sup>8a</sup> and some synthetic hydrophobic binding sites<sup>9b,c,17</sup> have been prepared and display enzyme-like properties, e.g., "active-site" binding via hydrophobic forces and catalytic turnovers. These results have proven to be interesting; however, the ability to truly imitate an enzyme is still lacking.<sup>16</sup>

For further progress to be made in the field of molecular recognition, a greater understanding of the binding event is required. Some of the factors that need addressing are fundamental in nature, while others are of a more applied bent. We set out to design and build a novel receptor molecule in an attempt to achieve a more thorough understanding of the binding event. Some of the questions that we wanted to answer were:

- (a) What is the effect of size and shape of both the receptor and the guest upon  $K_a$ ?
- (b) What is the role of charge in the recognition event?
- (c) How does flexibility in the receptor or the guest manifest itself in  $K_a$ ?

- (d) Do  $\pi$ -stacking interactions between aromatic rings of receptor and guest play a significant role?
- (e) How do these parameters affect the kinetics of binding and is there a correlation with  $K_a$ ?
- (f) Can a chiral receptor be designed that can efficiently discriminate between the enantiomers of a racemate?
- (g) If selectivity in binding is achieved, how can this result be used to do productive chemistry, e.g., separations, transport, etc?

While we have not succeeded in answering all these questions completely, the following chapters will present our approaches to answering some of them.

## References for Chapter 1

1. For two general reviews on the field see: *Topics in Current Chemistry* 1982, 101, and *Topics in Current Chemistry* 1981, 98.
2. (a) Dugas, H.; Penney, C. *Bioorganic Chemistry*; Springer-Verlag: New York, 1981.  
(b) *Design and Synthesis of Organic Molecules Based on Molecular Recognition*, Van Binst, G., Ed.; Springer-Verlag: Berlin, 1983.
3. (a) Cram, D.J.; *Angew. Chem., Int. Ed. Engl.* 1986, 25, 1039-1134.  
(b) Cram, D.J. *Science* 1983, 219, 1177-1183.  
(c) Cram, D.J.; Cram, J.M. *Science* 1974, 183, 803-809.
4. Kellogg, R.M. *Angew. Chem., Int. Ed. Engl.* 1984, 23, 782-794.
5. (a) Sam, D.J.; Simmons, H.E. *J. Am. Chem. Soc.* 1972, 94, 4024-4025.  
(b) Sam, D.J.; Simmons, H.E. *J. Am. Chem. Soc.* 1974, 96, 2252-2253.
6. (a) Franke, J.; Vögtle, F. *Topics in Current Chemistry* 1986, 132, 135-170.  
(b) Tabushi, I.; Yamamura, K. in *Topics in Current Chemistry* 1983, 113, 145-183.
7. (a) Bender, M.L.; Komiyama, M. *Cyclodextrin Chemistry*; Springer-Verlag: Berlin, 1978.  
(b) Saenger, W. *Angew. Chem., Int. Ed. Engl.* 1980, 19, 344-362.
8. (a) Breslow, R.; Emert, J. *J. Am. Chem. Soc.* 1975, 97, 670-672.  
(b) Tabushi, I.; Shimokawa, K.; Shimizu, N.; Shirakata, H.; Fujita, K. *J. Am. Chem. Soc.* 1976, 98, 7855-7856.  
(c) Breslow, R.; Czarniecki, M.F.; Emert, J.; Hamaguchi, H. *J. Am. Chem. Soc.* 1980, 102, 762-770.  
(d) Ueno, A.; Tomita, Y.; Osa, T. *J. Chem. Soc., Chem. Comm.* 1983, 976-977.

9. (a) Tabushi, I.; Kuroda, Y.; Kimura, Y. *Tetrahedron Lett.* 1976, 37, 3327-3330.  
(b) Tabushi, I.; Kimura, Y.; Yamaura, K. *J. Am. Chem. Soc.* 1978, 100, 1304-1306.  
(c) Tabushi, I.; Kimura, Y.; Yamaura, K. *J. Am. Chem. Soc.* 1981, 103, 6486-6492.
10. (a) Odashima, K.; Itai, A.; Iitaka, Y.; Koga, K. *J. Am. Chem. Soc.* 1980, 102, 2504-2505.  
(b) Odashima, K.; Itai, A.; Iitaka, Y.; Arata, Y.; Koga, K. *Tetrahedron Lett.* 1980, 21, 4347-4350.  
(c) Soga, T.; Odashima, K.; Koga, K. *Tetrahedron Lett.* 1980, 21, 4351-4354.  
(d) Odashima, K.; Soga, T.; Koga, K. *Tetrahedron Lett.* 1981, 22, 5311-5314.  
(e) Takahashi, I.; Odashima, K.; Koga, K. *Tetrahedron Lett.* 1984, 25, 973-976.
11. (a) Diederich, F.; Dick, K. *Tetrahedron Lett.* 1982, 23, 3167-3170.  
(b) Diederich, F.; Dick, K. *J. Am. Chem. Soc.* 1984, 106, 8024-8036.  
(c) Diederich, F.; Griebel, D. *J. Am. Chem. Soc.* 1984, 106, 8037-8046.  
(d) Diederich, F.; Dick, K.; Griebel, D. *Chem. Ber.* 1985, 118, 3588-3619.  
(e) Kreiger, C.; Diederich, F. *Chem. Ber.* 1985, 118, 3620-2621.
12. (a) Fendler, E.J.; Constien, V.G.; Fendler, J.H. *J. Phys. Chem.* 1975, 79, 917-926.  
(b) Mukerjee, P.; Mysels, K.J. *Natl. Stand. Ref. Data Ser., Natl. Bur. Stand., No. 36*, 1971.
13. Tanford, C. *The Hydrophobic Effect*, 2nd ed.; Wiley: New York, 1980.

14. The hydrophobic effect has also been used in the modeling of biological membranes by synthetic mimics. See Fendler, J. *Membrane Mimetic Chemistry*; Wiley: New York, 1982.
15. Tabushi, I. *Tetrahedron* 1984, 40, 269-292.
16. Breslow, R. in *Chemical Reactions in Organic and Inorganic Constrained Systems*; Setton, R., Ed.; D. Reidel: New York, 1986; pp 17-28.
17. (a) Schürmann, G.; Diederich, F. *Tetrahedron Lett.* 1986, 27, 4249-4252.  
(b) Lutter, H.-D.; Diederich, F. *Angew. Chem., Int. Ed. Engl.* 1986, 25, 1125-1127.

**CHAPTER 2**  
**Design and Synthesis of a**  
**New Host System**

## Design

In setting out to design a new receptor molecule with the ability to recognize and bind other organic molecules in aqueous solution, we set upon some design criteria. We wanted the molecules to be water-soluble; therefore, the number and placement of water-solubilizing groups would be crucial. We felt that a well-defined, rigid, hydrophobic cavity would provide an environment that would allow guests to bind in both an enthalpically and entropically favorable way. By designing a cavity that was more hydrophobic than a cyclodextrin, for example, we felt that our receptor would bind organic guests more strongly; we also felt that some of the adverse entropy associated with this bimolecular reaction could be reduced by using a preformed, rigid cavity.<sup>1a</sup> Our synthetic plan was to incorporate many features: it was to be efficient, variable and rational. We wanted to avoid the oligomeric-type syntheses typified by the calixarenes;<sup>1b,c</sup> we wanted to be able to alter the size and shape of our cavity at will; in contrast to the cyclodextrins, we wanted to be able to easily functionalize our system with transport or catalytic groups. Finally, we desired a binding site that was stably chiral so that we could examine the forces behind chiral recognition in aqueous solution.

These aforementioned criteria are quite demanding. However, we felt that if we could design and synthesize a molecule that satisfied these criteria, we would have an efficient receptor system with which we could attempt to study the phenomenon of molecular recognition.

In a manner similar to that of other workers in the field,<sup>2</sup> we chose to use a macrocyclic framework to enforce the cavity. In contrast, we chose ethenoanthracenes as our basic building blocks for our macrocycles. The general design is shown in Figure 2.1.

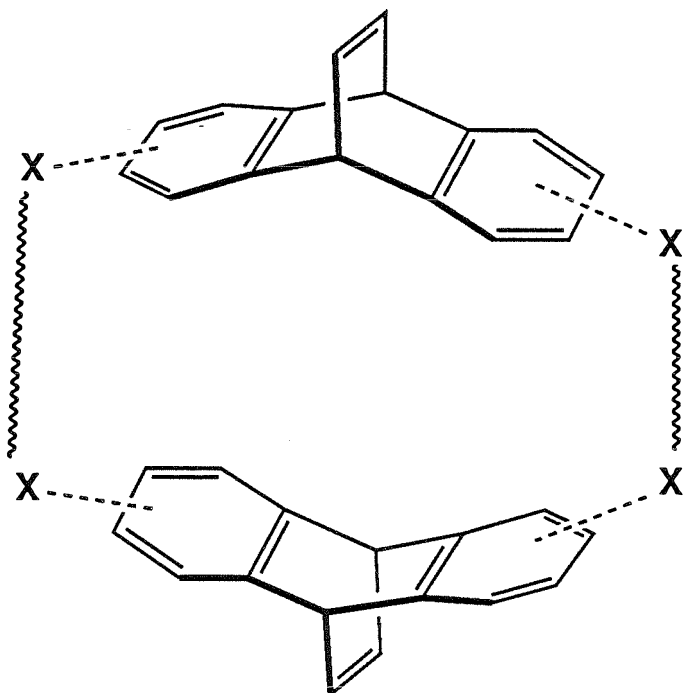


**FIGURE 2.1:** General Host Design

We chose the ethenoanthracene building block for many reasons. First, the molecule is rigid and provides a V-shaped cleft that forms the basis of our binding site. Linking two of these building blocks together via the appropriate linker would establish a macrocycle with a rigid, quite hydrophobic interior wherein we envisioned selected guests would bind. By varying the linker, a binding site of the desired size and shape could be constructed. The ethenoanthracene appeared to be easily prepared by Diels-Alder technology from the appropriate anthracene precursor. The requisite anthracenes are simple structures with many known substitution patterns. Choice of substituents and their placement would be critical to the design.

We envisioned that placement of a heteroatom such as oxygen on the basic building block would facilitate some of the synthetic considerations in the assembly of the macrocycle; furthermore, by using a 2,6-disubstituted anthracene precursor, the Diels-Alder adduct, when assembled into a macrocycle, would provide a host structure with a cavity having a gross sense of twist. We felt that a macrocycle with a helical cavity possessing either a grossly left-handed or grossly right-handed sense of twist would have a binding site with an optimum topography for chiral recognition. Our system, therefore, has at its heart an intrinsically chiral portion of space. We felt that this design would be superior to a design in which one constructs a sphere or a cube and achieves asymmetry by introducing stereogenic centers about the exterior.

The final design consideration is the placement of the water-solubilizing groups. They could be placed anywhere on the basic backbone; however, we felt that placement of the water-solubilizing groups exterior to and well removed from the hydrophobic cavity would be the most beneficial. We did not want to reduce the hydrophobicity of the cavity with nearby polar

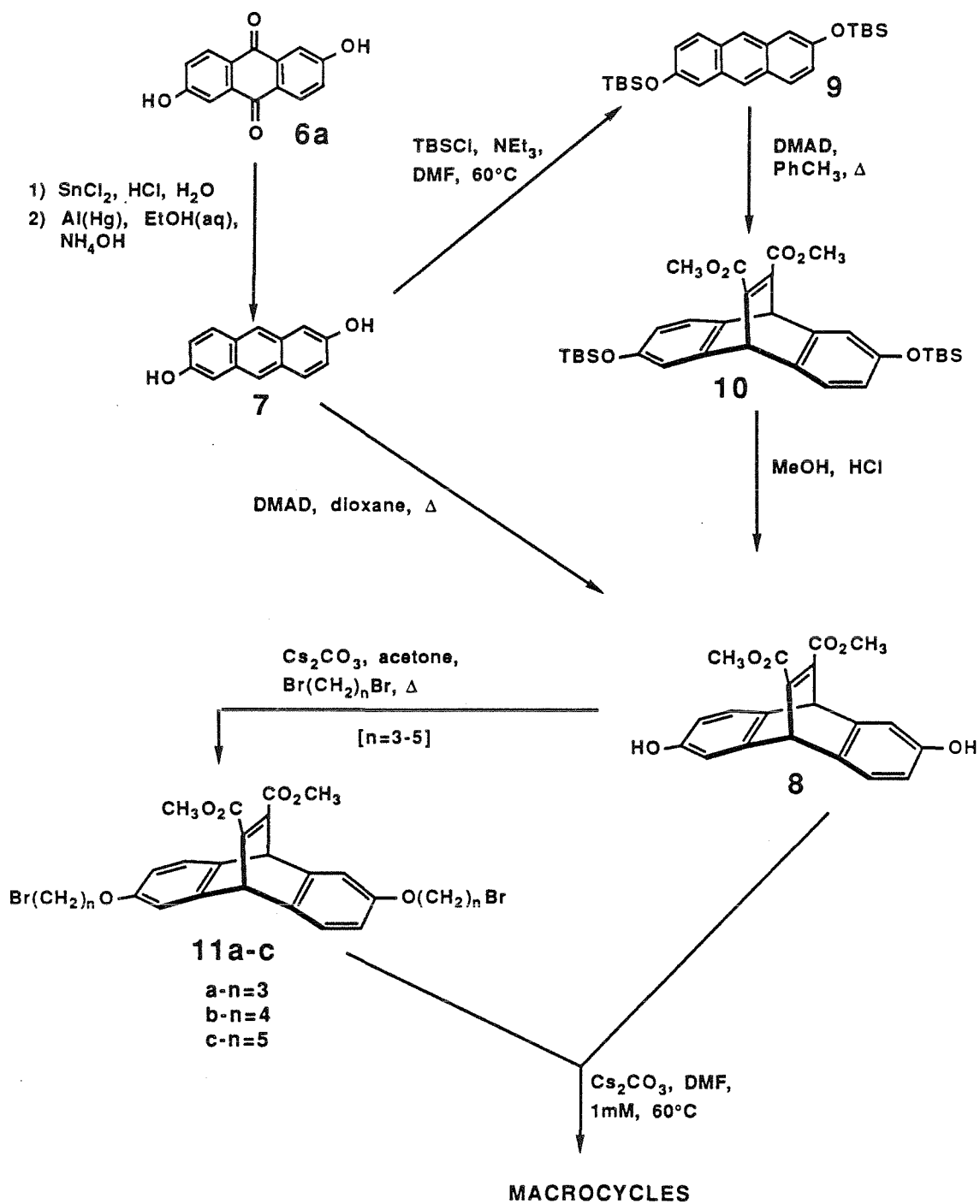
residues. We therefore chose to introduce four carboxylates -- two on each of the etheno bridges, well removed from the binding site -- to achieve water solubility.

## Synthesis

Our synthetic scheme is shown in Scheme 2.1. Reduction of the commercially available anthraflavic acid **6a** in either one step or two (via the anthrone derivative, **6b**), takes place readily at 65 °C to provide the known<sup>3</sup> 2,6-dihydroxyanthracene, **7**. A higher reaction temperature led to large amounts of the over-reduced dihydroanthracene by-product which could be removed by washing with dichloromethane.

2,6-Dihydroxyanthracene, **7**, undergoes a Diels-Alder reaction with dimethylacetylenedicarboxylate (DMAD) in refluxing dioxane over 48 hours to give the racemic ethenoanthracene derivative, **8**, in 60% yield.<sup>4</sup> Dioxane was chosen as solvent because of the insolubility of 2,6-dihydroxyanthracene in most typical Diels-Alder solvents (aromatic hydrocarbons). The low yield reflects the ease with which DMAD undergoes Michael-addition reactions. Many of the by-products in this reaction were Michael adducts of the phenol and DMAD along with DMAD oligomers. Protection of the phenolic hydroxyl groups as *tert*-butyldimethylsilylethers<sup>5</sup> eliminated the Michael addition problem and added tremendous solubility; the Diels-Alder reaction could now be conducted in toluene as solvent. Deprotection of the silylethers in the adduct, **10**, with mineral acid led to the diol with no difficulty.

The diol, **8**, can be alkylated with an excess of an  $\alpha,\omega$ -dibromide using  $\text{Cs}_2\text{CO}_3$  as a base and acetone as solvent.<sup>6</sup> Use of DMF as solvent led to lower yields of isolated products; use of  $\text{K}_2\text{CO}_3$  as a base led to longer reaction times and less clean reaction mixtures. These dibromides, **11a-c**, are formed in 65-70% yield and are ready for macrocyclization.



**SCHEME 2.1:** Synthetic Scheme to Ethenoanthracene based Hosts

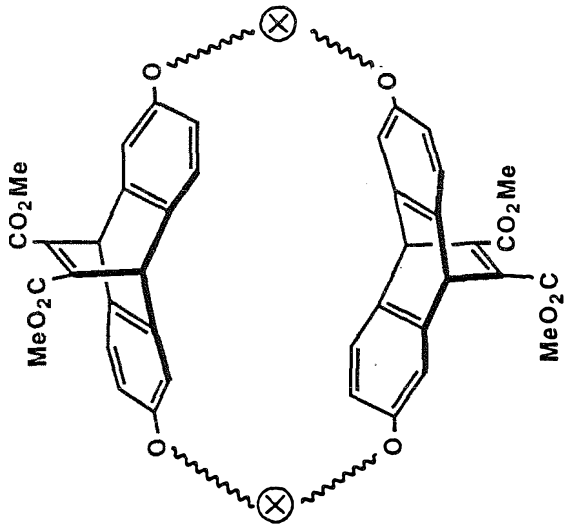
The macrocyclization reaction is conducted using one equivalent of the diol, **8**, and one equivalent of the appropriate dibromide, **11**, in DMF at 1mM concentration.  $\text{Cs}_2\text{CO}_3$ <sup>6</sup> is used as a base, with the reaction being complete after 4 days at 60 °C. The yields of the isolated macrocycles, **12a-c**, are shown in Table 2.1. These macrocycles are 26- to 30-membered rings and yet they are formed in good yields. We believe that these yields attest to the rigid, concave shapes of the precursors and to efficacy of the  $\text{Cs}_2\text{CO}_3/\text{DMF}$  reagent.<sup>6</sup>

Since all the basic building blocks are racemic, coupling of them gives rise to two diastereomers as shown in Figure 2.2. The *d,l* compound is chiral, having  $D_2$  symmetry; it is the homochiral coupling product. The *meso* compound has  $C_{2h}$  symmetry; it is the heterochiral coupling product. The chiral,  $D_2$  isomer is present as a racemate; optical resolution of **8** will give rise to only the *d* (or *l*) macrocycle, thus opening up a route to optically active host systems.<sup>7</sup> This molecule has the intrinsically dissymmetric helical cavity that we feel could be an exceptionally favorable topography for achieving chiral discrimination between the two enantiomers of a racemate.

The two diastereomers formed in the macrocyclization can be separated from higher molecular weight material by simple flash chromatography. Separation of the two diastereomers from each other is achieved by preparative reverse-phase, high-performance liquid chromatography (see experimental section for details). The only other major contamination in the mixture is a di- $\pi$ -methane<sup>8</sup> product, which is easily separated at the HPLC stage. These molecules are light-sensitive; simply protecting them from room light eliminates the di- $\pi$ -methane reaction. In all cases, the isomers are free from higher molecular weight material; <sup>1</sup>H NMR, <sup>13</sup>C NMR and mass spectral data (EI, FABMS, vapor phase osmometry) indicate the structures to be the desired dimers.

**Table 2.1:** Yields of macrocycles from high-dilution ring-closure reactions

LINKER ⊗	YIELD ( <i>Meso</i> + <i>DL</i> )
(CH <sub>2</sub> ) <sub>3</sub>	35%
(CH <sub>2</sub> ) <sub>4</sub>	51%
(CH <sub>2</sub> ) <sub>5</sub>	40%



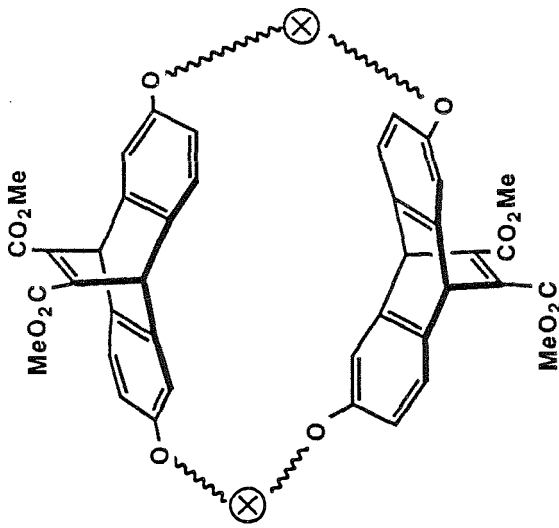
MESO ( $C_{2h}$ )

12

a:  $\otimes = (CH_2)_3$

b:  $\otimes = (CH_2)_4$

c:  $\otimes = (CH_2)_5$

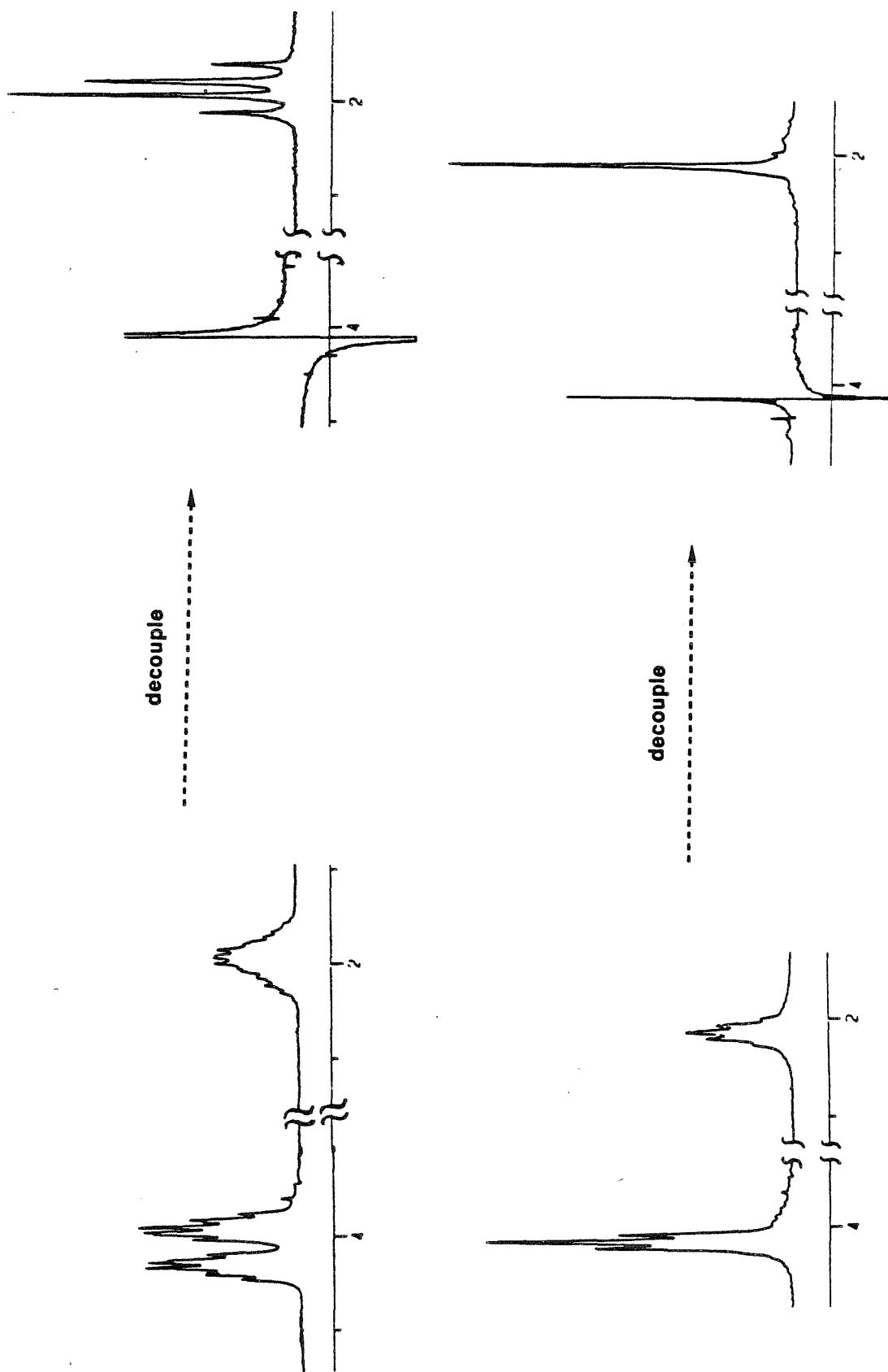


$D,L$  ( $D_2$ )

FIGURE 2.2: Meso and  $D,L$  Macrocycles

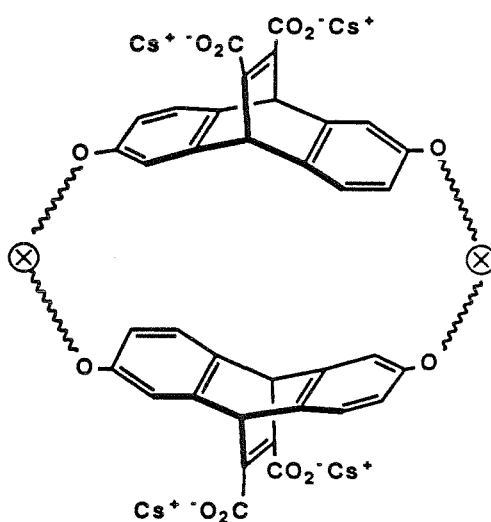
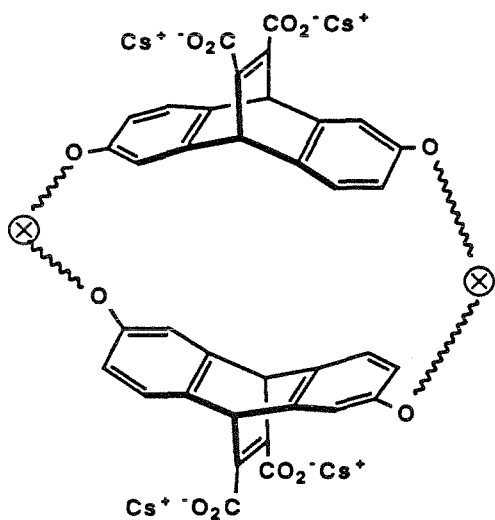
The final structural assignment was that of relative stereochemistry. The  $^1\text{H}$  NMR spectra of the *meso* and *d,l* isomers of **12** are qualitatively the same but quantitatively different in all these cases ( $\otimes = (\text{CH}_2)_n$ ,  $n = 3,4,5$ ). Nevertheless, the symmetry of these structures allows for the unambiguous assignment of stereochemistry when there are an odd number of methylene groups in the linking polymethylene chain. In the chiral,  $D_2$  isomer, the central methylene hydrogens are homotopic; decoupling of the hydrogens adjacent to this  $\text{CH}_2$  group should give rise to a singlet in the  $^1\text{H}$  NMR spectrum. In the *meso* compound ( $C_{2h}$ ), the methylene hydrogens of the central  $\text{CH}_2$  group are diastereotopic. A similar decoupling experiment should give rise to an AB pattern. Figure 2.3 shows the result of one of these decoupling experiments with host **12a**; the theoretical predictions are indeed borne out. A similar experiment proved successful for **12c**. With the assignment of the stereochemistry of the 3C and 5C macrocycles in hand, the stereochemistry of the 4C macrocycles was assigned on the basis of relative HPLC elution order using the 3C and 5C macrocycles as standards. This type of analysis was necessary, since the 4C macrocycles lack the unique central methylene group.

The final step in the synthetic scheme is shown in Scheme 2.2. The water-solubilizing groups were introduced by hydrolysis of the tetraesters ( $\text{CsOH}$ ,  $\text{H}_2\text{O}$ ,  $\text{DMSO}$ ). These tetra-cesium salts **13a-c** were ion-exchanged to give the ammonium carboxylates and then lyophilized to give the free carboxylic acids. These free acids were not very water-soluble. However, neutralization with  $\text{CsOD}/\text{D}_2\text{O}$  gave solutions of the very water-soluble tetra-cesium salts, ready for physical studies.

FIGURE 2.3: <sup>3</sup>C Macrocycle decoupling experiment

Tetraesters

12

CsOH, H<sub>2</sub>O, DMSO

13

a: ⊗ = (CH<sub>2</sub>)<sub>3</sub>b: ⊗ = (CH<sub>2</sub>)<sub>4</sub>c: ⊗ = (CH<sub>2</sub>)<sub>5</sub>

SCHEME 2.2: Introduction of water-solubilizing groups

These host structures define a cavity in space where appropriately sized guests can bind. Table 2.2 shows the approximate dimensions of the cavity as indicated by CPK model analysis. The idealized cavity is best thought of as cylindrical in shape. The depth of the macrocycle varies depending upon the linker; nevertheless, the ethenoanthracene framework provides a minimum of  $\sim 4\text{\AA}$  of depth.

The vertical dimension varies with the linker size (see Table 2.2), with longer linkers providing a cavity of greater width. However, a cavity of much different shape and size can be envisioned. These aliphatic-linked macrocycles are quite flexible and can fold into many different conformations. The NMR spectra of the molecules reflect time-averaged structures of the highest available symmetry. Attempts to detect conformational changes by low-temperature NMR experiments have been unsuccessful. This is quite consistent with an expected low barrier for polymethylene chain conformational dynamics.<sup>9</sup>

Hosts based upon aromatic xylylene-type linkers (ortho, meta and para) have been prepared.<sup>7</sup> These molecules are also fairly rigid, with fewer degrees of freedom than the hosts discussed here. The results of studies on these systems will be reported elsewhere.<sup>7</sup>

### CMC Studies

The tetra-cesium salts of these macrocycles are quite water-soluble; moreover, their behavior and structure are quite concentration- and pH-dependent in aqueous solution. These host structures are similar to surfactants having both hydrophobic and hydrophilic parts. At appropriate concentrations, the molecules associate to form an aggregate.<sup>10</sup> This aggregate is much like a micelle in its properties but probably more like a vesicle or bilayer in structure.

**Table 2.2:** Dimensions of the hydrophobic binding sites of the ethenoanthracene-based hosts

HOST	~ DIMENSIONS (Å x Å)
3C <i>Meso</i>	5.6 x 6.0
3C <i>DL</i>	5.6 x 5.6
4C <i>Meso</i>	6.8 x 6.4
4C <i>DL</i>	6.8 x 6.0
5C <i>Meso</i>	8.0 x 7.6
5C <i>DL</i>	8.0 x 6.8

The phenomenon of concentration-dependent structure is an important one. In this field, a precise geometry and specific interactions of a receptor site and its guest are often presented. However, without a knowledge of the state of aggregation of these receptors, the specific 1:1 receptor/guest interaction should be viewed with skepticism. Not until the concentration dependence of the receptor's structure has been determined can specific geometric and energetic interaction questions be addressed. While the binding of a guest molecule to an aggregate, whether it be a micelle or vesicle, is interesting, it is far from novel. The 1:1 interaction of a host receptor and a guest molecule is a much newer phenomenon and is the basis for the large amount of interest in the field of molecular recognition.

There are many methods available for determining the state of aggregation of surfactant-type molecules.<sup>10</sup> These methods have been reviewed and they fall into two categories. The first type of method is based on the addition of a probe molecule to the surfactant system and the measuring of some property of the probe molecule. The probe molecule typically undergoes a measurable change in one of its physical properties upon binding to the surfactant. This method of using a probe molecule has been criticized as being too intrusive, with the probe molecule changing the state of aggregation of the structure it was designed to probe.<sup>10</sup>

The other methods are of the "non-intrusive" type and typically involve spectroscopic studies. We chose to study our host systems by a non-intrusive <sup>1</sup>H NMR method. This method has been used often and quite successfully for determining the onset of aggregation of surfactant-type systems.<sup>10,11</sup> By recording the <sup>1</sup>H NMR spectrum of our host structures as a function of concentration, the critical micelle concentration (CMC) can be determined. While we probably do not have a system that forms micelles, it is

certain that the structures form some type of aggregate. Nevertheless, we will use the term CMC to describe the concentration above which aggregation begins.

Figure 2.4 shows the results of the NMR determination of the CMC for two of the hosts, **4CMeso** and **5CDL**. The change in chemical shifts as a function of concentration allows a determination of the CMC. At low concentrations, the  $^1\text{H}$  NMR spectrum is well-resolved and the peaks for the host are sharp. As the concentration increases, the peaks broaden and shift in position. The intermediate concentration range where the chemical shift changes rapidly is indicative of the onset of aggregation. At high concentration, the peaks of the host are very broad and considerably shifted and the solutions are visibly "soapy," indicative of an aggregated structure. The CMC is determined from this graph; it is the point at which the rapid change in chemical shift occurs. While the CMC is probably not a *single* concentration, we have used this convention for reporting purposes. Thus, the CMC for **5CMeso** is  $\approx 400 \mu\text{M}$  and for **4CMeso**,  $\approx 1000 \mu\text{M}$ . However, in all our studies, we stay well below the CMC (the flat plateau portion of the graph) to avoid aggregation effects. We can therefore be confident in assuming monomeric host structures in our studies.

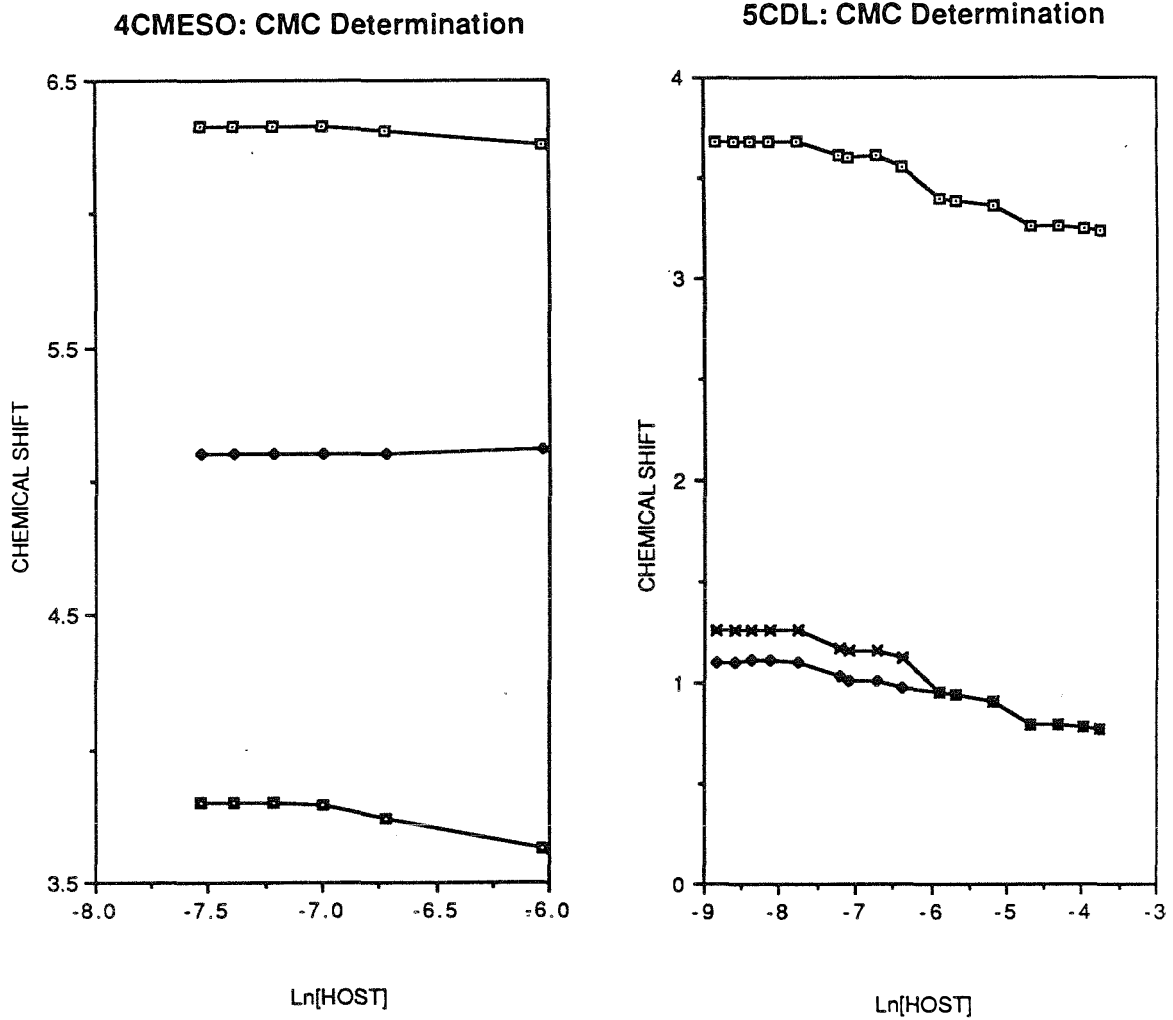


**FIGURE 2.4:** CMC Determination of 4CMESO and 5CDL by the NMR method

## EXPERIMENTAL SECTION

General;  $^1\text{H}$  NMR spectra were recorded on a Varian EM-390 spectrometer. Fourier transform NMR spectra ( $^1\text{H}$  and  $^{13}\text{C}$ ) were recorded on a JEOL FX-90Q, a Varian XL-200 or a JEOL GX-400 spectrometer. 500 MHz spectra were recorded on a Bruker WM500 spectrometer. All coupling constants are in hertz. Mass spectra were performed by Regional MS Facilities (UCR and UNeb). Analytical and preparative reversed phase HPLC were performed on a Perkin Elmer Series 2 LC with a Whatman Partisil 20 ODS-3 column using UV detection at 254 nm. All column chromatography was performed by the method of Still.<sup>12</sup>

### 2,6-Dihydroxyanthrone (6b)

A 1-L round-bottomed flask equipped with a reflux condenser was charged with anthraflavic acid, **6a**, (24.12 g, 0.1 mol, 1 eq),  $\text{SnCl}_2$  (112.8 g, 0.5 mol, 5 eq) and 600 mL of 25% HCl (v/v). The heterogeneous reaction mixture was heated to reflux for 18 hours. During this time the yellow-brown anthraquinone turned bright yellow in color indicative of the anthrone. The solution was cooled and filtered. The bright-yellow solid was washed with 500 mL of  $\text{H}_2\text{O}$  and air-dried. The material was purified by Soxhlet extraction using MeOH as the solvent. Yield: 19.52 g, 86%.  $^1\text{H}$  NMR ( $\text{DMSO}-d_6$ ):  $\delta$  7.00-8.20 (m, 8H), 4.20 (s, 2H).

### 2,6-Dihydroxyanthracene (7)

A 500-mL, three-neck, round-bottomed flask, equipped with a condenser, an  $\text{N}_2$  inlet, a mechanical stirrer, and a rubber septum was charged with the anthrone **6b** (9 g, 39.7 mmol, 1 eq) and 200 mL of 33% aqueous EtOH. Concentrated  $\text{NH}_4\text{OH}$  (34 mL) was added via syringe to the suspension. The solution turned deep red immediately. The aluminum

amalgam, prepared by mixing 18.8 g of aluminum (foil or shot) and 26.4 g of  $\text{HgCl}_2$  in 650 mL of  $\text{H}_2\text{O}$ , was added piecewise to the red solution with stirring. During the whole process, the solution was kept under  $\text{N}_2$  as much as possible. The reaction mixture containing the pieces of amalgam was then carefully heated to  $\sim 55\text{ }^\circ\text{C}$  until the red color faded to yellow ( $\sim 30\text{-}45$  min). The solution was cooled to  $0\text{ }^\circ\text{C}$  for 10 minutes and then poured into 100 mL of 5N HCl. The precipitate was collected by filtration. This yellow-brown solid was suspended in 900 mL of acetone, filtered through celite and concentrated, giving 7.12 g of a light-yellow-brown, air-sensitive solid. Yield = 86%. This procedure also worked with 6a as a starting material.  $^1\text{H}$  NMR (Acetone- $d_6$ ):  $\delta$  7.28 (dd, 2H,  $J=7.5, 1.5$ ), 7.38 (d, 2H,  $J=1.5$ ), 7.98 (d, 2H,  $J=7.5$ ), 8.28 (s, 2H), 8.68 (s, 2H, xch. with  $\text{D}_2\text{O}$ ).  $^{13}\text{C}$  NMR (acetone- $d_6$ ):  $\delta$  154.58, 132.29, 130.08, 124.23, 120.98, 107.92.

### 2,6-Bis(*tert*-butyldimethylsiloxy)anthracene(9)

A 200-mL, round-bottomed flask was charged with 2,6-dihydroxyanthracene, 7 (1 g, 4.8 mmol, 1 eq) and *tert*-butyldimethylsilylchloride (3.59 g, 23.8 mmol, 5 eq). Fifty milliliters of dimethylformamide was added and the solution placed under argon. Triethylamine (2.4 g, 3.25 ml, 23.8 mmol, 5 eq) was added and the solution was warmed to  $80\text{ }^\circ\text{C}$  for 2 hours. The solution was concentrated with the aid of a vacuum pump and dry-loaded onto silica gel. The material was chromatographed over silica gel using 15%  $\text{Et}_2\text{O}$ /petroleum ether and the fast-moving yellow band was collected and concentrated, giving 1.93 g (93%) of the desired compound as a yellow solid. It could be further purified by recrystallization from petroleum ether.  $^1\text{H}$  NMR ( $\text{CDCl}_3$ ):  $\delta$  8.15 (s, 2H), 7.80 (d, 2H,  $J=9.03$ ), 7.24 (d, 2H,  $J=2.44$ ), 7.05 (dd, 2H,  $J=9.03, 2.44$ ), 1.01 (s, 18H), 0.25 (s, 12H).

**2,6-Bis(*tert*-butyldimethylsiloxy)-9,10-dihydro-9,10-(1,2-dicarbomethoxy)ethenoanthracene (10)**

A 25-mL, round-bottomed flask was charged with **9** (1.35 g, 3.02 mmol, 1 eq), 3 mL of freshly distilled toluene and 1.9 mL of DMAD (2.19 g, 15.4 mmol, 5 eq). The solution was refluxed for 42 hours. The solution was concentrated and 20 mL of MeOH was added. The solution was sonicated and crystals formed. 1<sup>st</sup> crop: 805 mg. The mother liquors were chromatographed on silica gel using 80% Et<sub>2</sub>O/petroleum ether as an eluant, giving 720 mg of a white solid. Mp = 123-126 °C. Total yield = 1.525 g, 86% yield. <sup>1</sup>H NMR (CDCl<sub>3</sub>): δ 7.05 (d, 2H, *J*=8.05), 6.75 (d, 2H, *J*=2.2), 6.3 (dd, 2H, *J*=8.05, 2.2), 5.15 (s, 2H), 3.8 (s, 6H), 0.9 (s, 18H), 0.13 (s, 12H).

**2,6-Dihydroxy-9,10-dihydro-9,10-(1,2-dicarbomethoxy)ethenoanthracene (8)**

A suspension 2,6-dihydroxyanthracene (1.05 g, 5 mmol, 1 eq) in 20 mL of anhydrous, freshly distilled dioxane was stirred under N<sub>2</sub>. Dimethylacetylenedicarboxylate (7.2 g, 8.3 mL, 10 eq, 50 mmol) and pyrogallol (63 mg, 0.5 mmol, 1 eq) were added. The mixture was refluxed for 2 days. The dioxane was removed under reduced pressure and the resulting brown viscous oil was chromatographed on silica, using ether as an eluent. Yield: 1.05g (60%) of a yellow foam. <sup>1</sup>H NMR (acetone-*d*<sub>6</sub>): δ 3.80 (s, 6H), 5.50 (s, 2H), 6.50 (dd, 2H, *J*=1.5, 7.5), 7.00 (d, 2H, *J*=1.5) 7.25 (d, 2H, *J*=7.5). <sup>13</sup>C NMR (CDCl<sub>3</sub>): δ 166.50, 154.05, 147.50, 145.99, 135.04, 124.31, 112.02, 111.02, 52.52, 51.59.

**2,6-Dihydroxy-9,10-dihydro-9,10-(1,2-dicarbomethoxy)ethenoanthracene (8)**

The bis TBS ether, **10**, (800 mg, 1.38 mmol) was dissolved in 20 mL MeOH; 1 mL CH<sub>2</sub>Cl<sub>2</sub> and 1 mL conc. HCl were added. The reaction was stirred at room temperature for 6.5 hours. The solution was concentrated and

chromatographed over SiO<sub>2</sub>, using ether as an eluant to give 450 mg (93%) of a white solid. This material could be recrystallized from CHCl<sub>3</sub>. Mp = 235-237 °C. Mass Spectrum: (m/e) 352 (M<sup>+</sup>), 293 (100), 278, 261, 249, 234, 210, 181, 152, 59. HRMS: 352.0956 (calc.), 352.0947 (found). Analysis calculated: C (68.18), H (4.58); found: C (67.50), H (4.62).

**2,6-Bis(3-bromopropoxy)-9,10-dihydro-9,10-(1,2-dicarbomethoxy)-ethenoanthracene (11a)**

To a solution of the diol, **8** (704 mg, 2 mmol, 1 eq), in 35 mL of degassed acetone were added Cs<sub>2</sub>CO<sub>3</sub> (3.25 g, 10 mmol, 5 eq) and 1,3-dibromopropane (4.03 g, 20 mmol, 10 eq). The solution was gently refluxed for 18 hours. The excess Cs<sub>2</sub>CO<sub>3</sub> and precipitated CsBr were removed by filtration and washed with acetone. The solution was concentrated and chromatographed over SiO<sub>2</sub> using 30% ethyl acetate:petroleum ether as an eluant. Yield: 674 mg (57%) of a light yellow oil. <sup>1</sup>H NMR (CDCl<sub>3</sub>): δ 2.05 (quintet, 4H, *J* = 7.0), 3.50 (t, 4H, *J* = 7.0), 3.80 (s, 6H), 3.95 (t, 4H, *J* = 7.0), 5.39 (s, 2H), 6.50 (dd, 2H, *J* = 7.5, 2.0), 7.08 (d, 2H, *J* = 2.0), 7.25 (d, 2H, *J* = 7.5). <sup>13</sup>C NMR (CDCl<sub>3</sub>): δ 165.76, 156.42, 146.98, 145.72, 135.74, 124.06, 111.46, 109.71, 65.35, 52.24, 51.59, 32.11, 29.90.

**2,6-Bis(4-bromobutoxy)-9,10-dihydro-9,10-(1,2-dicarbomethoxy)-ethenoanthracene (11b)**

To a suspension of Cs<sub>2</sub>CO<sub>3</sub> (6.027 g, 18.5 mmol, 10 eq) in 30 mL of degassed acetone containing 2.2 mL of 1,4-dibromobutane (3.99 g, 18.5 mmol), 10 eq) was added a 10 mL solution of the diol, **8** (650 mg, 1.85 mmol, 1 eq), in acetone. The solution was refluxed in the dark for 15 hours. The excess Cs<sub>2</sub>CO<sub>3</sub> and precipitated CsBr were removed by filtration and washed with CH<sub>2</sub>Cl<sub>2</sub> and acetone. The solution was concentrated and chromatographed using 35% ethyl acetate:petroleum ether as an eluant. Yield: 689 mg (60%) of

a light yellow oil.  $^1\text{H}$  NMR ( $\text{CDCl}_3$ ):  $\delta$  1.90 (m, 8H), 3.40 (t, 4H,  $J=6.1$ ), 3.80 (s, 6H), 3.90 (t, 4H,  $J=6.1$ ), 5.30 (s, 2H), 6.45 (dd, 2H,  $J=7.5, 1.5$ ), 6.90 (d, 2H,  $J=1.5$ ), 7.20 (d, 2H,  $J=7.5$ ).  $^{13}\text{C}$  NMR ( $\text{CDCl}_3$ )  $\delta$  166.56, 157.35, 147.74, 146.43, 136.79, 124.75, 112.13, 110.32, 69.04, 52.99, 52.33, 34.07, 30.01, 28.42.

**2,6-Bis(5-bromopentoxy)-9,10-dihydro-9,10-(1,2-dicarbomethoxy)-ethenoanthracene (11c)**

To a 50 mL solution of the diol **8** (1 g, 2.84 mmol, 1 eq) in acetone were added 1,5-dibromopentane (6.53 g, 3.87 mL, 28.4 mmol, 10 eq) and  $\text{Cs}_2\text{CO}_3$  (9.25 g, 28.4 mmol, 10 eq). The solution was kept under  $\text{N}_2$  and gently refluxed for 6 hours. The solution was filtered and concentrated. The product was isolated as a yellow oil (1.248 g, 68%) by flash chromatography over silica gel, using 30% ethyl acetate:petroleum ether as an eluant.  $^1\text{H}$  NMR ( $\text{CDCl}_3$ ):  $\delta$  7.2 (d, 2H,  $J=7.5$ ), 6.9 (d, 2H,  $J=1.5$ ), 6.4 (dd, 2H,  $J=7.5, 1.5$ ), 5.3 (s, 2H), 3.8 (t, 4H,  $J=7$ ), 3.75 (s, 6H), 3.3 (t, 4H,  $J=7$ ), 1.9-1.3 (m, 12H).  $^{13}\text{C}$  NMR ( $\text{CDCl}_3$ ):  $\delta$  166.32, 157.35, 147.73, 146.43, 136.10, 124.66, 112.05, 110.23, 68.25, 52.85, 52.26, 34.33, 32.84, 28.81, 25.23.

### Macrocyclization Conditions

The 3C, 4C, 5C macrocycles were prepared in the same way. A flame-dried flask was charged with 1 eq of the diol and 1 eq of the appropriate dibromide. Enough DMF was added to make the solution 1 mM in these reactants. The DMF was distilled from BaO at reduced pressure and stored over 4Å molecular sieves prior to use.  $\text{Cs}_2\text{CO}_3$  (5 eq) was added. The flask was protected from light and kept over  $\text{N}_2$  while being warmed to 60 °C. The reaction was completed in 3-4 days. The DMF was removed with the aid of a pump. The residue was partitioned between  $\text{CH}_2\text{Cl}_2$  and 1 N HCl. The organic layer was washed with  $\text{H}_2\text{O}$  and then brine. The organic layer was dried over  $\text{MgSO}_4$  and concentrated. The crude reaction mixture was subjected to flash

chromatography to isolate the dimeric macrocycles. This mixture was then separated by preparative reverse-phase HPLC. Listed below are the conditions for all the chromatography and the spectral data for the macrocycles.

### 3C Macrocycles (12a)

Flash Chromatography: 50% ethyl acetate:petroleum ether

Yield = 35%

RPHPLC: 20% H<sub>2</sub>O/CH<sub>3</sub>OH, 12 ml/min flow rate  $t_R$  (Meso) = 17.5 min,  $t_R$  (d,l) = 21.9 min

Analysis calculated: C (70.40), H (5.14); found: C 9(69.89), H (5.11).

### 3C Meso

<sup>1</sup>H NMR (CDCl<sub>3</sub>): δ 7.01 (d, 4H,  $J$  = 7.1), 6.80 (d, 4H,  $J$  = 2.3), 6.39 (dd, 4H,  $J$  = 7.1, 2.3), 5.18 (s, 4H), 3.99 (m, 8H), 3.74 (s, 12H), 1.98 (m, 4H).

<sup>13</sup>C NMR (CDCl<sub>3</sub>): δ 165.53, 156.06, 146.48, 154.39, 135.34, 123.63, 111.32, 109.99, 63.51, 52.42, 51.75, 29.55.

Mass Spectrum: (FAB) 785 (MH<sup>+</sup>), 753, 725, 309, 155.

### 3C DL

<sup>1</sup>H NMR (CDCl<sub>3</sub>): δ 7.03 (d, 4H,  $J$  = 8.0), 6.82 (d, 4H,  $J$  = 2.5), 6.39 (dd, 4H,  $J$  = 8.0, 2.5), 5.17 (s, 4H), 4.03 (m, 8H), 3.75 (s, 12H), 2.03 (m, 4H).

<sup>13</sup>C NMR (CDCl<sub>3</sub>): δ 165.52, 156.37, 146.40, 145.29, 135.27, 123.54, 112.26, 108.96, 63.77, 52.44, 51.67, 29.41.

Mass Spectrum: (FAB) 785 (MH<sup>+</sup>), 753, 725, 309, 155.

### 4C Macrocycles (12b)

Flash Chromatography: 40% ethyl acetate:petroleum ether

Yield: 51%

RPHPLC: 15% H<sub>2</sub>O/CH<sub>3</sub>OH, 12 ml/min flow rate  $t_R$  (Meso) = 18.1 min,  $t_R$  (DL) = 28.8 min

Analysis calculated: C (70.92), H (5.46); found: C (68.81), H (5.29).

#### 4C Meso

$^1\text{H}$  NMR ( $\text{CDCl}_3$ ):  $\delta$  7.10 (d, 4H,  $J=8.3$ ), 6.86 (d, 4H,  $J=2.4$ ), 6.41 (dd, 4H,  $J=8.3, 2.4$ ), 5.25 (s, 4H), 3.90 (m, 8H), 3.79 (s, 12H), 1.78 (m, 8H).

$^{13}\text{C}$  NMR (acetone- $d_6$ ):  $\delta$  166.45, 157.73, 147.75, 136.88, 124.85, 112.62, 110.46, 68.15, 52.47, 52.16, 25.72.

Mass Spectrum: (FAB) 813 ( $\text{MH}^+$ ), 781, 753, 670, 309, 155, 119.

#### 4C DL

$^1\text{H}$  NMR ( $\text{CDCl}_3$ ):  $\delta$  7.10 (d, 4H,  $J=8.3$ ), 6.82 (d, 4H,  $J=2.44$ ), 6.36 (dd, 4H,  $J=8.3, 2.44$ ), 5.22 (s, 4H), 3.75 (m, 8H), 3.76 (s, 12H), 1.69 (m, 8H).

$^{13}\text{C}$  NMR (acetone- $d_6$ ,  $\text{CH}_2\text{Cl}_2$ ):  $\delta$  166.19, 157.40, 147.20, 146.58, 136.40, 124.41, 112.30, 110.16, 67.91, 52.33, 51.88, 25.60.

Mass Spectrum: (FAB) 813 ( $\text{MH}^+$ ), 781, 753, 670, 309, 155, 119.

#### 5C Macrocycles (12c)

Flash Chromatography: 10:1  $\text{CHCl}_3/\text{Et}_2\text{O}$

Yield: 40%

RPHPLC: 15%  $\text{H}_2\text{O}/\text{CH}_3\text{OH}$ , 12 mL/min flow rate,  $t_{\text{R}}(\text{Meso}) = 31.3$  min,  $t_{\text{R}}(\text{DL}) = 40$  min

Analysis calculated: C (71.42), H (5.75); found: C (71.27), H (5.58).

#### 5C Meso

$^1\text{H}$  NMR ( $\text{CDCl}_3$ ):  $\delta$  7.00 (d, 4H,  $J=8.07$ ), 6.77 (d, 4H,  $J=2.17$ ), 6.29 (dd, 4H,  $J=8.07, 2.17$ ), 5.15 (s, 4H), 3.79 (m, 8H), 3.69 (s, 12H), 1.61 (m, 8H), 1.55 (m, 4H).

$^{13}\text{C}$  NMR ( $\text{CDCl}_3$ ):  $\delta$  166.01, 156.67, 147.00, 145.79, 135.50, 124.00, 111.35, 109.90, 67.58, 52.31, 51.73, 28.44, 22.50.

Mass Spectrum: (FAB) 841 ( $\text{MH}^+$ ), 809, 781, 698, 361, 293, 210, 119.

**5C DL**

$^1\text{H}$  NMR ( $\text{CDCl}_3$ ):  $\delta$  7.07 (d, 4H,  $J=8.03$ ), 6.77 (d, 4H,  $J=2.14$ ), 6.34 (dd, 4H,  $J=8.03, 2.14$ ), 5.21 (s, 4H), 3.85 (m, 8H), 3.74 (s, 12H), 1.67 (m, 8H), 1.55 (m, 4H).

$^{13}\text{C}$  NMR ( $\text{CDCl}_3$ ):  $\delta$  166.00, 156.82, 146.94, 145.77, 135.49, 123.93, 111.61, 109.50, 67.68, 52.30, 51.68, 28.43, 22.48.

Mass Spectrum: (FAB) 841 ( $\text{MH}^+$ ), 809, 781, 698, 361, 293, 210, 119.

**Hydrolysis Conditions**

All the host macrocycles were hydrolyzed in a similar manner. The tetraesters 12 were dissolved in either DMSO or THF and CsOH (8-10 eq) was added. Five percent water was added and the reaction stirred overnight. The solution was lyophilized and the resulting solid dissolved in a minimum amount of  $\text{H}_2\text{O}$ . The aqueous solution was added to the top of a cation exchange column (neutral pH,  $\text{NH}_4^\oplus$  form) and the material eluted with doubly distilled water. The fractions containing the host(s) were determined by reverse-phase TLC. The samples were combined and lyophilized to give the free acids. Standard solutions of these hosts were achieved by adding the appropriate amount of CsOD and making the solution up to a certain volume in a volumetric flask with the desired buffer. The NMR data of the hosts 13 are given below.

**3C DL**

$^1\text{H}$  NMR (borate buffer, pH = 9, rel. to external TSP):  $\delta$  7.21 (d, 4H,  $J=8.05$ ), 7.05 (d, 4H,  $J=2.2$ ), 6.60 (dd, 4H,  $J=8.05, 2.2$ ), 5.20 (s, 4H), 4.22 (m, 8H), 2.05 (m, 4H).

$^{13}\text{C}$  NMR ( $\text{DMSO}-d_6$ . $\text{D}_2\text{O}$ ):  $\delta$  170.04, 159.91, 149.20, 148.48, 139.73, 125.54, 112.89, 66.41, 53.60, 29.87.

**3C Meso**

$^1\text{H}$  NMR (borate buffer, pH = 9, rel. to external TSP):  $\delta$  7.09 (d, 4H,  $J=8.3$ ), 7.01 (d, 4H,  $J=2.4$ ), 6.50 (dd, 4H,  $J=8.3, 2.4$ ), 5.14 (s, 4H), 4.22 (m, 4H), 4.11 (m, 4H), 2.05 (m, 4H).

$^{13}\text{C}$  NMR (borate buffer pH = 9, rel. to external TSP):  $\delta$  172.23, 153.27, 145.49, 144.68, 135.82, 121.86, 109.03, 107.97, 62.61, 50.31, 26.94.

**4C Meso**

$^1\text{H}$  NMR ( $\text{CD}_3\text{OD}$ ):  $\delta$  7.00 (d, 4H,  $J=8.0$ ), 6.94 (d, 4H,  $J=2.2$ ), 6.43 (dd, 4H,  $J=8.0, 2.2$ ), 5.46 (s, 4H), 3.88 (m, 8H), 1.75 (m, 8H).

$^{13}\text{C}$  NMR ( $\text{CD}_3\text{OD}$ ):  $\delta$  168.38, 157.55, 149.18, 147.06, 136.90, 124.73, 112.08, 111.07, 68.13, 53.49, 25.58.

**4C DL**

$^1\text{H}$  NMR ( $\text{CD}_3\text{CN}$ ):  $\delta$  7.08 (d, 4H,  $J=8.0$ ), 6.92 (d, 4H,  $J=1.7$ ), 6.38 (dd, 4H,  $J=8.0, 1.7$ ), 5.60 (s, 4H), 3.8 (m, 4H), 1.7 (m, 4H).

$^{13}\text{C}$  NMR ( $\text{CD}_3\text{OD}$ ):  $\delta$  168.79, 157.33, 151.05, 147.43, 137.57, 124.51, 112.15, 111.37, 68.61, 54.23, 26.04.

**5C Meso**

$^1\text{H}$  NMR ( $\text{D}_2\text{O}$ , phosphate buffer):  $\delta$  7.12 (d, 4H,  $J=2.2$ ), 6.97 (d, 4H,  $J=8.0$ ), 6.20 (dd, 4H,  $J=8.0, 2.2$ ), 5.23 (s, 4H), 3.98 (m, 4H), 3.82 (m, 4H), 1.58 (m, 8H), 1.45 (m, 4H).

$^{13}\text{C}$  NMR ( $\text{D}_2\text{O}$ ):  $\delta$  173.79, 154.37, 146.81, 146.25, 137.70, 123.16, 111.68, 110.09, 68.36, 57.92, 26.74, 21.04.

**5C DL**

$^1\text{H}$  NMR ( $\text{D}_2\text{O}$ , phosphate buffer):  $\delta$  7.04 (d, 4H,  $J=8.0$ ), 6.87 (d, 4H,  $J=2.2$ ), 6.30 (dd, 4H,  $J=8.0, 2.2$ ), 5.10 (s, 4H), 3.68 (m, 8H), 1.26 (m, 8H), 1.10 (m, 4H).

$^{13}\text{C}$  NMR ( $\text{D}_2\text{O}$ ):  $\delta$  171.95, 152.61, 145.00, 144.49, 136.09, 121.42, 110.26, 108.81, 66.94, 50.07, 24.62, 19.11.

**References for Chapter 2**

1. (a) For the importance of rigidity in host-guest systems, see: Cram, D.J. *Angew. Chem., Int. Ed. Engl.* **1986**, *25*, 1039-1134.  
(b) Gutsche, C.D. *Acc. Chem. Res.* **1983**, *16*, 161-170.  
(c) Gutsche, C.D. *Tetrahedron* **1983**, *39*, 409-426.
2. See references 9-11 in Chapter 1.
3. (a) Goodall, F.L.; Perkin, A.G. *J. Chem. Soc.* **1923**, 470-746.  
(b) Hall, J.; Perkin, A.G. *J. Chem. Soc.* **1923**, 2029-2037.
4. Sauer, J.; Wiest, H.; Mielert, A. *Chem. Ber.* **1964**, *97*, 3183-3207.
5. (a) Corey, E.J.; Venkateswarlu, A. *J. Am. Chem. Soc.* **1972**, *94*, 6190-6191.  
(b) Lalonde, M.; Chan, J.H. *Synthesis* **1985**, 817-845.
6. (a) van Keulen, B.; Kellogg, R.M.; Piepers, O. *J. Chem. Soc., Chem. Comm.* **1979**, 285-286.  
(b) Illuminati, G.; Mandolini, L. *Acc. Chem. Res.* **1981**, *14*, 95-102.
7. Shepodd, T.J., Ph.D. Thesis, California Institute of Technology, 1988.
8. (a) Ciganek, E. *J. Am. Chem. Soc.* **1966**, *88*, 2882-2883.  
(b) Rabideau, P.; Hamilton, J.B.; Friedman, L. *J. Am. Chem. Soc.* **1968**, *90*, 4465-4466.  
(c) Zimmerman, H.E.; Grunewald, G.L. *J. Am. Chem. Soc.* **1966**, *88*, 183-184.
9. (a) Masek, B.B.; Santarsiero, B.D.; Dougherty, D.A. *J. Am. Chem. Soc.* **1987**, *109*, 4373-4379.  
(b) Chang, M.H.; Masek, B.B.; Dougherty, D.A. *J. Am. Chem. Soc.* **1985**, *107*, 1124-1133.
10. (a) Fendler, E.J.; Constien, V.G.; Fendler, J.H. *J. Phys. Chem.* **1975**, *79*, 917-926.

(b) Mukerjee, P.; Mysels, K.J. *Natl. Stand. Ref. Data. Ser., Natl. Bur. Stand. No. 36*, 1971.

11. Diederich, F.; Dick, K. *Tetrahedron Lett.* 1982, 23, 3167-3170.
12. Still, W.C.; Kahn, M.; Mitra, A. *J. Org. Chem.* 1978, 43, 2932-2925.

**Chapter 3**  
**Physical Studies: The Case of**  
**Adamantyltrimethylammonium Iodide**

## NMR Studies

One of the most useful and successful methods for studying the interaction between two molecules is NMR spectroscopy.<sup>1</sup> For the field of host-guest chemistry, this technique is now emerging as a dominant one because it can provide geometry information on the host-guest complex;<sup>2</sup> in addition, the association constant ( $K_a$ ) and, under the proper circumstances, the forward and backward rate of reaction for complex formation can be measured. In the area of water-soluble receptor molecules,  $^1\text{H}$  NMR is now becoming a powerful tool for studying the binding event.<sup>3,4,5</sup>

The NMR method relies upon the change in the chemical shift of protons of the guest molecule when it is bound to the host receptor molecule. Three distinct domains are possible if a guest and a host were to interact (Figure 3.1). First, (Figure 3.1a) there could be no observable change in the chemical shift of the guest. This could be an indication of a weak or non-existent interaction between host and guest. Specifically, if the binding site of the host were lined with aromatic rings, the bound guest would reside near the shielding portion of the ring and would be expected to experience an upfield shift in its NMR resonance.

Second, (Figure 3.1b) upon addition of the host to a solution of the guest, two signals could appear. One signal would appear at the chemical shift of the free guest in the absence of host and one would appear upfield of this resonance and would be ascribable to the host-guest complex. This situation is the slow-exchange limit, where free guest in solution is exchanging places with the guest bound in the host at a rate that is slow relative to the NMR timescale. Integration of the areas of the peaks for free and bound guest along with the knowledge of all the initial concentrations of the host and the guest is sufficient to provide a determination of an

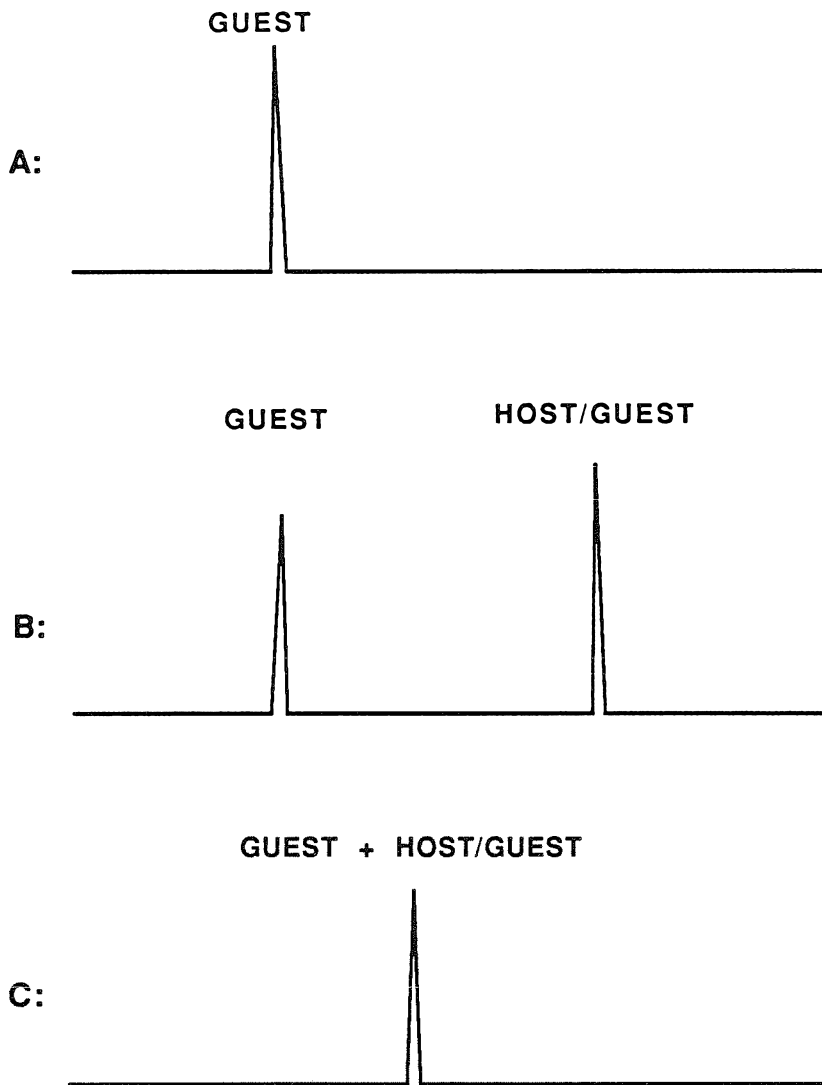


**FIGURE 3.1:** Three distinct domains that can occur when studying host-guest interactions by  $^1\text{H}$ NMR spectroscopy

association constant ( $K_a$ ) for the process. This is the ideal result and is not easily achieved with most systems. With the assumption of the forward reaction rate constant ( $k_{on}$ ) being close to the diffusion-controlled limit, the observation of resonances for free and bound guests requires that the process have a large binding constant.

Third, (Figure 3.1c) upon addition of the host to the guest, the observed guest signal could move upfield of the free position. However, now there is no signal for free guest. Furthermore, the position of the signal is concentration-dependent, whereas in the slow-exchange limit only the relative peak areas, not their respective positions change with concentration. If these situations obtain, then the experiment is in the fast-exchange limit, where the free guest and bound guest are exchanging places rapidly on the NMR timescale. In the fast exchange limit, the observed peak is a weighted average of the free and bound peaks, weighted in the respective proportions as determined by  $K_a$ .

The deconvolution of a fast-exchange spectrum and the evaluation of the association constant for the process are not simple tasks. One solution to this problem is to perform a saturation-binding experiment. This experiment consists of successively adding host to a solution of the guest, until the time-averaged guest peak stops shifting upfield. At this point, the solution is "saturated" with all the guest present being bound within the host. This type of experiment is expected to be successful for those systems where high host concentrations are achievable in the absence of interfering aggregation phenomena.

Another method for deconvoluting the fast-exchange spectrum to obtain an association constant is to submit the data to an iterative computer-fitting procedure. Equation (1) gives the chemical shift of the system as a weighted average between free and bound guest. Equation (1) assumes a 1:1

binding model between host and guest.  $\delta_{OBS}$  is the chemical shift observed in the

$$\delta_{OBS} = \delta_{HG}P_B + \delta_G(1 - P_B) \quad (1)$$

experiment. Its position is a function of the association constant ( $K_a$ ) and the concentrations employed in the experiment.  $\delta_{HG}$  is the chemical shift of the host-guest complex. It is an unknown in equation (1) and is observable only in the slow-exchange limit or in a saturation binding experiment.  $P_B$  is the percent of the guest that is bound in the experiment; it also is an unknown in the experiment.  $\delta_G$  is the chemical shift of the guest in absence of the host; this quantity is known from an NMR experiment of the guest without host. Thus, equation (1) represents an equation of two unknowns ( $\delta_{HG}$  and  $P_B$ ) with one observable ( $\delta_{OBS}$ ).

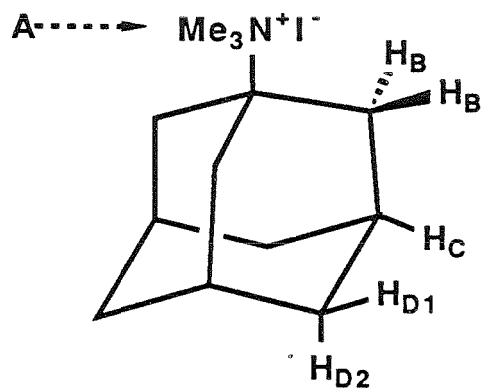
By conducting multiple experiments at differing host:guest ratios, numerous  $\delta_{obs}$  can be measured. A unique value of  $\delta_{HG}$  and  $K_a$  can be obtained that fits all the data by using a non-linear least-squares fitting procedure. From this computer-evaluation of the data, an association constant ( $K_a$ ) and  $\delta_{HG}$ , the chemical shift of the host-guest complex, are extracted. Therefore, in addition to the association constant, the NMR spectrum of the host-guest complex can be constructed, thereby providing potential geometry information on the complex. By reporting the maximum upfield shift,  $D$ , which is simply  $\delta_G - \delta_{HG}$ , rather than the chemical shift of the host-guest complex,  $\delta_{HG}$ , we feel that the data will be more comprehensible to the reader and more easily interpreted when making comparisons.

## The Case of ATMA

One of the first molecules that we chose to study by the NMR method was adamantyltrimethylammonium iodide (ATMA).<sup>5</sup> In contrast to earlier work by Diederich,<sup>3a</sup> we chose to study an aliphatic guest with a polycyclic framework. CPK model-building studies indicated that our host cavity was of the proper size to encapsulate an adamantyl derivative. This complementarity of fit led us to believe that a water-soluble adamantyl derivative would bind efficiently to our hosts. We chose the amine derivative, ATMA (see Figure 3.2) because it was easily prepared from the commercially available amine hydrochloride, it was quite water-soluble, and its high symmetry ( $C_{3v}$ ) made it amenable to low concentration  $^1\text{H}$  NMR studies.

We reasoned that if ATMA were to bind to our host molecules, its protons should experience shielding from the aromatic rings of the host. We hoped that the pattern of upfield shifts emerging from such an experiment would provide us with some information on the geometry of the host-guest complex. ATMA has five types of protons, labelled A, B, C, D<sub>1</sub> and D<sub>2</sub> in Figure 3.2. The cylindrical shape of ATMA places its protons in unique positions relative to each other. The A protons and B protons each form a ring that is perpendicular to the C<sub>3</sub> axis of ATMA. Protons C and D<sub>1</sub>, although they are different types of protons, form a third cylindrical ring of protons. Finally, the D<sub>2</sub> protons don't form such a cylindrical ring; they point parallel to the C<sub>3</sub> axis of ATMA.

Figure 3.2 shows a representation of a CPK model of ATMA. A reasonable binding orientation for ATMA to assume within the cavity of the host is one in which the C<sub>3</sub> axis of ATMA is parallel to the etheno bridges of the host. If such an orientation were to result, the "ring" protons of ATMA (A, B, C + D<sub>1</sub>) should be shifted upfield, whereas, the D<sub>2</sub> protons should not



ATMA

Adamantyltrimethylammonium iodide

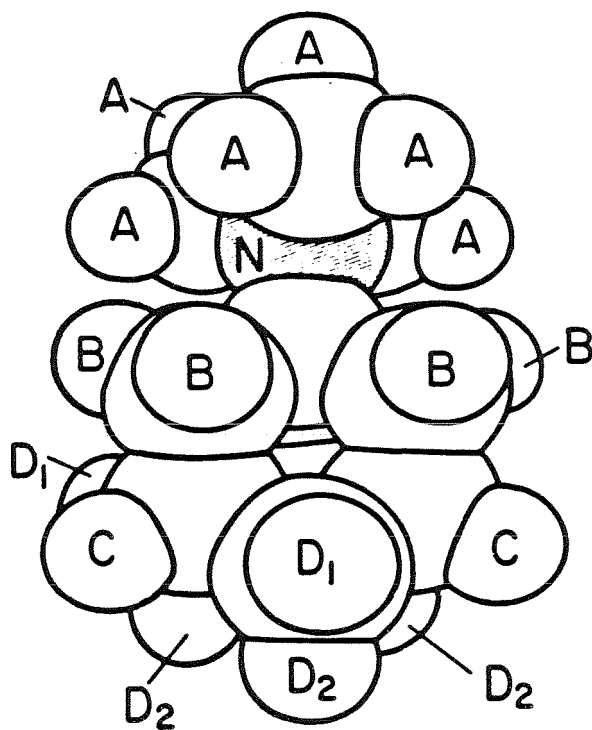


FIGURE 3.2: Adamantyltrimethylammonium iodide (ATMA), stick and CPK drawing

experience much shielding. The relative ordering of the shielding of the "ring" protons will depend upon the depth of penetration of ATMA within the binding site. If the nitrogen end of the molecule preferred to interact with the water, then perhaps the shielding pattern would be  $C \approx D_1 < B < < A$ ; however, other possible orderings are imaginable.

Table 3.1 shows the results of the study of the interaction of ATMA with our hosts.<sup>6</sup> The data for the polymethylene-linked macrocycles immediately allow the previously described binding orientation to be ruled out. For the 4C isomers, all the protons are shifted approximately the same amount; for the 5C isomers, some preference for the nitrogen end of the molecule to be bound within the hydrophobic cavity of the host is observed. Most importantly, for the aliphatic-linked macrocycles, the  $D_2$  protons of ATMA are substantially shielded. These results suggest that these hosts do not bind ATMA in the expected orientations. The hosts are quite flexible and could collapse to another perhaps cleft-shaped conformation which does not orient ATMA in a specific manner.

The data also indicate that a trimethylammonium group prefers to reside within the cavity of our host rather than in the surrounding water. Furthermore, these association constants are some of the largest ever measured for an aliphatic guest. The ability to bind ATMA is quite different than the ability to bind a polycyclic aromatic hydrocarbon.<sup>3c</sup> While these hydrocarbons are very insoluble in aqueous solution and not surprisingly do bind to a hydrophobic receptor molecule, ATMA is very water-soluble, yet it still prefers to reside in the binding site -- with the methyl groups attached to the positively charged nitrogen atom being the most shielded in some cases.

**Table 3.1:**  $K_a$  and D values for binding of ATMA to several hosts

ATMA DATA <sup>a</sup>						
Host	$D_A$	$D_B$	$D_C$	$D_{D1}$	$D_{D2}$	$K_a M^{(-1)}$ <sup>b</sup>
<b>4CMeso<sup>c</sup></b>	0.91	1.02	0.99	1.09	1.10	7500
<b>4CDL<sup>c</sup></b>	0.75	0.65	0.60	0.80	0.90	1300
<b>5CMeso<sup>c</sup></b>	2.51	2.84	0.96	1.10	0.97	2500
<b>5CDL<sup>c</sup></b>	2.44	2.80	1.43	1.52	1.33	1800
<b>PDL<sup>c</sup></b>	1.85	2.90	1.19	1.30	0.76	120000
<b>C6-L<sup>d</sup></b>	1.25	2.64	0.92	1.02	0.41	9500
<b>5CDL<sup>d</sup></b>	1.41	1.58	0.89	0.93	0.89	8100
<b>PDL<sup>d</sup></b>	1.80	2.90	1.20	1.30	0.70	92000

a)  $D = \delta_G - \delta_{HG}$  in ppm;  $D > 0$  indicates an upfield shift.

b) Average of the  $K_a$  for each proton.

c) In phosphate buffer,  $pD \approx 7.5$ .

d) In borate-D buffer.

If flexibility in the hosts is the cause of the random-type binding orientation, then by modifying the hosts with rigid linkers the expected binding orientation could be enforced. Furthermore, if the binding site is rigid then an increase in  $K_a$  could be expected.<sup>7,8</sup> This change in binding geometry and increase in  $K_a$  are observed when the linkers of the host are *p*-xylyl groups.<sup>5</sup> However, the increase in binding affinity is not due to the rigidity factor.

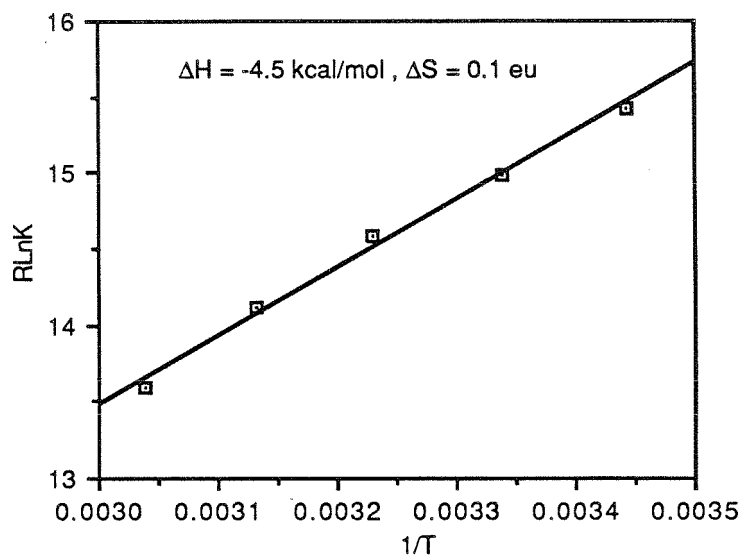
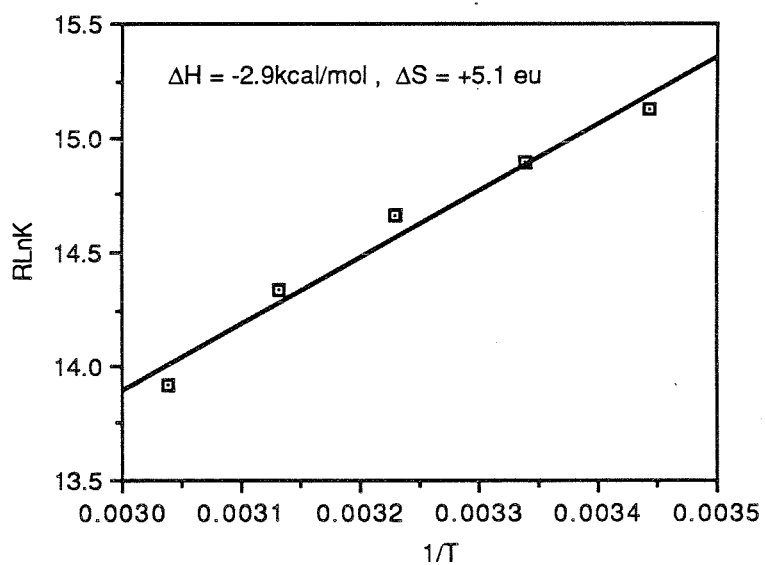
The idealized geometry of binding that the *p*-xylyl-linked host (**PDL**) displays with ATMA is also displayed by a *trans*-1,4-dimethylenecyclohexyl-linked host (**C6-L**). The data of Table 3.1 clearly demonstrate that these two similar hosts bind ATMA in the same geometry. Thus, the rigidity of the linker group (*p*-xylyl or *trans*-1,4-dimethylenecyclohexyl versus polymethylene) is the factor governing the host geometry upon binding. However, in this case,  $K_a$  seems not to be very rigidity-dependent. In fact, the ordered binding of ATMA by **C6-L** and the cleft-type binding typified by **5CDL** are of the same magnitude, in borate-D buffer. The enhanced binding affinity ( $\approx$  an order of magnitude) that **PDL** has for ATMA relative to **C6-L** is *not* a result of rigidity. Rather, there appears to be some special attraction of this guest for **PDL**.

### Variable Temperature Studies

We have also attempted to measure the enthalpy and entropy of reaction for ATMA and some of the hosts by examining the temperature dependence of the binding constant. Table 3.2 shows the binding constants for ATMA and *meso* hosts **4C** and **5C** as a function of temperature.<sup>9</sup> The thermodynamic parameters were determined from the van't Hoff plots shown in Figure 3.3.

**Table 3.2:** Temperature dependence of the association constant for ATMA with 4C and 5CMeso hosts

Host		
Temp (K)	4CMeso $K_a$	5CMeso $K_a$
290.5	2351	2027
299.6	1890	1804
309.7	1549	1599
319.4	1222	1357
329.0	934	1104

**4CMESO + ATMA---VT Data****5CMESO + ATMA---VT Data****FIGURE 3.3:** Variable temperature ATMA data

While the data span a small range of free energy, the trend in the data is clear. The decrease in  $K_a$  as the temperature increases implies that the enthalpy of reaction is negative. Furthermore, the entropy of reaction for this binding event is small and greater than zero.

The observed negative enthalpy of reaction for ATMA and our hosts is unexpected if the process is one of hydrophobic binding. The hydrophobic effect for aliphatic hydrocarbons has been studied<sup>10</sup> and the enthalpy change for the transfer of a hydrocarbon from water to pure liquid hydrocarbon is positive. The effect diminishes as the size of the hydrocarbon increases; interestingly, the transfer of aromatic hydrocarbons from water to pure liquid aromatic hydrocarbon is enthalpically favorable.

The understanding of this negative  $\Delta H$  for the binding event may not be trivial. Both the solvation of the host-guest complex and the desolvation of the host cavity and guest must be considered. If the cavity of the host is considered to be an aromatic hydrocarbon which, as a result of the binding of ATMA, is transferred from an aqueous to a hydrophobic environment, then the observed  $\Delta H_{\text{rxn}}$  can be rationalized. However, this neglects the desolvation of the guest and any possible ionic and/or van der Waals interaction between the host and guest.

The entropy of reaction is the interesting number in this study. Reactions of the type shown in equation 2, typically are entropically unfavorable because of the



increase in the order of the system that results when two molecules combine to form one. As a benchmark, the dimerization of formic acid in the gas phase<sup>11</sup>

has  $\Delta S_{\text{rxn}} = -36$  eu and the dimerization of  $\text{NO}_2$  to  $\text{N}_2\text{O}_4$  has  $\Delta S_{\text{rxn}} = -43$  eu.<sup>12</sup>

No reports of the thermodynamic parameters of reaction for the binding of a guest to a synthetic water-soluble host have appeared in the literature. The values for a host-guest type of association in organic solvents have been reported.<sup>13,14</sup> For the binding of an organic molecule to a synthetic host in *organic* solvents, the entropy change of reaction was  $\approx -14$  eu. This number again reflects the organization necessary to bring two molecules together.

If the binding phenomenon is hydrophobic in nature, then the entropy term is expected to favor the formation of the complex. The transfer of a hydrocarbon from water to pure hydrocarbon is entropically favorable.<sup>10</sup> The origin of this effect is thought to reside in the highly ordered water that surrounds the hydrocarbon in aqueous solution. Thus, desolvation releases this ordered water and an increase of entropy ensues.

Many workers have studied the binding of substrates to cyclodextrins<sup>15</sup> and have reported the thermodynamic parameters for these association processes. For the binding of aromatic compounds to cyclodextrins,<sup>15</sup> the reactions are enthalpically driven. In contrast to the classical hydrophobic effect, the vast majority of the guests studied are not entropically driven to bind to the cyclodextrin cavity. The few examples that are entropically driven show very little enthalpic driving force for binding (see Table 3.3). This compensation effect has been interpreted as an indication that water molecules are participating in the complex formation.<sup>15</sup>

With relevance to the current work, the binding of adamantyl derivatives to cyclodextrins has received some attention.<sup>16</sup> Both adamantyl amine and its hydrochloride salt bind to cyclodextrins, and the

**Table 3.3:** Thermodynamic parameters ( $\Delta H$  and  $\Delta S$ ) for the binding of aromatic guests to cyclodextrins

Guest	Cyclo-dextrin	$\Delta H$ (kcal/mol) <sup>a</sup>	$\Delta S$ (eu) <sup>a</sup>
<i>p</i> -Nitrophenol	$\alpha$	-4.2	-2.8
<i>p</i> -Nitrophenolate	$\alpha$	-7.2	-8.7
Benzoic Acid	$\alpha$	-9.6	-18.0
4-Aminobenzoic Acid	$\alpha$	-11.6	-26.0
2-Aminobenzoic Acid	$\alpha$	-0.3	21.0
<i>m</i> -Chlorophenyl acetate	$\beta$	-1.0	8.0
<i>m</i> -Ethylphenyl acetate	$\beta$	-4.6	-3.0
Benzoyl acetic acid	$\beta$	-5.7	-8.6

a) Data taken from ref. 15.

thermodynamic parameters have been measured.<sup>16a</sup> Furthermore, the binding of adamantyl carboxylic acid has also been examined.<sup>16b</sup> Table 3.4 lists the thermodynamic parameters that were measured in these studies.

For all of the adamantyl guests studied, when bound to both  $\alpha$ - and  $\beta$ -cyclodextrin, the enthalpy of binding ( $\Delta H_B$ ) is negative, whereas the entropy of binding ( $\Delta S_B$ ) is generally small and negative. It is difficult to generalize the entropy effects because of the uncertainties in the data; nevertheless, the observation of large negative enthalpies of reaction and small negligible entropies implies that these interactions display a "non-classical hydrophobic effect."<sup>17</sup> These data<sup>16</sup> have been interpreted in this light and some useful concepts were delineated.

Dissection of the thermodynamic parameters<sup>16c</sup> leads to two contributing components to the observed free energy of binding ( $\Delta G_B$ ). These components are an intrinsic binding component and a hydrophobic component. The intrinsic binding component is characterized by a large favorable enthalpy change ( $\Delta H_I$ ) and an unfavorable entropy change ( $\Delta S_I$ ). This pattern of thermodynamic parameters is consistent with this intrinsic binding component being a van der Waals type of interaction.<sup>16c</sup> A van der Waals interaction between two molecules would be expected to be enthalpically favorable, yet, because of the bimolecularity of the process, entropically unfavorable. The hydrophobic component to the observed binding is characterized by a small, unfavorable enthalpy change ( $\Delta H_H$ ) upon binding coupled with a large favorable entropic change ( $\Delta S_H$ ).<sup>16a,c</sup> This pattern is consistent with the traditional hydrophobic effect.<sup>10,17</sup>

The thermodynamic parameters for  $\alpha$ - and  $\beta$ -cyclodextrin with all the adamantyl derivatives (except A-NH<sub>3</sub><sup>+</sup>) show a similar pattern. A reduction in the size of the cavity leads to a more unfavorable enthalpy of binding and a

**Table 3.4:** Thermodynamic parameters ( $\Delta H$  and  $\Delta S$ ) for the complex formation between cyclodextrins and adamantyl derivatives

Guest <sup>a</sup>	Cyclo-dextrin	$\Delta H$ (kcal/mol) <sup>b</sup>	$\Delta S$ (eu) <sup>b</sup>
A-NH <sub>2</sub>	$\alpha$	-4.84	-5.1
	$\beta$	-6.92	0.1
A-NH <sub>3</sub> <sup>+</sup>	$\alpha$	-3.66	-4.5
	$\beta$	-6.65	-4.4
A-CO <sub>2</sub> H	$\alpha$	-3.2	-1.0
	$\beta$	-7.53	-0.1
	$\gamma$	-0.1	22.0
A-CO <sub>2</sub> <sup>-</sup>	$\alpha$	-3.22	-0.3
	$\beta$	-4.85	3.4
	$\gamma$	1.20	20.2

a) A = adamantyl

b) Data taken from reference 16.

more unfavorable entropy of binding. These results have been interpreted to mean<sup>16b</sup> that the adamantyl ring cannot bind deeply within the smaller cavity. Consequently, less van der Waals interactions are possible (a decrease in  $-\Delta H_B$  is observed) and less hydrophobic interactions are possible (a more unfavorable  $\Delta S_B$  is observed). CPK models support the poor fit of an adamantyl skeleton to  $\alpha$ -cyclodextrin, while  $\beta$ -cyclodextrin encompasses an adamantyl skeleton quite snugly.

The most interesting results are observed with  $\gamma$ -cyclodextrin and the adamantane carboxylate derivatives. For both the free acid and the anion, weak enthalpic and strong entropic binding interactions are observed in agreement with the accepted hydrophobic effect. The authors<sup>16a</sup> suggest that the exothermic van der Waals effect observed with the other cyclodextrins are absent in the  $\gamma$ -isomer because of the large cavity size. Therefore, in this instance, hydrophobic binding is observed; the adamantyl skeleton does not fit tightly into the cavity, and the critical distance needed for the van der Waals effect to operate cannot be attained. Unlike the  $\beta$ -isomer, the  $\gamma$ -isomer cannot tightly encapsulate the guest and maximize the van der Waals interactions. These results underscore the delicate balance between van der Waals and hydrophobic interactions. Nevertheless, the authors conclude that the size of the cavity and their complementarity of fit correlate well with the observed free energy change.

Our data concerning the binding of ATMA to our macrocyclic hosts also display a "non-classical hydrophobic effect." It is therefore obvious that van der Waals interactions are an important component to the observed binding event. A comparison of the enthalpies and entropies of binding as a function of cavity size does not parallel the pattern observed with the cyclodextrin and the adamantyl derivatives. If the *4CMESO/5CMESO* couple

is analogous to  $\alpha$ -/ $\beta$ -cyclodextrin, then the trend in  $\Delta S_B$  is consistent but the trend in  $\Delta H_B$  is not. If more van der Waals interactions are present in the **5CMESO** isomer, then a larger  $\Delta H_B$  is expected. In fact, the opposite is observed. This turnaround could be rationalized by assuming that a change in conformation of **5CMESO** precedes binding. Such a conformational event would cost enthalpy and thus would reduce the observed enthalpy of binding. This, in fact, may be the case (see Chapter 4); however, at this time it is only a rationalization of the data.<sup>18</sup>

The rather limited range of free energy over which the experiments were conducted limits a differentiation between these hosts. A conservative error of 250 cal/mol in the measured free energy of binding causes these measured enthalpies and entropies to be indistinguishable from each other. In addition, the poorer quality of **5CMESO** data relative to the **4CMESO** data does not allow a fine distinction to be made between these data sets. Nevertheless, the thermodynamic parameters that we have measured follow the "non-classical hydrophobic effect" in a manner reminiscent of the cyclodextrins with adamantyl guests.

**References for Chapter 3**

1. Forster, R.; Fyfe, C.A. *Prog. Nucl. Magn. Reson. Spectrosc.* 1969, 4, 1-89.
2. (a) Jarvi, E.T.; Whitlock, H.W. *J. Am. Chem. Soc.* 1982, 104, 7196-7204.  
(b) Whitlock, B.J.; Whitlock, H.W. *J. Am. Chem. Soc.* 1983, 105, 838-844.  
(c) Adams, S.P.; Whitlock, H.W., Jr. *J. Org. Chem.* 1981, 46, 3474-3478.  
(d) Jarvi, E.T.; Whitlock H.W., Jr. *J. Am. Chem. Soc.* 1980, 102, 657-662.
3. (a) Diederich, F.; Griebel, D. *J. Am. Chem. Soc.* 1984, 106, 8024-8036.  
(b) Diederich, F.; Dick, K. *Chem. Ber.* 1985, 118, 3817-3829.
4. (a) Takahashi, I.; Odashima, K.; Koga, K. *Tetrahedron Lett.* 1984, 25, 973-976.  
(b) Odashima, K.; Itai, A.; Iitaka, Y.; Arata, Y.; Koga, K. *Tetrahedron Lett.* 1980, 21, 4347-4350.
5. Shepodd, T.J.; Petti, M.A.; Dougherty, D.A. *J. Am. Chem. Soc.* 1986, 108, 6085-6087.
6. The concentrations of the stock host solutions, in 10 mM cesium phosphate buffer ( $D_2O$ ,  $pD \approx 7.5$ ), were determined by integration against four internal standards. All NMR spectra were obtained under fast-exchange conditions on a JEOL GX400 spectrometer with all chemical shifts being relative to external DSS. All NMR experiments were performed significantly below the  $cmc$ 's of these hosts. The host-guest ratio varied from 2:1 to 1:4 with typical  $[host] = 40-500 \mu M$  and  $[guest] = 100-800 \mu M$ . The ATMA reference spectrum

was recorded at 450  $\mu\text{M}$  in  $\text{D}_2\text{O}$ . Control studies with cesium maleate and ATMA or the "half-molecule" (2,6-diethoxy-9,10-dihydro-9,10-(1,2-dicarboxy)-ethenoanthracene, dicesium salt) and ATMA were performed. In each case only very small ATMA shifts were seen, which were attributable to ionic interactions.

7. See, for example: Cram, D.J. *Angew. Chem., Int. Ed. Engl.* **1986**, *25*, 1039-1134.
8. Breslow, R. *Isr. J. Chem.* **1979**, *18*, 187-191.
9. These association constants were determined using a multifit program where the data for all the protons of the guest are fitted to one  $K_a$  that best fits all the data (R.E. Barrans, Jr., unpublished results). Furthermore, the difference in the  $K_a$ s to those in Table 3.1 reflect the fact that the temperature-dependent  $K_a$ s were determined in a pH = 9.5-10 phosphate buffer. Furthermore, the ionic strength of the buffer differed from the pH = 7.5 phosphate buffer.
10. Tanford, C. *The Hydrophobic Effect*, 2nd ed.; Wiley: New York, 1980.
11. Green, J.H.S. *J. Chem. Soc.* **1961**, 2241-2242.
12. Woods, T.L.; Garrels, R.M. *Thermodynamic Values at Low Temperatures for Natural Inorganic Materials*; Oxford:New York, 1987.
13. Cram, D.J.; Stewart, K.D.; Goldberg, I.; Trueblood, K.N. *J. Am. Chem. Soc.* **1985**, *107*, 2574-2575.
14. Diederich, F.; Dick, K.; Griebel, D. *J. Am. Chem. Soc.* **1986**, *108*, 2273-2286.
15. Saenger, W. *Angew. Chem., Int. Ed. Engl.* **1980**, *19*, 344-362.

16. (a) Gelb, R.I.; Schwartz, L.M.; Laufer, D.A. *J. Chem. Soc., Perkin Trans. 2* 1984, 15-21.  
(b) Cromwell, W.C.; Byström, K.; Eftink, M.R. *J. Phys. Chem.* 1985, 89, 326-332.  
(c) Harrison, J.C.; Eftink, M.R. *Biopolymers* 1982, 21, 1153-1166.
17. Jencks, W.P. *Catalysis in Chemistry and Enzymology*; McGraw-Hill: New York, 1969.
18. Another possible explanation is that the **4CMESO/5CMESO** couple is analogous to the  $\beta$ -/ $\gamma$ -cyclodextrin results. The observed thermodynamic parameters are consistent with this analogy, although on a much smaller scale. If ATMA is not totally engulfed by the **5CMESO** host (much like  $\gamma$ -cyclodextrin), then a decrease in  $\Delta H$  and an increase in  $\Delta S$  should be observed. While this is the case, the change in the thermodynamic parameters is not nearly as dramatic as the change observed in the  $\beta$ -/ $\gamma$ -cyclodextrin couple. In addition, CPK models fail to support the assumed lack of fit of ATMA to the cavity of **5CMESO**.

Chapter 4

**Physical Studies: Substituted Ammonium Ions  
and Aromatic Heterocyclic Guests**

## Introduction

Subsequent to our study of adamantyltrimethylammonium iodide (ATMA), we set out to examine our hosts' abilities to bind other closely related guests. We have found the trimethylammonium substituent to be an effective NMR probe as well as an easy, convenient way to introduce water solubility. We have therefore chosen to study a series of substituted trimethylammonium salts of the general formula,  $R-N(CH_3)_3^+ X^-$ . By varying the guest and host structure, such parameters as the shape and size of both components involved in the molecular recognition event can be examined. Furthermore, we hoped to assess other factors such as the effect of counter-ion and the effect of charge on the binding event.

Table 4.1 displays the array of hosts and guests that have been examined in this study. The association constants were determined by the NMR method described previously (see Chapter 3). Figure 4.1 shows other structures used in these studies.

## Synthesis

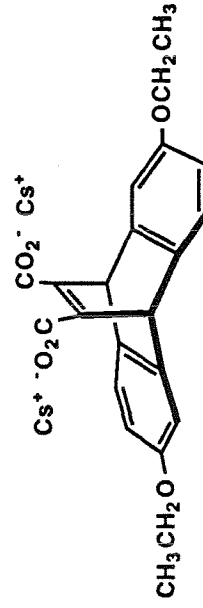
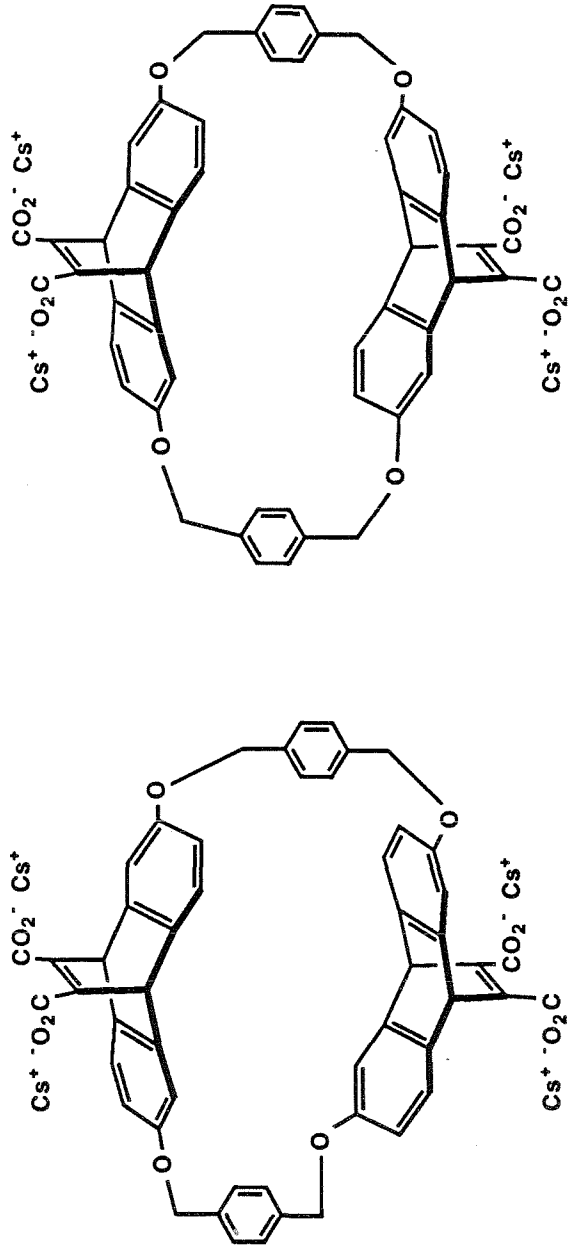
The guests used in this study were prepared from the commercially available amines (see Experimental Section). A new host, depicted in Scheme 4.1, was prepared. This *trans*-1,4-dimethylenecyclohexyl-linked host (**14**) was prepared in enantiomerically pure form from an enantiomerically pure precursor diol.<sup>1</sup> The macrocyclic ring closure was effected in a different manner than that used to synthesize the previously described hosts (**12a-c**). Attempts to cyclize the diol with the appropriate dibromide were unsuccessful; E<sub>2</sub> elimination was competing with the

**TABLE 4.1:** Grand table of Association constants

GUEST	HOST			
	<i>5CMESO</i>	<i>PMESO</i>	<i>5CDL</i>	<i>C6-L</i>
PhCH <sub>2</sub> N(CH <sub>3</sub> ) <sub>3</sub> <sup>+</sup> Br <sup>-</sup>	2.5 x 10 <sup>3</sup>	6.0 x 10 <sup>3</sup>	2.5 x 10 <sup>3</sup>	4.2 x 10 <sup>3</sup>
4-NO <sub>2</sub> PhCH <sub>2</sub> N(CH <sub>3</sub> ) <sub>3</sub> <sup>+</sup> I <sup>-</sup>	5.6 x 10 <sup>3</sup>	1.3 x 10 <sup>4</sup>	8.4 x 10 <sup>3</sup>	7.5 x 10 <sup>3</sup>
PhCH <sub>2</sub> N(CH <sub>3</sub> ) <sub>3</sub> <sup>+</sup> Cl <sup>-</sup>			2.0 x 10 <sup>3</sup>	
PhCH <sub>2</sub> NEt <sub>3</sub> <sup>+</sup> Br <sup>-</sup>	1.7 x 10 <sup>3</sup>	1.4 x 10 <sup>4</sup>		
C <sub>10</sub> H <sub>7</sub> CHCH <sub>3</sub> N(CH <sub>3</sub> ) <sub>3</sub> <sup>+</sup> I <sup>-</sup>	2.3 x 10 <sup>3</sup>	2.2 x 10 <sup>4</sup>		
PhN(CH <sub>3</sub> ) <sub>3</sub> <sup>+</sup> BF <sub>4</sub> <sup>-</sup>		5.5 x 10 <sup>3</sup>	2.5 x 10 <sup>3</sup>	
4- <sup>t</sup> BuPhN(CH <sub>3</sub> ) <sub>3</sub> <sup>+</sup> BF <sub>4</sub> <sup>-</sup>		1.6 x 10 <sup>4</sup>	1.5 x 10 <sup>4</sup>	
4-(CH <sub>3</sub> ) <sub>3</sub> NPhN(CH <sub>3</sub> ) <sub>3</sub> <sup>++</sup> 2BF <sub>4</sub> <sup>-</sup>		8.9 x 10 <sup>3</sup>	5.3 x 10 <sup>3</sup>	
C <sub>6</sub> H <sub>11</sub> N(CH <sub>3</sub> ) <sub>3</sub> <sup>+</sup> I <sup>-</sup>	2.9 x 10 <sup>3</sup>	1.2 x 10 <sup>4</sup>	4.3 x 10 <sup>3</sup>	small shifting observed
C <sub>10</sub> H <sub>7</sub> CH <sub>2</sub> N(CH <sub>3</sub> ) <sub>3</sub> <sup>+</sup> I <sup>-</sup>			1.8 x 10 <sup>4</sup>	1.4 x 10 <sup>4</sup>
(n-C <sub>4</sub> H <sub>9</sub> ) <sub>3</sub> NCH <sub>3</sub> <sup>+</sup> I <sup>-</sup>			1.4 x 10 <sup>3</sup>	small shifting observed
C <sub>10</sub> H <sub>15</sub> N(CH <sub>3</sub> ) <sub>3</sub> <sup>+</sup> I <sup>-</sup>			8.1 x 10 <sup>3</sup>	9.5 x 10 <sup>3</sup>
N(CH <sub>3</sub> ) <sub>3</sub> <sup>+</sup> OH <sup>-</sup>	2.8 x 10 <sup>2</sup>			

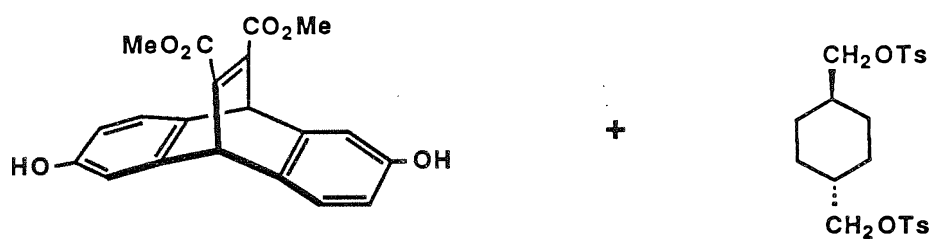
TABLE 4.1: continued

GUEST	HOST	
	5CDL	C6-L
Isoquinoline	$1.5 \times 10^3$	$4.6 \times 10^4$
<i>N</i> -Methylisoquinoline	$6.1 \times 10^3$	$2.7 \times 10^4$
1-Methylisoquinoline	$1.2 \times 10^3$	$1.0 \times 10^5$
Quinoline	$8.1 \times 10^2$	$2.2 \times 10^4$
<i>N</i> -Methylquinoline	$8.1 \times 10^3$	$4.7 \times 10^4$
4-Methylquinoline	$1.0 \times 10^3$	$3.0 \times 10^4$
2-Methylquinoline	$3.9 \times 10^2$	$2.0 \times 10^4$
Indole	small shifting observed	$1.6 \times 10^3$
<i>N</i> -Methylindole	small shifting observed	$3.8 \times 10^3$



17

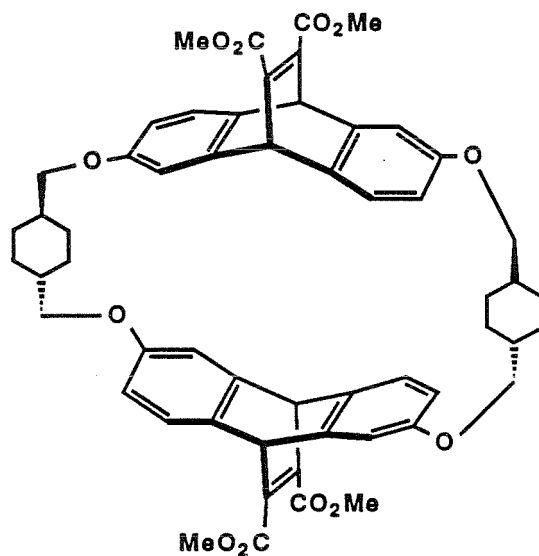
**FIGURE 4.1:** P-xylyl-linked hosts and half-molecule control



(+) - R,R

8

$\text{Cs}_2\text{CO}_3$ , DMF, 60°C,  
syringe pump addition



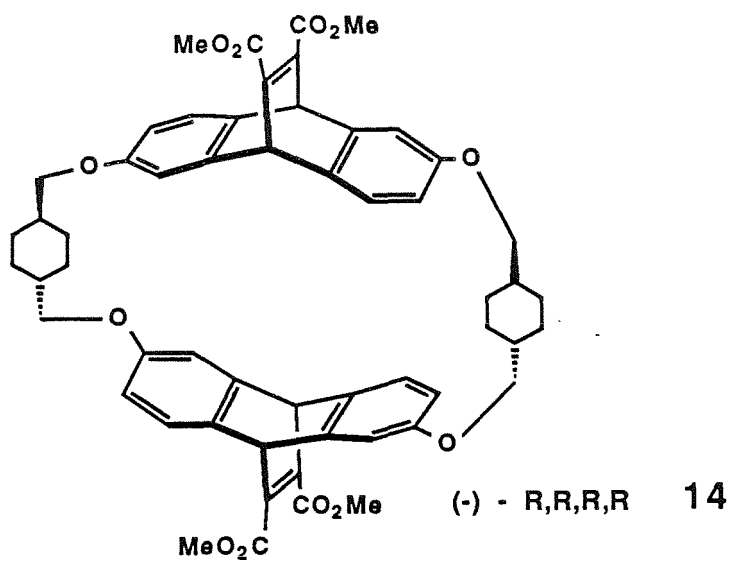
(-) - R,R,R,R

14

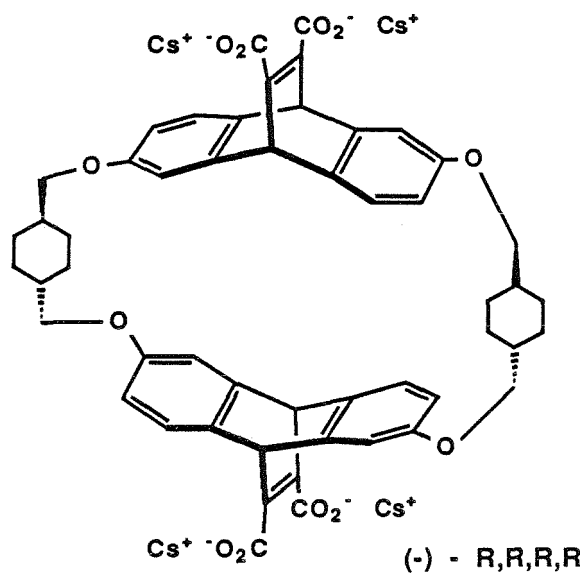
**SCHEME 4.1:** Synthetic scheme for cyclohexyl-linked host

macrocyclization, and products with exocyclic methylene groups were observed by  $^1\text{H}$  NMR. By switching to a ditosylate linker, the elimination pathway was not observed, and macrocyclization occurred, albeit in low yield. This macrocyclization is the slowest yet observed and may be due to the branching *beta* to the electrophilic carbon in the linker. Nevertheless, some material was available, and we hoped that this host would make an interesting comparison to the *p*-xylyl-linked hosts.<sup>1</sup> Hydrolysis proceeded as before (see Scheme 4.2) giving the tetra-cesium salt of the host (**C6-L**, **15**).

In an attempt to ascertain some structural information on these macrocycles, a difference NOE experiment was conducted. For **14** in  $\text{CDCl}_3$ , irradiation of  $\text{H}_3$  of the host (using the anthracene numbering system) led to a small but real enhancement of one of the two diastereotopic hydrogens of the methylene group  $\alpha$  to the ethereal oxygen of the *trans*-1,4-dimethylenecyclohexyl linker. Irradiation of the other aromatic hydrogens of **14** ( $\text{H}_1$  and  $\text{H}_4$ ) led to no such enhancement. This experiment suggests that the conformation about the aryl ether oxygen is relatively fixed, with one of the hydrogens of the  $\alpha$ -methylene group lying in-plane (or nearly in-plane) fairly close to  $\text{H}_3$ . Thus, the linker chain faces away (*trans*) from the bridgehead; this arrangement places the  $\alpha$ -carbon of the linker towards  $\text{C}_3$  and away from  $\text{C}_1$  of the ethenoanthracene unit. This experiment has also been successful with the *p*-xylyl-linked hosts;<sup>1</sup> this time, however, the enhancement is more significant because the signal is



CsOH, DMSO, H<sub>2</sub>O



SCHEME 4.2: Hydrolysis of cyclohexyl-linked host

not extensively *J*-coupled to adjacent hydrogens. For the aliphatic-linked macrocycles described in Chapter 2 (**12a-c**), the difference NOE experiment failed to give any convincing results. The extent to which this *trans* conformation exists for the tetra-cesium salts in aqueous solution remains to be seen; however, these experiments provide some data for future computational efforts on these systems.

### CMC Studies

CMC studies on the hosts **C6-L** and **5CDL** were attempted in the pH=9 borate-D buffer. The chemical shifts of the protons of **C6-L** were concentration-independent over the range 85-2030 $\mu$ M. However, at high concentrations, the peaks were broader and the *J*-couplings were not resolvable. As the concentration was lowered, the resonances of **C6-L** sharpened. Other studies from these laboratories<sup>1</sup> have indicated that the resolution of the fine *J*-coupling is not necessarily an indication of monodisperse host. In light of the fact that a structurally similar host (**P-D** or **L**) has a CMC of  $\approx$  250 $\mu$ M in this buffer, all binding studies on **C6-L** were performed at concentrations <150 $\mu$ M to avoid aggregation.

The chemical shifts of the protons of **5CDL** respond undramatically to changes in concentration. The lack of an obvious abrupt change in the chemical shift, analogous to that seen earlier (see Chapter 2), makes the assignment of a CMC difficult. To minimize aggregation effects, yet still achieve reasonable amounts of bound guest in the physical studies, all studies with **5CDL** were performed at concentrations < 250 $\mu$ M.

Other work from this laboratory<sup>1</sup> has shown that above the CMC,

random upfield shift patterns of the guest and poor fits of the data to the 1:1 binding model are observed. The lack of such behavior for the data on **C6-L** and **5CDL**, while not evidence against aggregation, lessens the suspicion that aggregation effects are present. If aggregation is occurring, its effect is not as significant as has been previously observed.

### Background

Previous binding studies with synthetic hydrophobic receptor molecules have focused upon anionic guests because the hosts used cationic water-solubilizing groups (see Chapter 1). The interaction of a host and guest bearing like charges has been assumed to be weak because of charge-charge repulsions. Nevertheless, Diederich and Dick<sup>2</sup> have studied the interactions of cationic guests with their cationic host **5** (see Chapter 1).

The observed  $K_a$  values for the cationic guests were far less than those observed with analogous anionic guests. Cationic guests displayed less affinity for the binding site of **5**, relative to their neutral precursors. Specifically, a decrease in  $K_a$  by a factor of  $\approx 10$  was observed with *N,N,N',N'*-tetramethylbenzidine upon changing the acidity of the solution from pH=11 to pH=1.2. The same change in pH with the guest 1,5-bis(dimethylamino)naphthalene resulted in no complexation ( $K_a < 10M^{-1}$ ) in acidic solution! This represented a drop in  $K_a$  by three orders of magnitude and was not explainable by the authors.<sup>2</sup> Interestingly, the change in  $K_a$  was less than a factor of 7 upon quaternization: 1-

dimethylaminonaphthalene forms a complex with **5** having a  $K_a=9300\text{M}^{-1}$ , while 1-trimethylammoniumnaphthalene forms a complex having a  $K_a = 1700\text{M}^{-1}$ . The association of 1-dimethylaminonaphthalene to **5** at  $\text{pH}=1.2$  was not reported. Importantly, in all these studies, the naphthalene moiety was included within the cavity of **5** in preference to the appended substituents. The authors concluded that the substituents were oriented towards the aqueous medium, based upon the small upfield shifts observed for these groups when the guests were bound to **5**.

More recently,<sup>3</sup> in a manner similar to the studies to be presented in this chapter, the association of cationic guests to synthetic hydrophobic hosts having anionic solubilizing groups has been examined. Dhaenens *et al.*<sup>4</sup> and Vögtle *et al.*<sup>3b</sup> have prepared diphenylmethane-based macrocyclic hosts, which have carboxylate groups around the binding site. The observed binding of cationic guests, including TMA derivatives, is mainly a result of electrostatic interactions. The lack of a rigid macrocyclic framework allows the carboxylates in these structures to form close contacts easily with the cationic guests resulting in very favorable electrostatic interactions.

Dhaenens *et al.*<sup>4</sup> have observed in their system that bis TMA derivatives have higher binding affinities than mono TMA derivatives. However,  $K_a$  varied little upon changing the substituent R in the TMA derivatives,  $\text{R-N}(\text{CH}_3)_3^+ \text{X}^-$ . This system also displayed a similar lack of

discrimination in  $K_a$  with several bis TMA derivatives. Changing the TMA group to an ammonium group led to stronger association because of increased hydrogen bonding and electrostatic effects.

These results indicate that the effect here is solely electrostatic in nature. Particularly compelling is the fact that tetramethylammonium, benzyltrimethylammonium and acetylcholine(2-acetoxyethyltrimethylammonium) bind the same within the reported experimental error ( $\pm 0.2$  in  $\log K_a$ ). If hydrophobicity were playing a major role, then some variation in  $K_a$  would be expected.

The results of Vögtle *et al.*<sup>3b</sup> are far from compelling. The authors correlate association constants with observed upfield shifts. Furthermore, on the basis of this limited data (three NMR experiments), conclusions on the fit of the guest to the cavity of the host are drawn. Without knowledge of CMC effects, association constants, control studies and more experimental detail, the results are simply preliminary and highly qualitative.

### **Effect of Charge**

The use of a trimethylammonium substituent (TMA) in the guests used for these studies was one of convenience. However, this group is quite often directed into the interior of the macrocycle, rather than exposed to the aqueous environment.<sup>5</sup> The fact that the TMA group is buried in the hydrophobic binding site of our hosts could be ascribed to two effects. First, the TMA group is hydrophobic and prefers the binding site to water; or second, our host system, with four external carboxylates, generates a large

negative field, the center of which is the energetically most favorable place for a cation to reside.

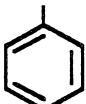
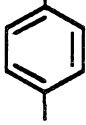
Ascribing the observed binding of these substituted TMA derivatives solely to one of these effects will be difficult, and it is possible that both these effects are operating. The thought that a charged TMA group is hydrophobic may not be as contradictory as it would seem.<sup>6</sup> A charged group, such as a carboxylate ( $\text{RCO}_2^-$ ) or an ammonium ion ( $\text{RNH}_3^+$ ), is far more hydrophilic than a TMA group ( $\text{RN}(\text{CH}_3)_3^+$ ). This hydrophilicity is undoubtedly due to the stronger solvation of a carboxylate or an ammonium ion by water. In addition to the ion-dipole interaction, there is an added hydrogen-bonding interaction of these groups with the water.<sup>6,7</sup> Desolvation of such charged species must disrupt the hydrogen bonds; therefore, these charged species are very hydrophilic. A TMA on the other hand, lacks these hydrogen-bonding interactions (yet still has the ion-dipole interaction). Desolvation of this structure would not be as energetically expensive as it would be for the analogous ammonium ion. Thus, a TMA would be more hydrophobic.

One might argue that the observed binding of our hosts to the TMA derivatives is simply a consequence of the charge. While it is true that, for most of the simple TMA derivatives that we have studied, the TMA group is recognized by the binding site and buried therein, the observed trends in  $K_a$  (see Table 4.1) suggest that the substituent that is attached to the TMA plays an important role in the observed molecular recognition.

In an attempt to address the charge issue, we studied the guests shown in Table 4.2. These guests are all simple substituted benzenes; by adding a substituent and observing a change in  $K_a$  we wanted to assess that substituent's hydrophobicity. Thus, for both hosts **5CDL** and **PMESO**, *p-tert*-butylphenyltrimethylammonium was more tightly bound than phenyltrimethylammonium. The addition of a *tert*-butyl group enhances both the hydrophobicity of the molecule and its  $K_a$ . The addition of a TMA group (phenyltrimethylammonium versus 1,4-bis(trimethylammonium)-phenyl) also led to a higher  $K_a$ ; therefore, a TMA group would appear to enhance binding. This effect is especially significant, considering that the addition of a TMA group also greatly increases the water solubility of the molecule.

Perhaps the most interesting comparison is between the TMA-substituted and the *tert*-butyl-substituted derivatives. Here, the issue of charge is being addressed. If the binding is governed by the charge, then the doubly charged 1,4-bis(trimethylammonium)phenyl should bind better than the singly charged *p-tert*-butylphenyltrimethylammonium. If hydrophobicity were the only factor behind the observed trends in  $K_a$  for these phenyl-substituted TMA derivatives, then the very water-soluble 1,4-bis(trimethylammonium)phenyl should bind significantly less than *p-tert*-butylphenyltrimethylammonium. Both these molecules have the same shape and size; thus, the trends in the data cannot be ascribed to a difference in the fit of these guests to the cavity of the hosts.

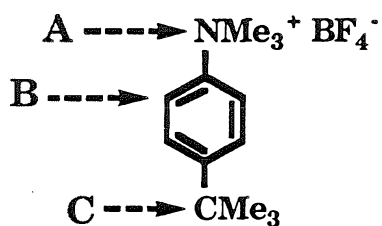
TABLE 4.2: Effect of charge on  $K_a$ 

GUEST	HOST	
	<i>5CDL</i>	<i>PMESO</i>
$\text{NMe}_3^+ \text{BF}_4^-$ 	$2.5 \times 10^3$	$5.5 \times 10^3$
$\text{CMe}_3$  $\text{NMe}_3^+ \text{BF}_4^-$	$1.5 \times 10^4$	$1.6 \times 10^4$
$\text{NMe}_3^+ \text{BF}_4^-$  $\text{NMe}_3^+ \text{BF}_4^-$	$5.3 \times 10^3$	$8.9 \times 10^3$

These results for **5CDL** suggest that a *tert*-butyl group is more hydrophobic than a TMA and that for this host, hydrophobicity plays some role in the observed binding. However, the fact that 1,4-bis(trimethylammonium)phenyl and *p-tert*-butylphenyltrimethylammonium bind about the same to **PMESO** may suggest that charge is important in the interactions of these guests with **PMESO**. Unfortunately, the change of a carbon for a nitrogen not only added a charge to the molecule but also increased its water solubility. The deconvolution of these effects is difficult, but the data suggest that both effects are operating to differing degrees in these systems.

Interestingly, it is not necessarily the most hydrophobic group that is buried within the cavity of the host. In fact, for *p-tert*-butylphenyltrimethylammonium and both hosts, the geometry of the host-guest complex is one where the TMA end of the molecule is the most shielded by the host. Therefore, when presented with a *tert*-butyl or a TMA group to bind and orient within the binding site, these hosts prefer to place the less hydrophobic, charged group in this shielding region. Figure 4.2 shows the D values for the guest in these host-guest combinations. Clearly, the TMA end of the molecule is that portion of the guest residing within the binding site of the host.

While the results of Table 4.2 support the idea that a *tert*-butyl group is more hydrophobic than a TMA and that charge is not the overriding factor in the observed binding, it is clear that a charged (or possibly electron-deficient) group prefers to reside within the cavity of our hosts.



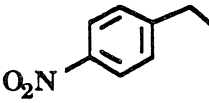
HOST	D <sub>A</sub>	D <sub>B</sub>	D <sub>C</sub>
<i>5CDL</i>	1.40	2.10	0.30
<i>PMESO</i>	1.89	3.14	0.54

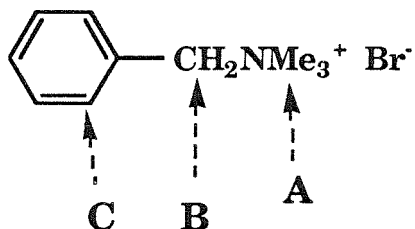
**FIGURE 4.2:** D values (in ppm) for *p-tert*-butylphenyl-trimethylammonium and the hosts *5CDL* and *PMESO*

Table 4.3 presents evidence for an electron-deficient group binding within the cavity of our macrocycles. The *p*-nitrobenzyltrimethylammonium guest binds more strongly to all the hosts than does benzyltrimethylammonium. This "nitro effect" is undoubtedly a donor-acceptor interaction, an effect previously observed in host-guest complexes.<sup>8</sup> The electron-rich anisole-like aromatic rings of our host can interact favorably with the electron-deficient nitroaromatic ring of the guest. This effect appears to be worth  $\approx 500$ - $700$  cal/mol if the observed association constants are transformed into free energies of binding ( $\Delta G_{\text{binding}} = -RT \ln K_a$ ). This analysis neglects differential guest solubility effects. This donor-acceptor effect appears to be fairly general with these hosts and will be discussed later.

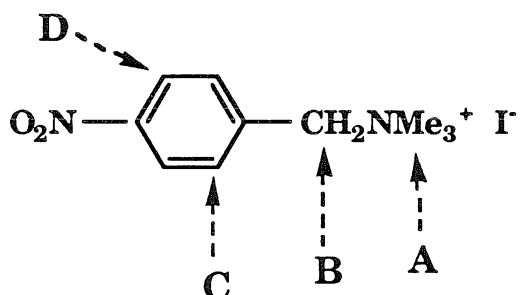
In addition to the increase of  $K_a$  upon the introduction of a nitro group, an interesting geometry change occurs upon binding. Figure 4.3 shows the *D* values for the protons of the guest in these complexes. Clearly, for the **5CMESO** complex, the nitro end of the guest is within the cavity of the host. A similar recognition of the nitro aromatic is seen in the **5CDL** complex, while for the **PMESO** complex the effect is not quite so pronounced. For **C6-L** the nitroaromatic portion of the guest molecule is recognized by this host; interestingly, the aromatic ring of the benzyl guest is also recognized in preference to the TMA group. This recognition of aromatic rings by **C6-L** will be seen to be quite general for this host (*vide infra*).

TABLE 4.3: The "nitro effect"

GUEST	HOST			
	<i>5CMESO</i>	<i>PMESO</i>	<i>5CDL</i>	<i>C6-L</i>
 $\text{NMe}_3^+ \text{Br}^-$	$2.5 \times 10^3$	$6.0 \times 10^3$	$2.5 \times 10^3$	$4.2 \times 10^3$
 $\text{NMe}_3^+ \text{I}^-$	$5.6 \times 10^3$	$1.3 \times 10^4$	$8.4 \times 10^3$	$7.5 \times 10^3$



HOST	D <sub>A</sub>	D <sub>B</sub>	D <sub>C</sub>
<i>PMESO</i>	2.24	3.01	2.60 (ortho)
<i>5CMESO</i>	1.40	2.04	1.47 (ortho)
<i>5CDL</i>	1.73	2.37	1.72 (ortho)
<i>C6-L</i>	0.57	-----	2.70 (ortho) 2.13 (meta)



HOST	D <sub>A</sub>	D <sub>B</sub>	D <sub>C</sub>	D <sub>D</sub>
<i>PMESO</i>	1.53	2.20	2.54	1.70
<i>5CMESO</i>	0.45	0.94	1.90	2.57
<i>5CDL</i>	0.61	1.24	2.07	1.52
<i>C6-L</i>	0.43	-----	2.26	2.32

**FIGURE 4.3:** D values (in ppm) for benzyltrimethylammonium and *p*-nitrobenzyltrimethylammonium with various hosts

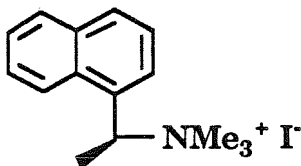
### Cavity Size: **5CMESO** vs. **PMESO**

The question of cavity size and shape relative to chemical structure is addressed by the data listed in Table 4.4. The two hosts, **5CMESO** and **PMESO**, are of approximately the same size (**PMESO** is slightly larger than **5CMESO**); however, the cavity of **PMESO** is "deeper" in that the aromatic rings provide some depth by functioning as walls that line the macrocyclic cavity. The **5CMESO** host appears to be much more flexible than the **PMESO** host and therefore could collapse upon smaller-sized guests. Thus, the **5CMESO** host could be more selective than **PMESO** for smaller guests, while **PMESO** might be more adept at covering the hydrophobic surface of a guest. Furthermore, desolvation of the host is expected to be an important factor in the binding event. Consequently, desolvation of the **PMESO** host is expected to be enthalpically favorable whereas the same desolvation is expected to be enthalpically less favorable for **5CMESO**, if the desolvation of aromatic and aliphatic hydrocarbons is taken as a guide.<sup>9</sup>

The data for these two host with various guests show some interesting trends. For all the guests studied, **5CMESO** binds them with essentially little difference in  $K_a$  values. On the contrary, **PMESO** displays some selectivity. **PMESO** discriminates among the guests, responding more to guests of increased hydrophobicity. Furthermore, the data suggest that larger-sized guests give larger association constants with **PMESO**.

**PMESO** responds more to the guest hydrophobicity than does **5CMESO**. About a factor of 1:0 decrease in  $K_a$  is observed for benzyltriethylammonium upon changing the host from **PMESO** to

TABLE 4.4: Cavity Size Data

GUEST	HOST	
	<i>5CMESO</i>	<i>PMESO</i>
	$2.5 \times 10^3$	$6.0 \times 10^3$
	$1.7 \times 10^3$	$1.4 \times 10^4$
	$2.3 \times 10^3$	$2.2 \times 10^4$
	$2.9 \times 10^3$	$1.2 \times 10^4$

**5CMESO**. This could also be a result of the poorer fit of this guest to the cavity of **5CMESO** relative to **PMESO**. CPK modeling and the data for benzyltrimethylammonium versus benzyltriethylammonium support this argument. While this is a limited data set, in all direct comparisons of the polymethylene-linked macrocycles to the *p*-xylyl-linked macrocycles, the latter are always the more efficient hosts.<sup>1</sup>

The **5CMESO** data raise the possibility that the TMA group may be all that is recognized in the binding event. While this may certainly be true to some extent, tetramethylammonium binds weakly to **5CMESO** (see Table 4.1). The leveling effect on  $K_a$  exerted over these guests by **5CMESO** may be conformational in origin. The **5CMESO** host has a unique geometry as revealed by <sup>1</sup>H NMR studies (see Experimental Section, Chapter 2, for details). Upon binding, *even to non-aromatic guests*, significant shifting of the aromatic protons of **5CMESO** is observed. Such a shifting of the protons of the host is expected if the guest were aromatic. However, the shifting observed with all the guests studied, both aliphatic and aromatic, suggests this molecule is conformationally quite mobile and a change in host geometry accompanies binding. This conformational change would be expected to cost energy and could lead to a reduction in the observed  $K_a$  values relative to a model where such a conformational change was absent.

Nevertheless, these guests are bound by **5CMESO** and the host does exert a profound influence over the guest. In all the guests studied, a "shift-reagent effect" is observed. The host resolves overlapping protons of

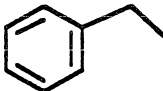
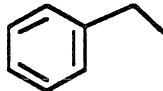
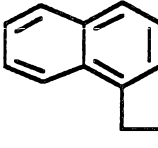
the guest; for the simple benzyl-substituted guests, the  $^1\text{H}$  NMR of the aromatic region of the guest in the absence of host is a broad singlet. Upon binding to the host, the peaks resolve and a doublet and two triplets appear in the ratio of 2:2:1. These protons are assignable as the *ortho*, *meta* and *para* protons, respectively, of the aromatic ring of the guest. It is clear that the aromatic ring of these guests is experiencing the anisotropic environment provided by the host cavity. The shift-reagent effect is observed in many of the host-guest combinations and is strong evidence for binding of the guest by encapsulation within the macrocyclic cavity.

### **5CDL**

The **5CDL** host binds the guests listed in Table 4.5 with some selectivity. **5CDL** binds both the chloride and bromide of benzyltrimethylammonium equally well. Thus, within the limit of the accuracy of the NMR method, there is no significant counter-ion effect upon binding. We expected little dependence on counter-ion, especially in a 10mM borate buffer.

Several interesting comparisons can be made with the data of Table 4.5. Generally, the more hydrophobic the R group<sup>6</sup> in the TMA, the larger is  $K_a$ . **5CDL** seems quite different from **5CMESO** in this respect. Thus, naphthyl > adamantyl > cyclohexyl > benzyl; the cyclohexyl/benzyl comparison holds for all three hosts : **PMESO**, **5CMESO**, **5CDL** (see Table 4.6), with little difference observed for **5CMESO**. Nevertheless, these differences, while small, do suggest that in these systems cyclohexyl is more hydrophobic than benzyl.<sup>3a,6</sup>

TABLE 4.5: Association Constants for **5CDL** and various guests

		HOST
GUEST		<b>5CDL</b>
 $\text{NMe}_3^+ \text{Br}^-$		$2.5 \times 10^3$
 $\text{NMe}_3^+ \text{Cl}^-$		$2.0 \times 10^3$
 $\text{NMe}_3^+ \text{I}^-$		$4.3 \times 10^3$
$\text{Bu}_3\text{NMe}^+ \text{I}^-$		$1.4 \times 10^3$
 $\text{NMe}_3^+ \text{I}^-$		$1.8 \times 10^4$
 $\text{NMe}_3^+ \text{I}^-$		$8.1 \times 10^3$

**TABLE 4.6:** Cyclohexyl versus Benzyl Comparison

GUEST	HOST		
	<i>5CMESO</i>	<i>PMESO</i>	<i>5CDL</i>
 <chem>CN(C)C[N+](C)(C)Br-</chem>	$2.5 \times 10^3$	$6.0 \times 10^3$	$2.5 \times 10^3$
 <chem>CN(C)C[N+](C)(C)I-</chem>	$2.9 \times 10^3$	$1.2 \times 10^4$	$4.3 \times 10^3$

A second interesting result is the comparison between ATMA and  $\text{Bu}_3\text{NCH}_3^+$ . Both guests have the same number of carbon atoms in their skeleton, yet ATMA is much more strongly bound. We made this comparison to assess the role of guest rigidity in the binding event. Thus, the rigid, preorganized guest binds more tightly to the host than does the flexible guest. Rigidity in the guest is just as important as rigidity in the host.<sup>10</sup> Both guests are of similar size and shape; therefore, the observed differences in binding do not appear to be due to steric factors. While the  $\text{Bu}_3\text{NCH}_3^+$  guest can exist in many conformations, in an aqueous environment we would expect it to be in a shape similar to that of ATMA to minimize the exposed hydrophobic surface area.

### ***C6-L***

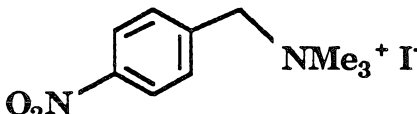
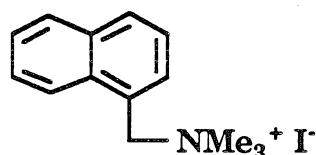
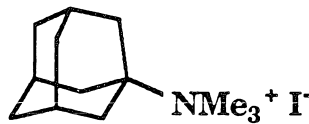
This host was synthesized for the purpose of having an aliphatic-linked macrocycle of some rigidity with the same dimensions as the *p*-xylyl-linked macrocycles. This host could be used to assess such questions as the role of aromatic  $\pi$ -stacking interactions<sup>11</sup> and host rigidity on  $K_a$ . If hydrophobicity were the most significant factor in the binding, then ***C6-L*** would be a better host than ***PDL***, since cyclohexyl is generally considered to be more hydrophobic than phenyl.<sup>3a,6,9,13</sup> CPK models indicate that this host does in fact have a similar geometry to ***PDL***; the cavity of ***C6-L*** is slightly smaller because of the axial cyclohexyl hydrogens that must protrude into the interior of the macrocycle.

The surprising result of the data shown in Table 4.7 is the small upfield shifts observed for the two guests  $C_6H_{11}N(CH_3)_3^+$  and  $Bu_3NCH_3^+$ . The small upfield shifts observed in the  $^1H$  NMR spectra of these experiments could mean that these guests do not bind strongly to **C6-L**; however, in light of the fact that ATMA does bind, the observed small shifting could be due to the fact that these guests reside near the cyclohexyl rings of the host and do not experience the usual strong upfield shifts of the other guests in the host-guest complexes.

The other interesting result of this host is that it does not necessarily recognize a TMA group. For the benzyl-type TMA guests studied, it is the aromatic ring of the guest that is recognized (see Figure 4.2 for these D values). Unfortunately, the D values for the benzylic methylene groups are generally obscured, but when visible, they form a clear AB pattern with a large  $\Delta\nu$ . These enantiotopic protons, in the presence of the chiral host, become formally diastereotopic, couple to one another and form an AB pattern. This result is again strong evidence for binding by encapsulation.

For the naphthyl guest, a small upfield shift of the TMA is also observed ( $D=0.37$  ppm). The methylene group of this guest is obscured by the solvent in these experiments; however, it is clear from these experiments that this guest is strongly bound to the host with the naphthalene ring of the guest aligned parallel to the cyclohexyl rings of **C6-L**. Large upfield shifts of the protons of the host protons are observed, with some of the cyclohexyl protons upfield of the TSP reference. The methylene

TABLE 4.7: Association Constants for **C6-L** and various guests

		HOST
GUEST		<b>C6-L</b>
	$\text{NMe}_3^+ \text{Br}^-$	$4.2 \times 10^3$
	$\text{NMe}_3^+ \text{I}^-$	$7.5 \times 10^3$
	$\text{NMe}_3^+ \text{I}^-$	$1.4 \times 10^4$
	$\text{NMe}_3^+ \text{I}^-$	$9.2 \times 10^3$
	$\text{NMe}_3^+ \text{I}^-$	small shifting observed
$\text{Bu}_3\text{NMe}^+ \text{I}^-$		small shifting observed

group  $\alpha$  to the oxygen of the linker of the host also undergoes strong upfield shifts, whereas the aromatic protons of the host shift much less. The aromatic protons of the guest are broad and difficult to assign, but it is clear from the  $^1\text{H}$  NMR spectra of this experiment that more than just the two aromatic hydrogens near the TMA substituent are involved in this binding event. Once again, **C6-L** recognizes the aromatic ring of the guest; furthermore, **C6-L** orients the guest so as to minimize the exposed surface area of the cyclohexyl rings. This unique effect will be elaborated upon later.

#### **Donor-Acceptor $\pi$ -Stacking and Ion-Dipole Effects**

Donor-acceptor interactions<sup>11</sup> have already been shown to be an important component of the binding of certain guests to our hosts. The observation of a donor-acceptor interaction in synthetic host-guest systems is not new. Ferguson and Diederich<sup>8</sup> have described host-guest complexation in organic solution dominated by electron donor-acceptor interactions.

Host **4** (see Chapter 1) was shown to associate with a variety of 2,6-disubstituted naphthalenes of differing electronic properties. The studies, conducted in methanol- $d_4$  as solvent, indicated that all the guests bound in the same geometry to **4** but with different binding affinities. The differences observed in the association constants were attributed to donor-acceptor interactions. The guests were divided into three classes: donor-donor guests (both substituents electron-donating), donor-acceptor guests

(one donor and one acceptor substituent) and acceptor-acceptor guests (both substituents electron-accepting). Host 4, composed of electron-rich aromatic rings, was considered to be a donor host. The degree of complexation of the guests with 4 was acceptor-acceptor > donor-acceptor > donor-donor. The authors interpreted these results to mean that electron donor-acceptor interactions were responsible for determining the relative stability of these complexes.

A disturbing piece of data is the complex between 2,6-dimethylnaphthalene and 4 ( $K_a = 67 \text{ M}^{-1}$ ,  $\Delta G^\circ = -2.53 \text{ kcal/mol}$ ). This complex is 730 cal/mol more stable than the complex of 2,6-di(hydroxymethyl)naphthalene and 4. This result is surprising because these two substituents (methyl and hydroxymethyl) should have about the same donating ability. The fact that the complex of 2,6-di(hydroxymethyl)naphthalene with 4 is also less stable than the complexes of 4 with other donor-donor guests (diamino, dihydroxy and dimethoxynaphthalenes) suggests that some other effect is operative in this case. It is possible that guest solubility is an unrecognized factor affecting complex formation in this case.

Ferguson and Diederich<sup>8</sup> determined the enthalpic and entropic contributions to the free energy of binding for host 4 and 2,6-dicyanonaphthalene in methanol-*d*<sub>4</sub>. On the basis of these values,  $\Delta H^\circ = -7.6 \text{ kcal/mol}$  and  $\Delta S^\circ = -14.1 \text{ eu}$ , the authors concluded that the observed differences in complexation among the guests were due to attractive interactions rather than to entropically favorable desolvation effects.

Furthermore, studies conducted in dimethylsulfoxide- $d_6$  indicated that although the absolute magnitude of the  $K_a$  values decreased, the same trends among the guests observed earlier in methanol- $d_4$  were observed in this solvent. Nevertheless, the low complexing ability of 2,6-di(hydroxymethyl)naphthalene was not addressed. Interestingly, in 60% aqueous methanol, a leveling effect was observed. These substituted naphthalenes were bound to **4** with little variation in  $K_a$ ; Ferguson and Diederich<sup>8</sup> concluded that in this instance, hydrophobic effects provided the major driving force for complexation.

Table 4.8 displays the association constants for **P-D** and **C6-L** with several quite water-soluble, aromatic, heterocyclic guests.<sup>12</sup> These two hosts were chosen as a pair with very similar binding-site dimensions and comparable degrees of preorganization.<sup>10</sup> Importantly, control studies with 2,6-diethoxy-9,10-dihydro-9,10-(1,2-dicarboxy)ethenoanthracene biscesium salt (**17** in Figure 4.1) show no significant association with these guests.

For **C6-L** and these guests, the geometry of binding is unique relative to the other hosts. However, it is consistent with this host's ability to encapsulate aromatic guests (*vide supra*). Upon binding these guests, upfield shifts of the cyclohexyl protons of the host are observed. In addition, H<sub>4</sub> of the host (using the anthracene numbering system) is shifted downfield. This pattern has been observed for *all* aromatic guests studied when bound to **C6-L**.

**Table 4.8:** Association Constants for aromatic heterocyclic guests and Hosts **C6-L** and **P-D**

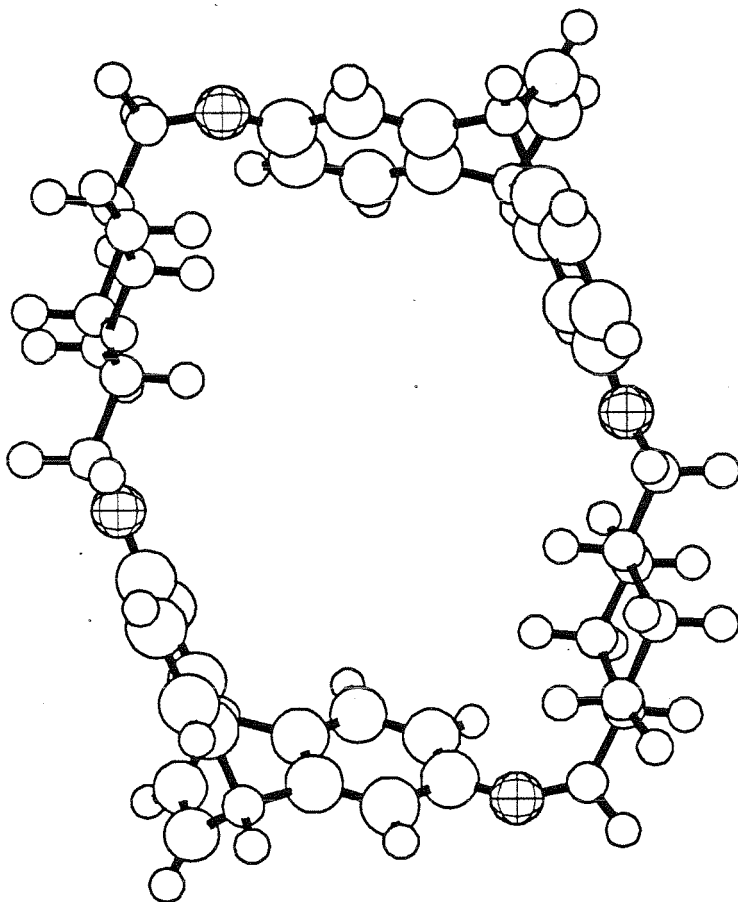
GUEST	Solubility [M] <sup>a</sup>	HOST	
		<b>P</b>	<b>C</b>
		K(M <sup>-1</sup> ) [-ΔG°] <sup>b</sup>	K(M <sup>-1</sup> ) [-ΔG°] <sup>b</sup>
quinoline	0.078	10000 [5.4]	22000 [5.9]
2-methylquinoline	0.023	11000 [5.5]	20000 [5.8]
4-methylquinoline	0.014	38000 [6.2]	30000 [6.0]
isoquinoline	0.037	47000 [6.3]	46000 [6.3]
1-methylisoquinoline	0.030	55000 [6.4]	100000 [6.7]
indole	0.016	1400 [4.2]	1600 [4.3]
<i>N</i> -methylindole	0.0032	2100 [4.5]	3800 [4.8]
<i>N</i> -methyloquinoline	0.45	200000 [7.2]	27000 [6.0]
<i>N</i> -methylquinoline	0.52	400000 [7.6]	47000 [6.3]

a: Solubilities as determined in our operating buffer (10mM cesium borate, pD=9).

b: In kcal/mol at 295K; values listed are accurate to ± 0.2 kcal/mol

These host shifts are consistent with a second type of geometry that is accessible to these macrocycles. These hosts can exist in a conformation where the hydrophobic cavity is quite different from the idealized, cylindrical geometry. This idealized geometry may be well suited for the recognition of a TMA group;<sup>5</sup> however, the ability of this host to encapsulate a flat aromatic ring in a manner superior to the encapsulation of a TMA requires a flattened cavity that can maximize van der Waals contacts between host and guest. CPK modeling indicates that **C6-L** can exist in this type of geometry reminiscent of a rhombus. The long side of the rectangle contains the cyclohexyl ring of the linker and one aromatic ring of the ethenoanthracene. The corner of this rectangle is provided by the cleft of the ethenoanthracene. The short side of the rectangle is formed from the remaining aromatic ring of the ethenoanthracene. This binding conformation is of  $\sim C_2$  symmetry with the approximate dimensions of 9.5Å x 4Å. Figure 4.4 shows a ball-and-stick model of this conformation. The hatched atoms represent the ether oxygens of the host; the carboxylates are omitted for clarity.

Isoquinoline or quinoline fits perfectly into this binding site. Furthermore, CPK models indicate that if either of these guests were placed in the binding site, then the H<sub>4</sub> proton of the host would be expected to undergo a downfield shift. This host proton resides near the deshielding region of the guest molecule. Moreover, this geometry nicely accommodates the upfield shifts of the cyclohexyl linker protons; they reside over the aromatic rings of the guest and therefore should shift

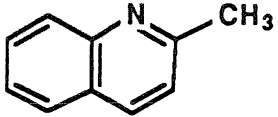
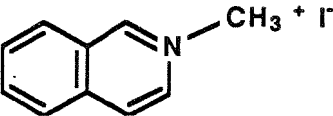
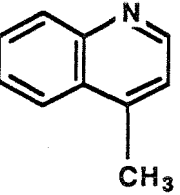
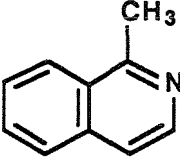
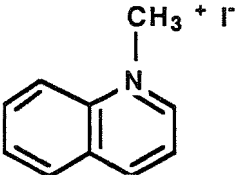


**FIGURE 4.4:** Rhomboid conformation of **C6-L** (carboxylates omitted for clarity)

upfield. This is precisely what is observed. This geometry also seems to allow for the maximization of the van der Waals contacts between the host and guest. This host "collapses" around the guest, providing efficient encapsulation, thereby protecting it from the aqueous surroundings. A similar geometry is proposed for **P-D**.<sup>1</sup>

The maximum upfield shifts of these guests in their complexes with **C6-L** clearly indicate no strong orientational preference within the cavity. Unlike the results of Koga<sup>13</sup> or Diederich<sup>13</sup> (Chapter 1), the shifts of the guests in these NMR experiments do not provide compelling evidence for just one binding geometry (equatorial or axial, for instance). Instead, the observed shifts appear to be an average of many geometries. Nevertheless, it is clear that for the 2-substituted quinoline or isoquinoline derivatives, the equatorial geometry is not a favorable one. In such an arrangement, the methyl group of these guests would protrude into the cleft of the ethenoanthracene. The D values for the methyl groups of the 2-substituted and 1-substituted guests are shown in Figure 4.5. Clearly, the lack of significant shielding of the methyl groups in the 2-substituted derivatives argues against the equatorial geometry. We feel that the guests tip slightly within the binding site to minimize non-bonded contacts between the methyl groups and the ethenoanthracene rings of the host. The  $K_a$  values are still quite high, indicating that significant van der Waals interactions of the host and guest are achieved.

Hosts **P-D** and **C6-L** are assembled from electron-rich alkoxyethenoanthracenes. Therefore, they should bind electron-deficient

GUEST	DCH <sub>3</sub>
	0.48
	0.44
	0.85
	1.35
	1.33

**FIGURE 4.5:** D values (in ppm) of the methyl groups for the complexes of **C6-L** and various isostructural methyl-substituted quinolines and isoquinolines

guests such as the quinolines and isoquinolines better than they bind the electron-rich indoles. The results indicate that this analysis is correct, even though the indoles are the less water-soluble compounds. Clearly, the differences observed here are not due to hydrophobic effects but to donor-acceptor interactions. We attribute the lack of significant differences between **P-D** and **C6-L** to the dominant interaction of the anisole-type rings of these hosts with these guests.

Methylation of quinoline and isoquinoline afforded the very water-soluble *N*-methylquinolinium and *N*-methylisoquinolinium. We expected that alkylation could further enhance donor-acceptor interactions; however, the hydrophilicity of these guests could significantly reduce the driving force for association with a hydrophobic binding site. Hence, the relatively constant values of  $K_a$  for these guests with **C6-L** indicate a substantial enhancement in attractive host-guest interactions for these cationic guests.

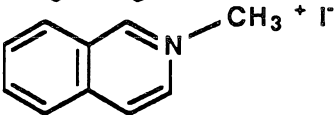
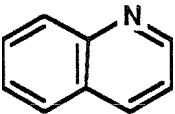
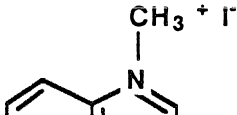
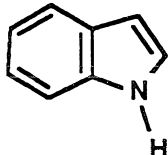
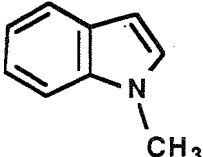
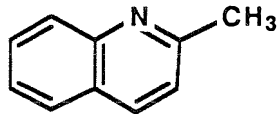
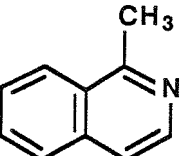
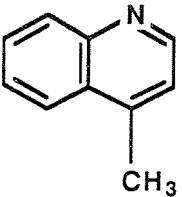
**P-D** binds these charged guests much more tightly than **C6-L**. Studies with the "isostructural" guest pairs (2-methylquinoline/*N*-methylisoquinoline, 1-methylisoquinoline/*N*-methylquinoline and 4-methylquinoline/*N*-methylquinoline) indicate that this is not a steric or hydrophobic effect (see Table 4.8 and Figure 4.4). In light of the ability of this type of host to form strong complexes with TMA-substituted guests relative to other hosts (e.g., ATMA),<sup>1</sup> we attribute the enhanced binding of these cationic guests to a polarization of **P-D** in response to the positive charge of the guest. This ion-dipole effect is significant and can be worth

more than 1 kcal/mol in binding free energy.

This charge effect is not an electrostatic effect similar to that observed by other workers<sup>3,4,13</sup> (see Chapter 1). In our systems, the rigid macrocyclic framework prevents the carboxylates from coming into close contact with the positively charged guests. The placement of ionic groups, complementary in charge to potential guests, around a hydrophobic receptor site has been shown to lead to quite high association constants via close-proximity electrostatic interactions.<sup>3,4,13</sup> The ion-dipole effect that we describe here is distinct from such an electrostatic effect in its origin but can lead to analogously high association constants. Furthermore, enormously hydrophobic guests are not required to achieve tight binding.<sup>13</sup> The operation of this ion-dipole effect in conjunction with donor-acceptor interactions results in tight binding of very hydrophilic guests to our synthetic receptors.<sup>14</sup>

Table 4.9 lists the association constants for the heterocyclic guests with **5CDL** and **C6-L**. The dramatic decrease in  $K_a$  between the hosts could be due to the flexibility of **5CDL**. Importantly, the host-guest geometries are quite different. For **5CDL** and the *N*-methyl derivatives of the heterocycles, all aromatic protons of the host shift upfield, the bridgehead proton shifts upfield and the linker protons shift *downfield*. These host shifts are consistent with an edge-on geometry with the edge of the aromatic ring of the guest adjacent to the linkers of the host. Less dramatic host shifts are apparent with this host and the parent heterocycles; nevertheless, for all

**TABLE 4.9:** Association Constants for **5CDL** and **C6-L** and aromatic heterocyclic guests

GUEST	HOST	
	<b>5CDL</b>	<b>C6-L</b>
	$1.5 \times 10^3$	$4.7 \times 10^4$
	$6.1 \times 10^3$	$2.7 \times 10^4$
	$8.1 \times 10^2$	$2.2 \times 10^4$
	$8.1 \times 10^3$	$4.7 \times 10^4$
	small shifting observed	$1.6 \times 10^3$
	small shifting observed	$3.8 \times 10^3$
	$3.9 \times 10^2$	$2.0 \times 10^4$
	$1.2 \times 10^3$	$1.0 \times 10^5$
	$1.0 \times 10^3$	$3.0 \times 10^4$

these electron-deficient heterocycles, the geometry appears to be the same, with the aromatic ring of the guest stacked under the ethenoanthracene moiety of the host. **5CDL** does exert a strong shift-reagent effect over the protons of these guests. Clearly, the aromatic ring of these guests is bound within the macrocyclic cavity of our host. The rhomboid geometry typified by **C6-L** seems not to be favorable for **5CDL**.

While the factors responsible for the lower binding affinity of **5CDL** with respect to **C6-L** for these heterocyclic guests are not completely clear, the results suggest that the stronger binding to **C6-L** is due to a combination of effects. Clearly, the ethenoanthracene rings provide some favorable donor-acceptor interactions if **5CDL** is taken as a model for these effects. However, the matching of guest shape and binding-site topography is also quite important and could account for the observed differences.<sup>3a,11</sup>

In contrast to **5CDL**, all the simple aromatic guests (see Table 4.7) bind to **C6-L** in the rhomboid conformation. The naphthyl ammonium guest in this geometry would clearly cause an upfield shift of the cyclohexyl protons, at the same time placing the TMA towards the aqueous environment. A similar geometry for the benzyl-type guests would also be expected to place the TMA group towards the water; the lower binding affinities of these benzyl-type guests for **C6-L** relative to the aromatic heterocyclic guests probably reflects their poorer fit to the cavity. The match of topography with the cavity is best for the aromatic heterocyclic guests. Therefore, **C6-L** binds the flat aromatic portions of the guest and places the spherical TMA group towards the water.

## Conclusions

Our studies on host-guest interactions in aqueous solution have revealed some interesting effects. The choice of a linker group is crucial to the design of efficient hosts. Significant variations in  $K_a$  occur upon changing the structural and/or electronic properties of the linker groups in these macrocycles. In addition, studies with the same guest indicate that different linker-dependent host conformations are produced upon complexation.

These host structures display a strong affinity for alkyl TMA salts despite the significant water solubility of these guests. The spherical shape of a TMA matches the idealized cylindrical binding site of the hosts. Moreover, there appears to be an added attraction between cationic guests and the *p*-xylyl-linked hosts. Several other factors, including steric complementarity, rigidity, donor-acceptor interactions and hydrophobicity have been shown to contribute to efficient association. Maximization of these effects can lead to  $K_a$  values  $> 10^5 \text{ M}^{-1}$ .

The aliphatic guest ATMA binds equally well to either **5CDL** or **C6-L**. However, the geometries of binding are distinctly different. We anticipated that the increase in linker rigidity upon changing from **5CDL** to **C6-L** would lead to a change in binding geometry and a significant increase in  $K_a$ . However, only the former was observed, with the change in  $K_a$  being insignificant. The large increase in  $K_a$  observed with the *p*-xylyl series of hosts relative to the aliphatic-linked macrocycles is indicative of the

additional attraction of TMA groups for this host. The direct comparison of *PDL* and *C6-L* allows for a probing of this phenomenon.

Tight binding of water-soluble aromatic heterocycles to *PDL* and *C6-L* has been achieved. Strong donor-acceptor interactions between host and guest overcome the intrinsic hydrophilicity of these guests, and large  $K_a$  values result. Electron-deficient guests associate with the hosts more strongly than do electron-rich guests. Upon the binding of these aromatic guests, specific shifts of host protons indicate that these hosts adopt a new, rhomboid-shaped conformation. This conformation maximizes van der Waals interactions between host and guest and provides efficient guest encapsulation. In addition, for *C6-L*, this conformation is proposed for all bound aromatic guests. The increased binding affinity of *PDL* for *N*-methylquinoline and *N*-methyloquinoline relative to *C6-L* has been ascribed to an additional ion-dipole effect in this host. The positive charge of the guest responds more favorably to the polarizable *p*-xylyl-linked host.

The studies with these heterocyclic guests show that high binding constants can be obtained with hydrophilic guests. Furthermore, our host design keeps the negatively charged carboxylates well removed from the binding site and well removed from bound guests. Hence, the observed charge effect is not of the electrostatic type but can lead to just as tight binding. Appending negatively charged groups around the binding site, accessible to bound, positively charged guests, would be expected to lead to even stronger binding. Nonetheless, the ability to bind and orient highly water-soluble molecules now allows the chemist to act upon a greater

range of potential guests with synthetic receptor molecules.

## EXPERIMENTAL SECTION

General:  $^1\text{H}$  NMR spectra were recorded on a JEOL FX-90Q or a JEOL GX400 spectrometer. All binding studies were performed in a borate-D buffer (pH=9) with the reported chemical shifts relative to an external TSP reference in the same buffer. The  $^1\text{H}$  NMR spectra were accumulated in the same manner for all the studies, using a 2 sec acquisition time and a 0.5 sec pulse delay. All coupling constants are in hertz.

**Binding Experiments:** All the binding experiments were performed by successive titrations of an aqueous borate-buffered solution of the host with aliquots of guest in the same buffer;  $[\text{Host}] = 150\text{--}400\ \mu\text{M}$  and  $[\text{Guest}] = 150\text{--}1000\ \mu\text{M}$ . Control studies were performed with  $[\text{17}] = 800\ \mu\text{M}$  and  $[\text{Guest}] = 500\ \mu\text{M}$ .

**Buffer Preparation:** A fresh bottle of  $\text{D}_2\text{O}$  (from the CIT stockroom, Aldrich 99.8 atom %D, 100g) was opened and 31.4 mg of anhydrous boric acid (HP 60 Mesh, Technical Grade, U.S. Borax) was added. CsOD (450  $\mu\text{L}$  ~1M solution in  $\text{D}_2\text{O}$ ) was added to bring the pH to 9.

**Concentration Determinations:** All concentrations were determined by  $^1\text{H}$  NMR integration (4 sec acquisition time, 30 sec pulse delay) against a potassium acid phthalate standard.

### **C6-L Host (14)**

A 10-mL syringe was charged with a DMF solution of optically pure (*R,R*)-diol **8** ( $[\alpha]_{\text{D}} = +64^\circ$  ( $c=0.9$ ,  $\text{CH}_3\text{CN}$ ), 70 mg, 0.1989 mmol, 1 eq) and *trans*-1,4-cyclohexanedimethanol-ditosylate (90 mg, 0.1991 mmol, 1 eq).

Cs<sub>2</sub>CO<sub>3</sub> (326 mg, 1 mmol, 5 eq) was suspended in 90 mL of anhydrous DMF. This flask was kept over argon and protected from light while it was warmed to 60 °C. The contents of the syringe were added slowly over 4 days. After the addition, the solution was stirred for 1 day at 60 °C. The DMF was removed by high vacuum distillation. The residue was dissolved in 25 mL of CH<sub>2</sub>Cl<sub>2</sub>. Ten milliliters of H<sub>2</sub>O was added and the phases were separated. The organic phase was extracted with H<sub>2</sub>O again (2x15mL each). The organic phase was finally washed with saturated brine solution. The organic layer was dried over MgSO<sub>4</sub> and concentrated. The product plus higher molecular weight materials were isolated by flash chromatography using 5% Et<sub>2</sub>O/CHCl<sub>3</sub> as an eluent. The individual cyclic oligomers could be isolated by preparative TLC with multiple elutions using 1% Et<sub>2</sub>O/CHCl<sub>3</sub> as eluent. The highest R<sub>f</sub> material was the dimer with the higher homologues running progressively more slowly. Dimer: 5 mg (5.5% yield). <sup>1</sup>H NMR (CDCl<sub>3</sub>): δ 7.09 (d, 4H, *J*=8.05), 6.82 (d, 4H, *J*=2.20), 6.38 (dd, 4H, *J*=8.05, 2.20), 5.20 (s, 4H), 3.86 (dd, 4H, *J*=5.86, 10.98), 3.73 (s, 12H), 3.71(dd, 4H, *J*=5.86, 10.98), 1.60 (m, 12H), 0.85 (m, 8H). <sup>13</sup>C NMR (CDCl<sub>3</sub>): δ 165.97, 156.61, 146.93, 145.82, 135.68, 123.79, 112.16, 110.66, 73.62, 52.24, 51.72, 36.45, 28.46. Mass Spectrum: (FAB) 921(MH<sup>+</sup>), 889, 779, 613, 461, 397. [α]<sub>D</sub> = -44° (c=0.12, CH<sub>3</sub>CN). Some presumed trimer and tetramer

could be isolated. Trimer: (2.5 mg);  $^1\text{H}$  NMR ( $\text{CDCl}_3$ ):  $\delta$  7.18 (d, 6H,  $J=8.05$ ), 6.88 (d, 6H,  $J=2.20$ ), 6.42 (dd, 6H,  $J=8.05$ , 2.20), 5.24 (s, 6H), 3.74 (s, 18H), 3.68 (m, 12H), 1.60 (m, 36H), 0.85 (m, 24H);  $[\alpha]_{\text{D}} = -8.4^\circ$  ( $c=0.154$ ,  $\text{CH}_3\text{CN}$ ).

Tetramer: (0.8 mg);  $^1\text{H}$  NMR ( $\text{CDCl}_3$ ):  $\delta$  7.17 (d, 8H,  $J=8.05$ ), 6.90 (d, 8H,  $J=2.20$ ), 6.43 (dd, 8H,  $J=8.05$ , 2.20), 5.26 (s, 8H), 3.76 (s, 24H), 3.66 (m, 16H), 1.60 (m, 48H), 0.85 (m, 32H);  $[\alpha]_{\text{D}} = +27.5^\circ$  ( $c=0.08$ ,  $\text{CH}_3\text{CN}$ ).

#### **C6-L: Tetra-cesium salt (15)**

The tetraester **14** (4 mg, 0.0043 mmol, 1 eq) was dissolved in 300  $\mu\text{L}$  of DMSO. Water (50  $\mu\text{L}$ ) was added, the solution protected from light and kept under argon. The CsOH (3.3 mg, 0.0215 mmol, 5 eq) was added and the reaction stirred for 8 hours. The volatiles were removed via lyophilization.

The crude mixture was applied to an ion-exchange column (Dowex,  $\text{NH}_4^+$  form). The fraction containing the desired ammonium salts of the host was isolated and lyophilized. The white foam remaining was dissolved in the borate-D buffer; CsOD/ $\text{D}_2\text{O}$  was added to bring the pH to 9.  $^1\text{H}$  NMR (borate-D buffer, relative to external TSP):  $\delta$  7.27 (d, 4H,  $J=8.05$ ), 7.05 (d, 4H,  $J=2.20$ ), 6.57 (dd, 4H,  $J=8.05$ , 2.20), 5.27 (s, 4H), 3.83 (m, 8H), 1.66 (m, 12H), 0.72 (m, 8H).  $^{13}\text{C}$  NMR ( $\text{DMSO-}d_6/\text{D}_2\text{O}$ ):  $\delta$  169.80, 157.01, 148.14, 147.45, 139.81, 125.18, 113.55, 112.31, 75.80, 53.70, 37.43, 29.44;  $[\alpha]_{\text{D}} = -133^\circ$  ( $c=0.0372$ ,

borate-d buffer, pH=9).

**2,6-Diethoxy-9,10-dihydro-9,10-(1,2-dicarbomethoxy)ethenoanthracene (16)**

A 10-mL, round-bottomed flask was charged with racemic **8** (100mg, 0.284 mmol, 1 eq) and Cs<sub>2</sub>CO<sub>3</sub> (650 mg, 1.988 mmol, 7 eq). Degassed acetone (5 mL) was added and the solution stirred under nitrogen. Ethyl iodide (160μL, 647 mg, 1.988 mmol, 7 eq) was added and the solution gently refluxed for 12 hours. The solution was filtered and concentrated. The product (76 mg, 65% yield) was isolated by column chromatography over silica gel using 60% ethyl ether/petroleum ether as an eluent. <sup>1</sup>H NMR (CDCl<sub>3</sub>): δ 7.20 (d, 2H, *J*=7.5), 6.90 (d, 2H, *J*=1.5), 6.45 (dd, 2H, *J*=7.5,1.5), 5.30 (s, 2H), 3.90 (q, 4H, *J*=6.6), 3.75 (s, 6H), 1.30 (t, 6H, *J*=6.6). <sup>13</sup>C NMR (CDCl<sub>3</sub>): δ 165.99, 156.82, 147.20, 145.79, 135.51, 124.11, 111.49, 109.75, 63.65, 52.34, 51.77, 14.84.

**2,6-Diethoxy-9,10-dihydro-9,10-(1,2-dicarboxy)ethenoanthracene biscesium salt (17)**

Bisester **16** (118 mg, 0.29 mmol, 1 eq) was dissolved in 1 mL of DMSO. Water (300μL) was added and the solution stirred for 4 hours. The solution was lyophilized and the residue ion-exchanged. The first three fractions containing the product were collected and lyophilized. The foamy white residue was dissolved in pH=9 borate-D buffer and the CsOD/D<sub>2</sub>O solution

was added to bring the pH to 9.  $^1\text{H}$  NMR (borate-D buffer, relative to external TSP):  $\delta$  7.31 (d, 2H,  $J=8.3$ ), 7.06 (d, 2H,  $J=2.44$ ), 6.55 (dd, 2H,  $J=8.3$ , 2.44), 5.28 (s, 2H), 4.00 (d of q, 4H,  $J=7.08$ ), 1.30 (t, 6H,  $J=7.08$ ).  $^{13}\text{C}$  NMR (borate-D buffer):  $\delta$  172.41, 153.33, 145.60, 144.75, 136.15, 121.74, 109.12, 108.10, 62.69, 50.03, 11.80.

**Guests:** The heterocyclic guests, alkyltrimethylammonium bromides and chlorides were commercially available from Aldrich Chemical Company. The iodides were prepared by the alkylation of the amine with excess iodomethane in DMF. The products were precipitated with  $\text{Et}_2\text{O}$  and recrystallized prior to use. The tetrafluoroborate salts were prepared by the action of Meerwein's reagent on the dimethylamino precursors in  $\text{CH}_2\text{Cl}_2$ . Addition of MeOH, concentration of the mixture and trituration with  $\text{Et}_2\text{O}$  gave the crude products. These salts were recrystallized prior to use.

#### **4-Nitrobenzyltrimethylammonium iodide**

The product was formed in 95% yield and was recrystallized from  $\text{CH}_3\text{CN}/\text{Et}_2\text{O}$ .  $^1\text{H}$  NMR (borate-D buffer):  $\delta$  8.39 (d, 2H,  $J=7.0$ ), 7.82 (d, 2H,  $J=7.0$ ), 4.65 (s, 2H), 3.17 (s, 9H).  $^{13}\text{C}$  NMR ( $\text{DMSO}-d_6/\text{D}_2\text{O}$ ):  $\delta$  150.06, 135.25, 135.21, 125.31, 69.44, 54.28.

#### **1-Naphthyltrimethylammoniummethyl iodide**

The product was formed in 82% yield and was recrystallized from

CH<sub>3</sub>CN. <sup>1</sup>H NMR (borate-D buffer): δ 8.28 (d, 1H, *J*=10.6), 8.17 (d, 1H, *J*=10.6), 8.09 (d, 1H, *J*=10.6), 7.81 (d, 1H, *J*=10.6), 7.74 (mt, 1H), 7.67 (t, 2H, *J*=10.6), 5.06 (s, 2H), 3.16 (s, 9H). <sup>13</sup>C NMR (DMSO / D<sub>2</sub>O): δ 135.1, 133.3, 130.7, 129.3, 128.1, 126.8, 124.8, 124.6, 66.9, 54.6.

#### **Phenyltrimethylammonium tetrafluoroborate**

The product was formed in 84% yield and was recrystallized from CH<sub>3</sub>CN/ Et<sub>2</sub>O. <sup>1</sup>H NMR (borate-D buffer): δ 7.83 (bd, 2H), 7.64 (m, 3H), 3.65 (s, 9H). Analysis calculated: C(48.47), H(6.33), N(6.27); found: C(48.41), H(6.53), N(6.27).

#### **4-*tert*-Butylphenyltrimethylammonium tetrafluoroborate**

The product was formed in 88% yield and was recrystallized from CH<sub>3</sub>CN/ Et<sub>2</sub>O. <sup>1</sup>H NMR (borate-D buffer): δ 7.75 (d, 2H, *J*=7.0), 7.70 (d, 2H, *J*=7.0), 3.63 (s, 9H), 1.34 (s, 9H). Analysis calculated: C(55.93), H(7.94), N(5.02); found: C(55.61), H(7.94), N(4.99).

#### **1,4-Bis(trimethylammonium)benzene bis(tetrafluoroborate)**

The product was formed in 95% yield and was recrystallized from CH<sub>3</sub>CN. <sup>1</sup>H NMR (borate-D buffer): δ 8.14 (s, 4H), 3.71 (s, 18H). Analysis calculated: C(39.17), H(6.14), N(7.61); found: C(39.07), H(6.14), N(7.34).

**References for Chapter 4**

1. For details see Shepodd, T.J. Ph.D. Thesis, California Institute of Technology, 1988.
2. Diederich, F.; Dick, K. *Chem. Ber.* **1985**, *118*, 3817-3829.
3. (a) Franke, J.; Vögtle, F. *Topic in Current Chemistry* **1986**, *132*, 135-170.  
(b) Vögtle, F.; Merz, J.; Wirtz, H. *Angew. Chem., Int. Ed. Engl.* **1985**, *24*, 221-222.
4. Dhaenens, M.; Lacombe, L.; Lehn, J.-M.; Vigneron, J.P. *J. Chem. Soc., Chem. Comm.* **1984**, 1097-1099.
5. Shepodd, T. J.; Petti, M.A.; Dougherty, D.A. *J. Am. Chem. Soc.* **1986**, *108*, 6085-6087.
6. Wolfenden, R. *Science* **1983**, *222*, 1087-1093.
7. For a good discussion of chemical forces see Huheey, J.E. *Inorganic Chemistry*, 3rd ed.; Harper&Row: New York, 1983; Chapter 6.
8. Ferguson, S. B.; Diederich, F. *Angew. Chem., Int. Ed. Engl.* **1986**, *25*, 1127-1129.
9. Tanford, C. *The Hydrophobic Effect*, 2nd ed.; Wiley: New York, 1980.
10. Cram, D.J. *Angew. Chem., Int. Ed. Engl.* **1986**, *25*, 1039-1134.
11. For an overview of  $\pi$ -stacking effects see:  
(a) Saenger, W. *Principles of Nucleic Acid Structure*; Springer-Verlag: New York, 1984; Chapter 6.

$\pi$ -Stacking effects have been observed in synthetic host-guest systems. See:

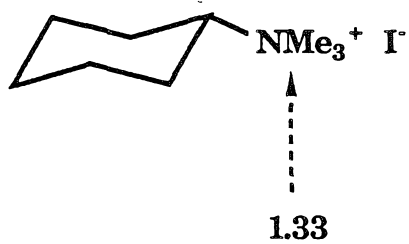
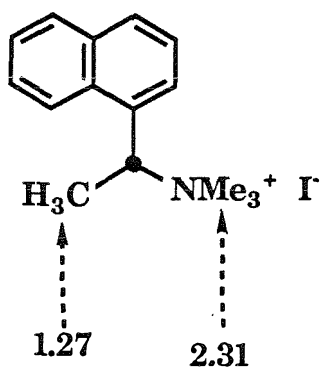
- (a) Rebek, J., Jr.; Askew, B.; Ballester, P.; Buhr, C.; Jones, S.; Nemeth, D.; Williams, K. *J. Am. Chem. Soc.* **1987**, *109*, 5033-5035.
- (b) Hamilton, A. D.; Van Engen, D. *J. Am. Chem. Soc.* **1987**, *109*, 5035-5036
12. Joule, J. A.; Smith, G.F. *Heterocyclic Chemistry*, 2nd ed.; Van Nostrand Reinhold: London, 1978.
13. See references 10 and 11 in Chapter 1.
14. We have also observed a similar ion-dipole effect in a *meta*-xylyl-linked macrocycle. In this case, the effect is worth  $\approx 2$  kcal/mol.<sup>1</sup>

**Appendix A:**  
**Calculated D Values for**  
**Host/ Guest Complexes**

**5CMESO**

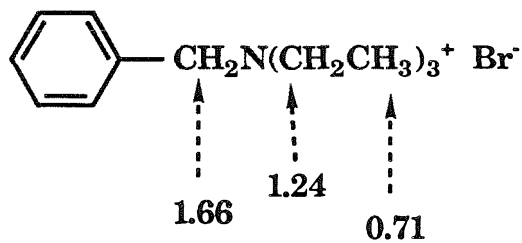
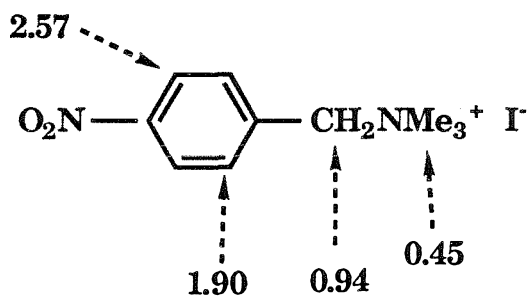
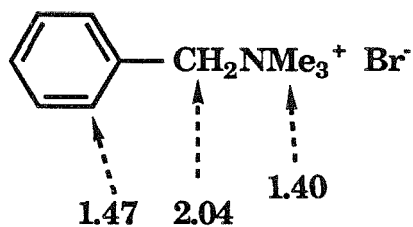
## Calculated D values (in ppm)

Host: 5CMESO

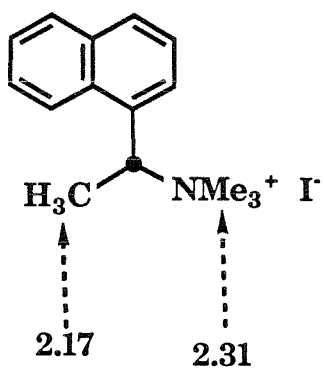
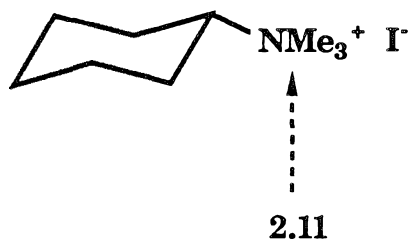
1.83 -----> NMe<sub>4</sub><sup>+</sup> OH<sup>-</sup>

## Calculated D values (in ppm)

Host: 5CMESO

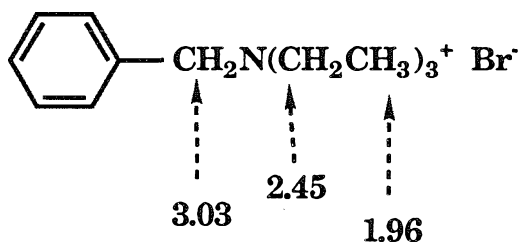
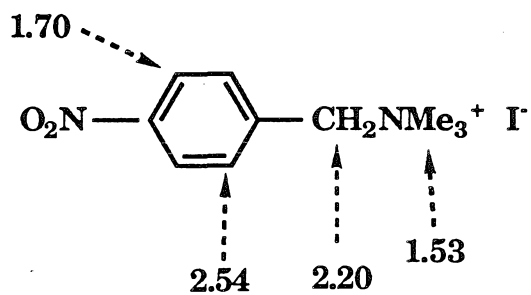
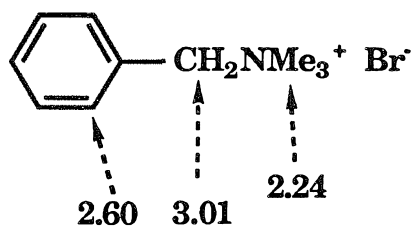


**PMESO**

**Calculated D values (in ppm)****Host: PMESO**

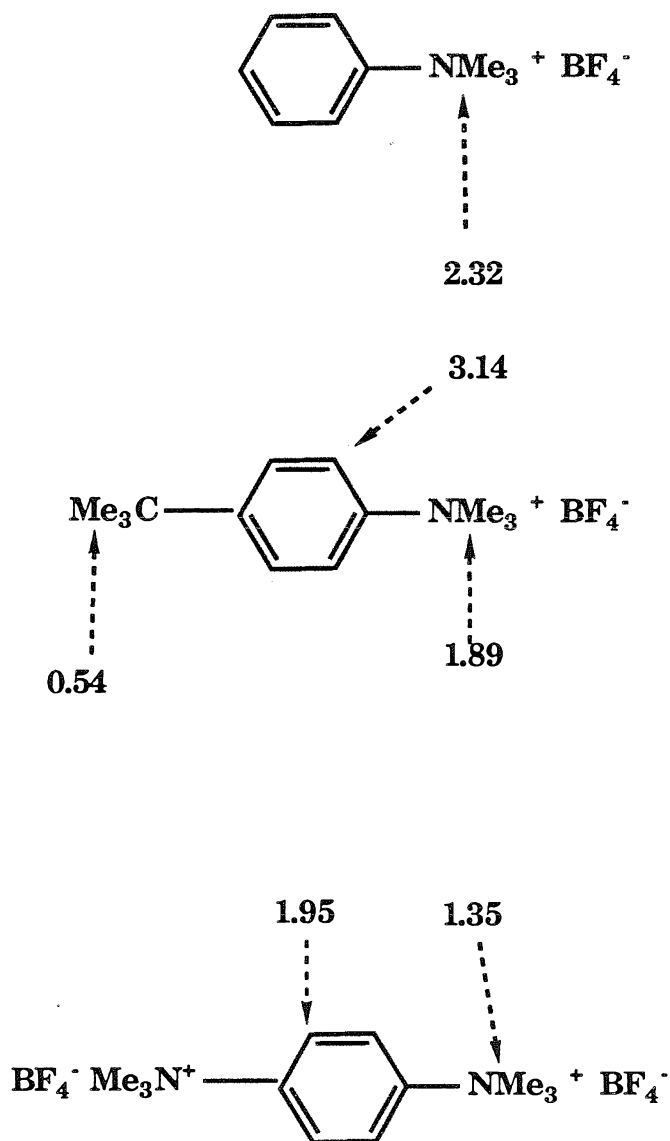
## Calculated D values (in ppm)

Host: PMESO



## Calculated D values (in ppm)

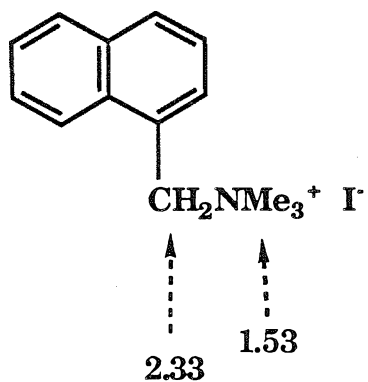
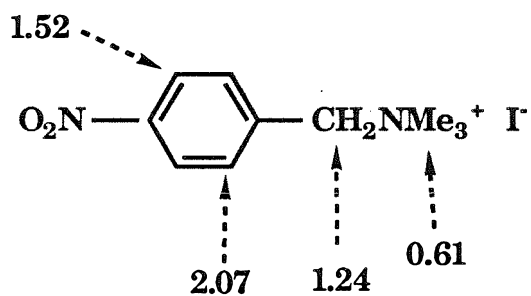
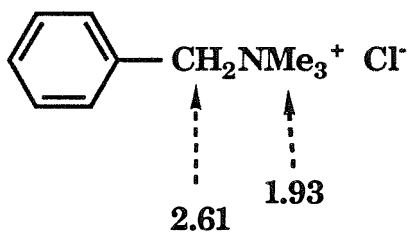
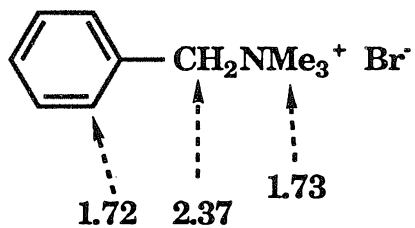
Host: PMESO



**5CDL**

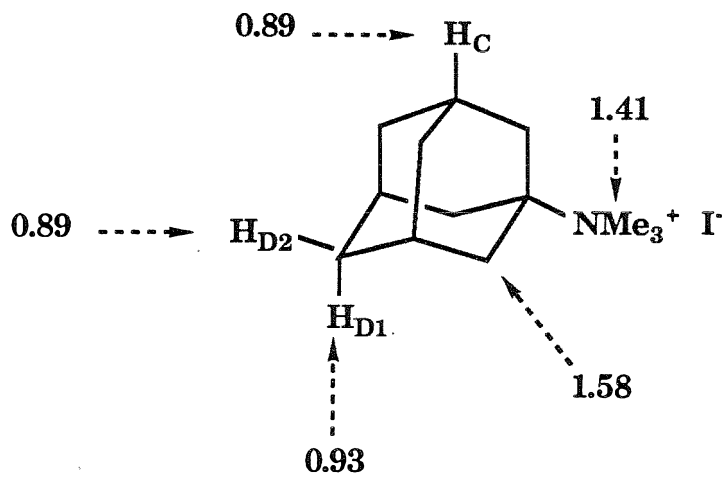
## Calculated D values (in ppm)

Host: 5CDL



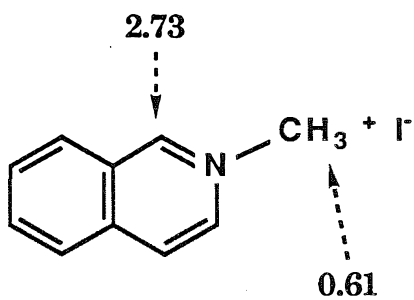
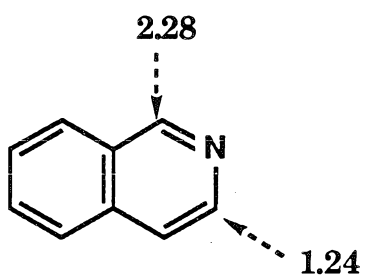
## Calculated D values (in ppm)

Host: 5CDL



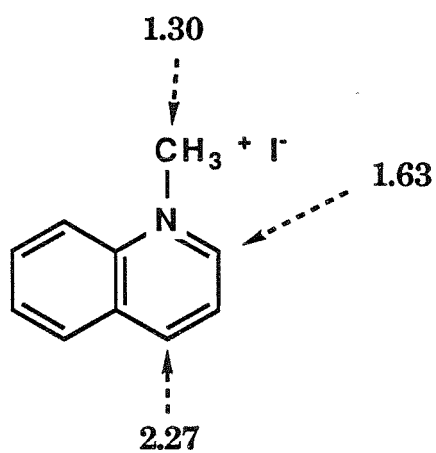
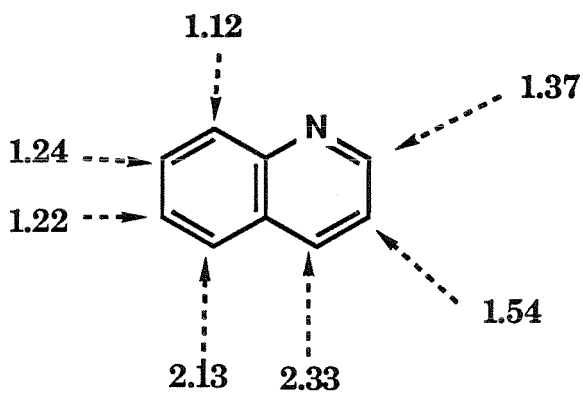
## Calculated D values (in ppm)

Host: 5CDL



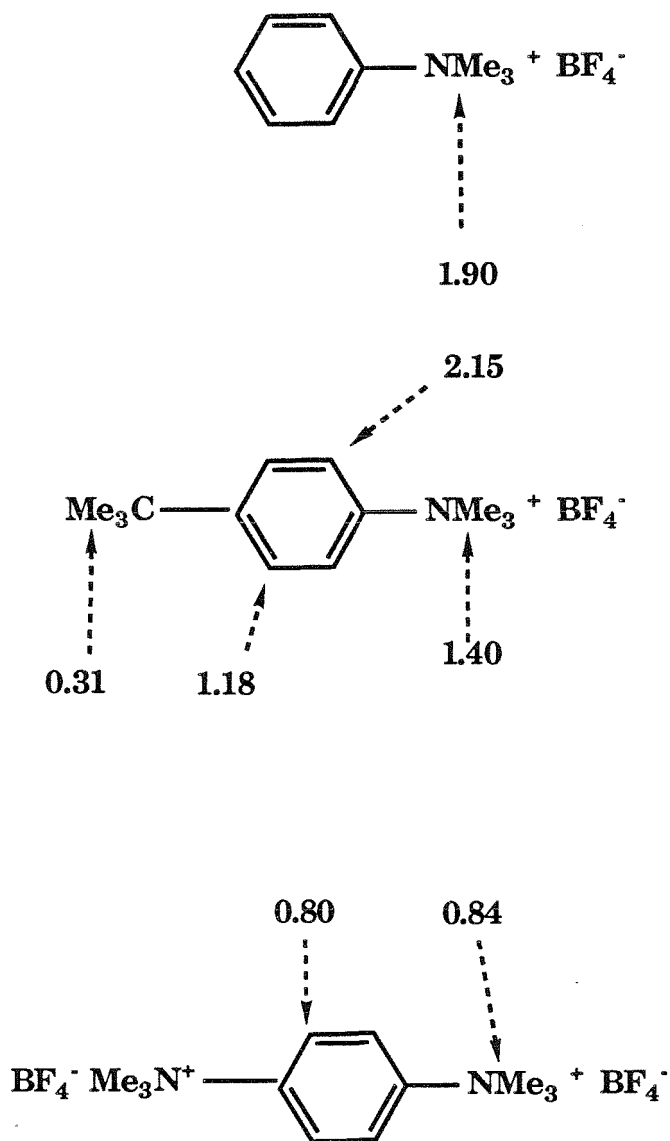
## Calculated D values (in ppm)

Host: 5CDL



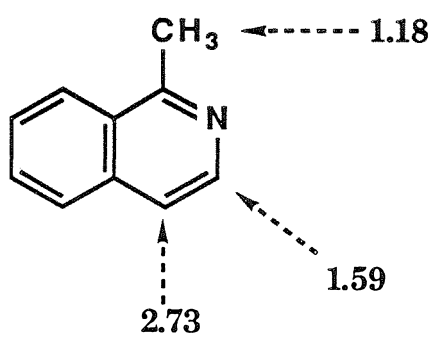
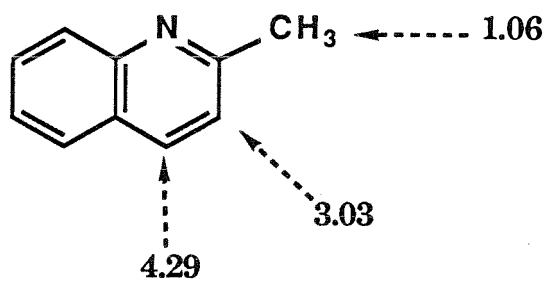
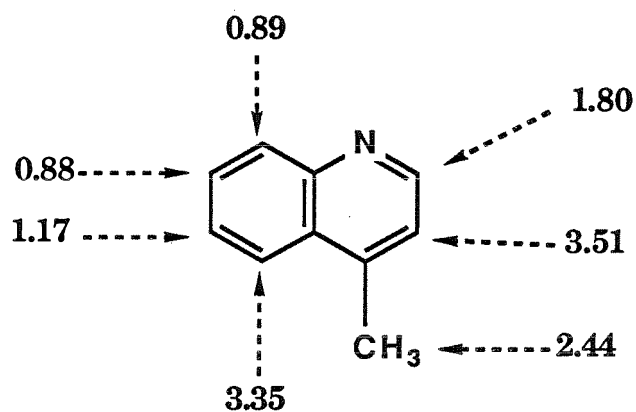
## Calculated D values (in ppm)

Host: 5CDL



## Calculated D values (in ppm)

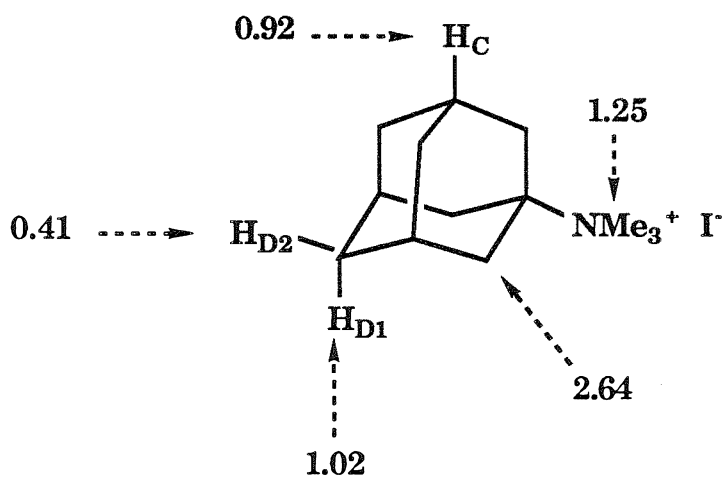
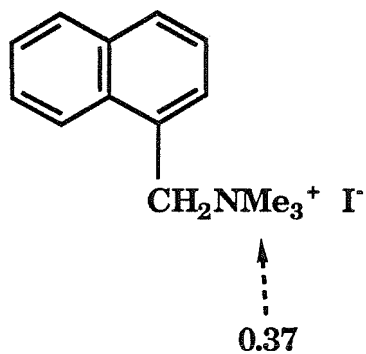
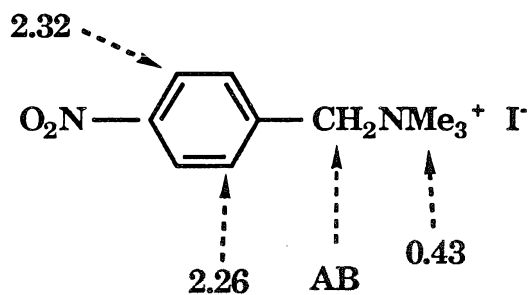
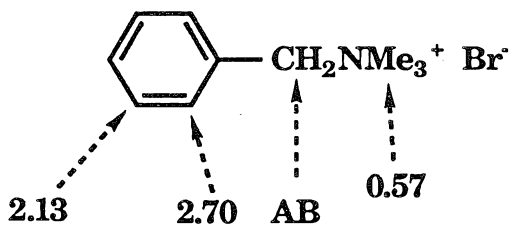
Host: 5CDL



**C6-L**

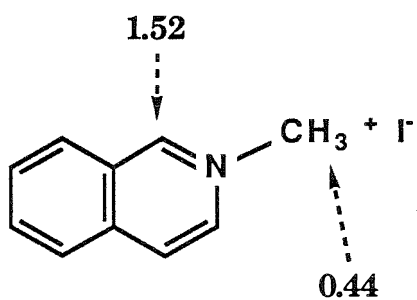
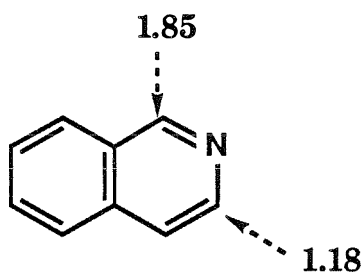
## Calculated D values (in ppm)

Host: C6-L



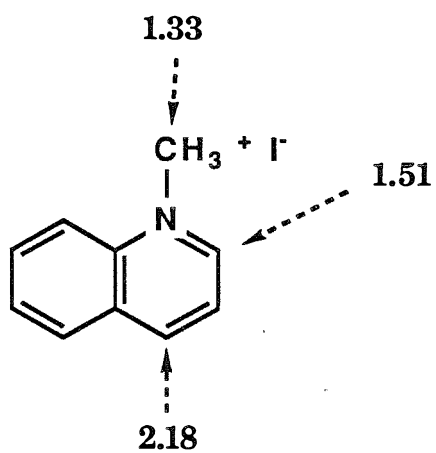
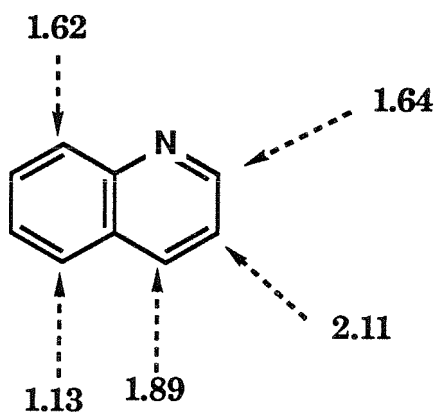
## Calculated D values (in ppm)

Host: C6-L



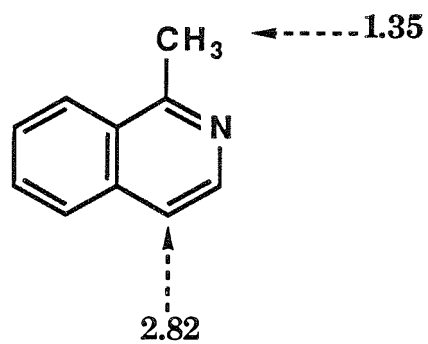
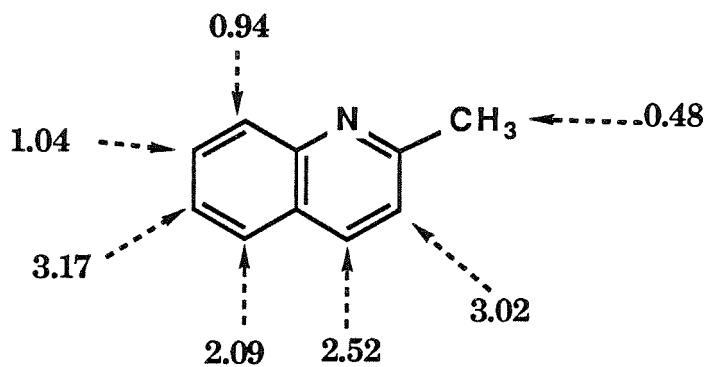
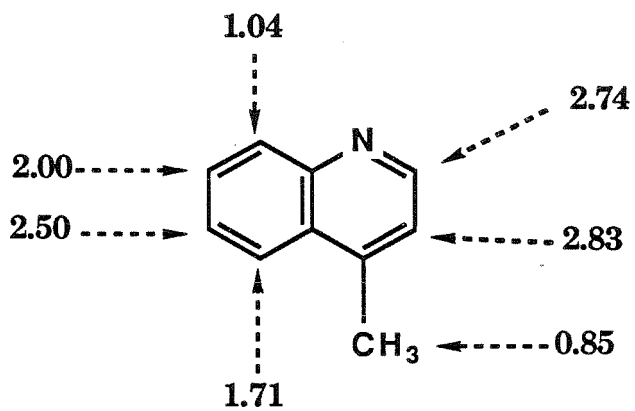
## Calculated D values (in ppm)

Host: C6-L



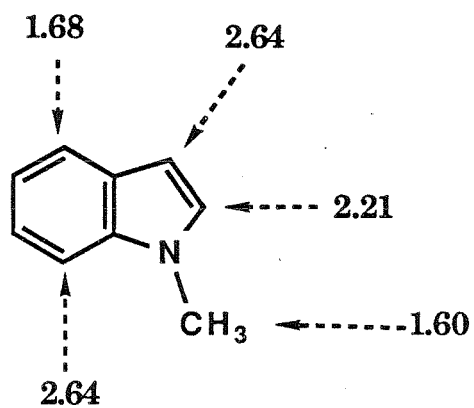
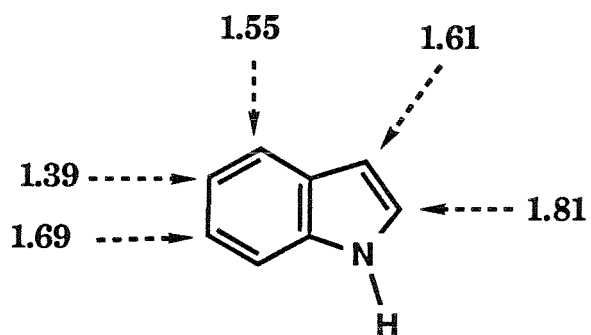
## Calculated D values (in ppm)

Host: C6-L



## Calculated D values (in ppm)

Host: C6-L



**Chapter 5**

**Design and Synthesis of Novel Building  
Blocks to New Host Structures**

This chapter describes our efforts directed towards the synthesis of new basic building blocks for novel host structures. These target structures were designed with certain structural constraints and properties in mind. The hosts derived from these building blocks could have some novel properties that we desired. Figure 5.1 shows the structures that we have prepared.

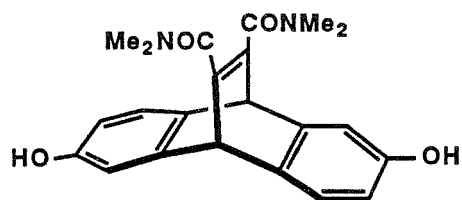
### Solubilization at Neutral pH

The carboxylate-based hosts described in Chapter 2 function quite well as molecular receptors. However, the operative pH range for these structures is limited, and a similar type of host structure having a much broader range of solubility could be very useful. One group that is soluble over a larger pH range is the quaternary ammonium group. This group has been used by ourselves and others<sup>1</sup> to introduce water solubility into otherwise lipophilic molecules. We envisioned that placing these groups exterior to our macrocycles would also allow for a greater range of water solubility. Therefore, we attempted the synthesis of precursors to such quaternary ammonium-ion based hosts.

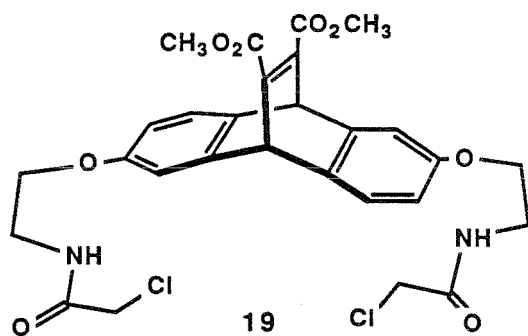
Scheme 5.1 outlines our proposed synthetic route; bis-amide, **18**, is the key precursor to the macrocycles. Macrocyclization of **18** with an appropriate linker, followed by reduction and exhaustive methylation would provide a macrocycle with four exterior alkyltrimethylammonium groups. Such a substance would be highly crystalline and water-soluble from pH=4 to pH=10.

We set out to synthesize bis-amide, **18**, by a modification of our Diels-Alder technology. Furthermore, we modeled some of the unknown steps in the

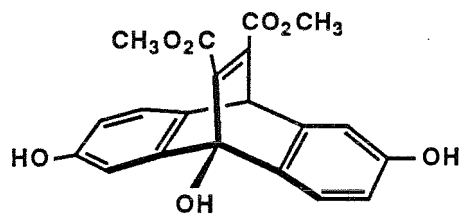
## SYNTHETIC TARGETS



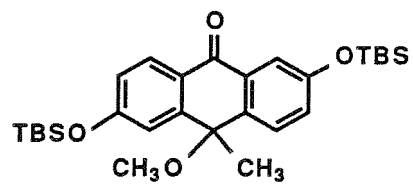
18



19

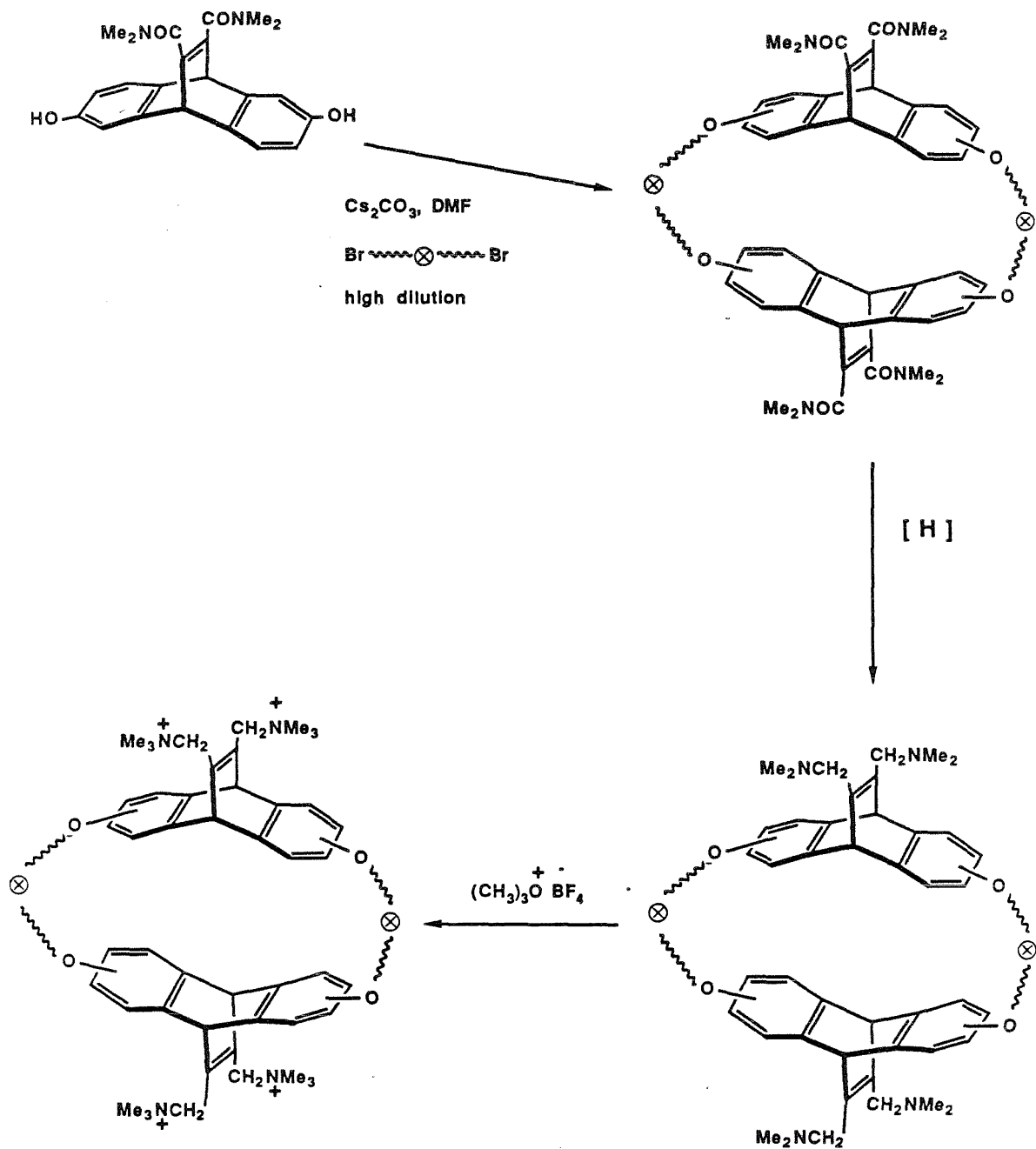


20



21

FIGURE 5.1: Novel Building Blocks



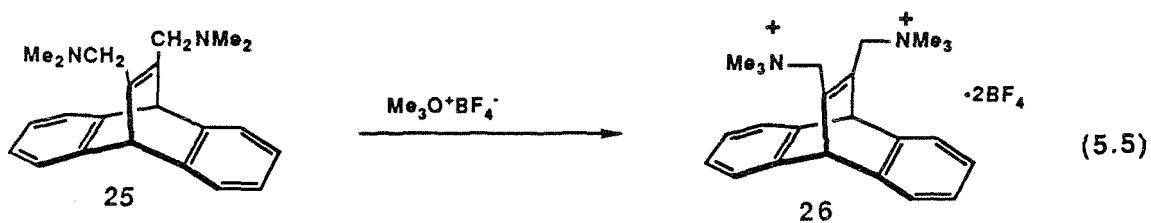
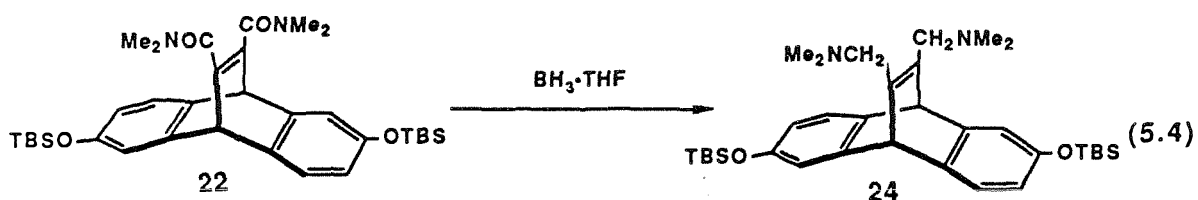
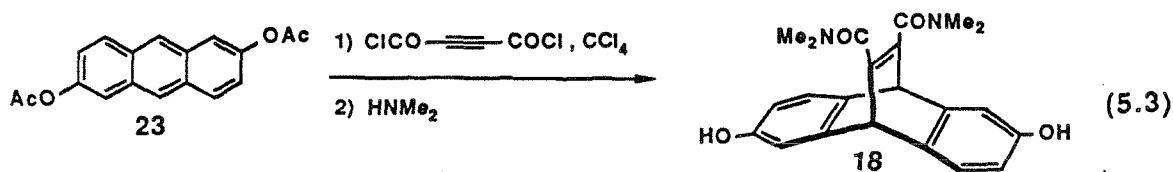
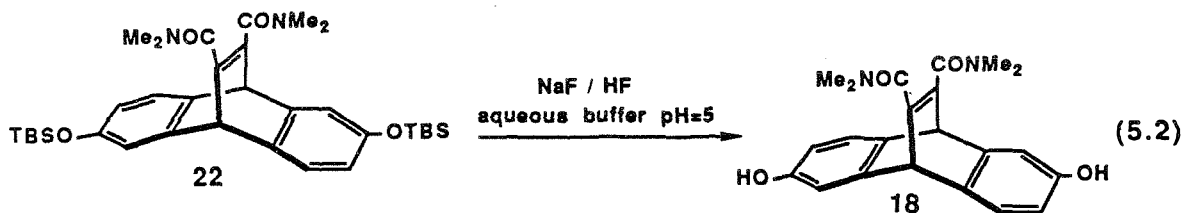
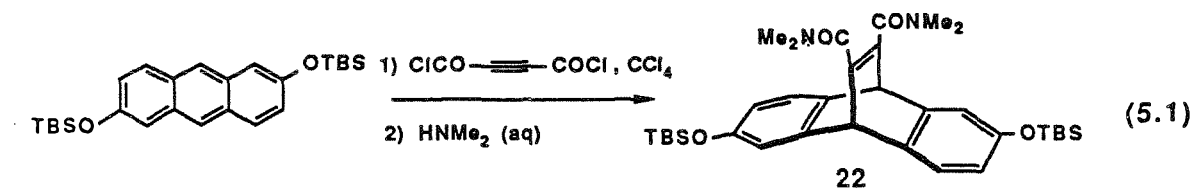
**SCHEME 5.1:** Proposed Synthetic Route to Alkylammonium-Based Macrocyclic Host System

overall synthetic scheme. Scheme 5.2 details the results of our synthetic efforts.

An analysis of the literature revealed that the only easily prepared acetylene bis-carboxamide was the parent compound prepared from dimethylacetylene dicarboxylate and ammonium hydroxide.<sup>2</sup> This material was difficult to purify, very insoluble in organic solvents and sluggish in Diels-Alder reactions. We therefore sought out the more powerful dienophile, acetylenedicarbonyldichloride.<sup>3</sup> This molecule is a potent dienophile and will add to furan<sup>3</sup> under certain conditions. It readily adds to 2,6-bis-*tert*-butyldimethylsiloxyanthracene, **9**, or to 2,6-diacetoxyanthracene, **23**, (eqns 5.1 and 5.3, respectively, in Scheme 5.2). The reaction mixture, when quenched with either neat or aqueous dimethylamine, affords the amide derivatives **22** and **18**, respectively.

This Diels-Alder reaction is capricious at best. The formation of the dienophile, as called for in the literature procedure,<sup>3</sup> requires that argon be bubbled through the solution vigorously. We have found that this is crucial to the success of the reaction. The dienophile is formed in high yield if the solution is vigorously degassed during dienophile formation, if efficient condenser ( $<0$  °C) cooling is provided for the reaction vessel, and if a large reaction vessel is employed. The two most common problems are no formation of the dienophile and the addition of HCl to the triple bond of the dienophile. The resulting fumarate derivative unfortunately often undergoes the Diels-Alder reaction.

In the quenching of the reaction mixture with dimethylamine, the acetate protecting groups are removed to afford the amidephenol **18** directly (eq 5.3). However, the Diels-Alder reaction of **23** with acetylenedicarbonyldichloride (eq 5.3) is more sluggish than the analogous reaction of **9** with



SCHEME 5.2: Synthetic Routes to Exocyclic Amines

acetylenedicarbonyldichloride (eq. 5.1). While both methods (eqs. 5.1 and 5.3) are capable of being scaled up, the isolation of the amidephenol **18** is difficult due to its appreciable water solubility. The two-step sequence (eqs. 5.1 and 5.2) allows for easier isolation of the products. While the pH=5 fluoride buffer was used to remove the silyl protecting groups (eq. 5-2), any mineral acid would probably be equally effective (*vide supra*).

The reduction of the *N,N*-dimethylamides to *N,N*-dimethylamines without concomitant reduction of the double bond was easily achieved with borane-tetrahydrofuran complex (Eq. 5.4).<sup>4,5</sup>

To model the final step in the synthetic scheme, bisamine **25** was quaternized with Meerwein's reagent.<sup>6</sup> While other alkylating agents (iodomethane, dimethylsulfate) gave incomplete reaction, Meerwein's reagent gave the product rapidly and cleanly provided that the starting amine was free from water.<sup>6</sup>

### Macrobicyclic Host Systems

The design and synthesis of macrobicyclic hosts for use in the study of molecular recognition have received some attention.<sup>7</sup> While these types of molecules can be difficult to synthesize, the possible advantages that they offer can outweigh their painstaking synthesis.

We envisioned that our basic host skeleton could easily be transformed into a macrobicyclic array. Figure 5.2 shows two possible topographies for macrobicyclic hosts, derived from our published system. We thought that the obvious points to attach a tether would be from the middle of one linker to the middle of another or from the bridgehead position of one ethenoanthracene to the bridgehead position of the other. We hoped that if the synthesis were successful, such molecules would provide us with systems having a deeper

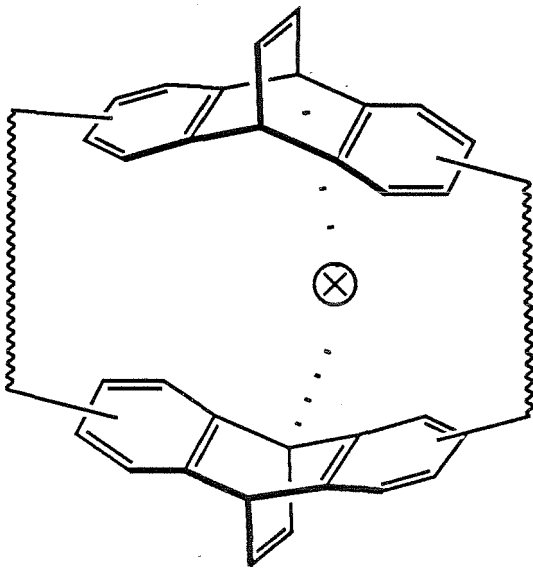
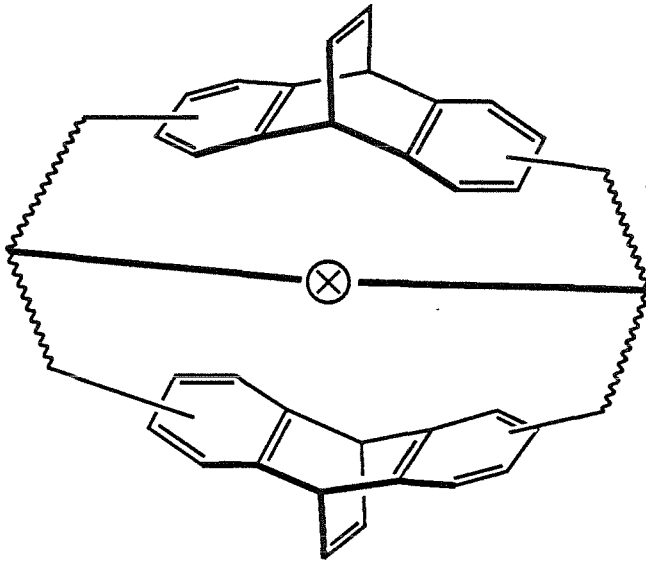


**FIGURE 5.2:** Two possible Topographies for Macrobicyclic Host Geometries

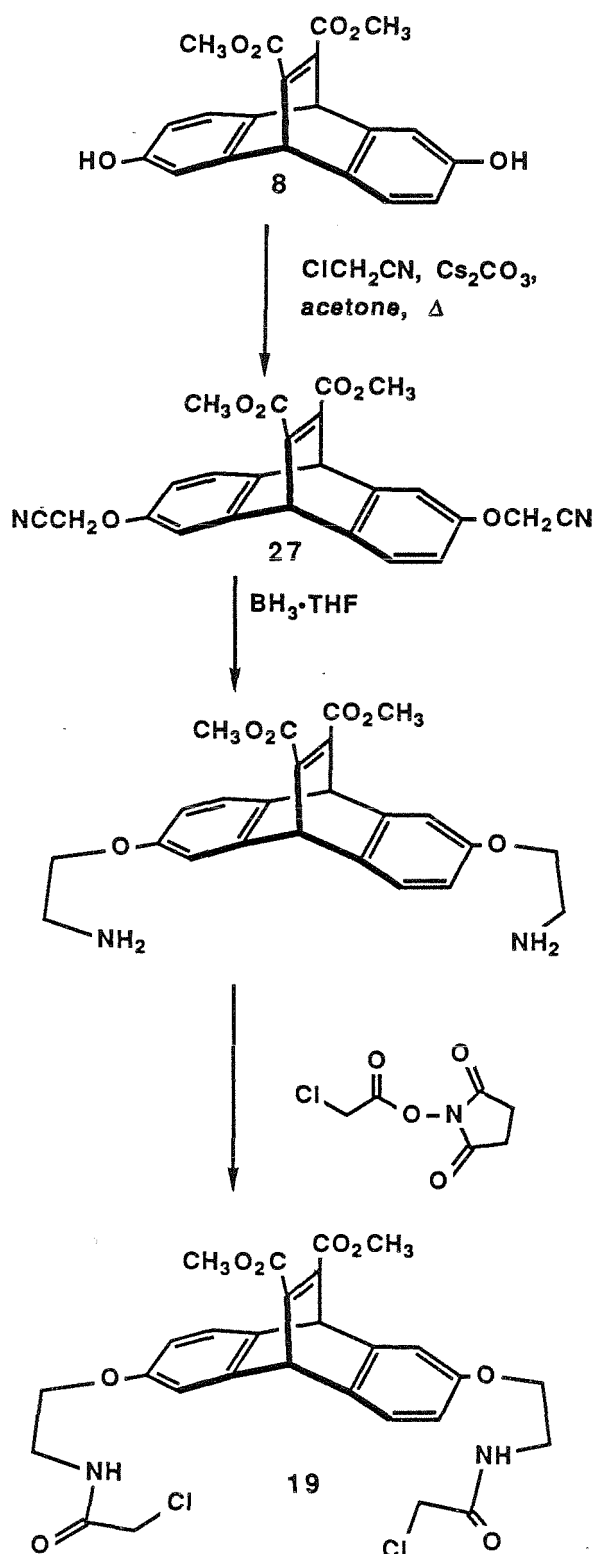
binding site to provide for more efficient encapsulation of the guest. Furthermore, by the appropriate placement of water-solubilizing groups on this macrobicycle, we hoped to raise the CMC of the host to allow for easier physical studies. The new tether that defines the macrobicycle could add rigidity to the host while also physically blocking one face of the host, thereby possibly slowing the on- or off-rates of a guest to or from the cavity. This rate decrease, if achieved, could simplify the physical studies; if both the guest and host-guest complex could be observed in the  $^1\text{H}$  NMR, the slow exchange limit would be reached, and simple integration of the signals would give the association constants.

### Linker Attachment Studies

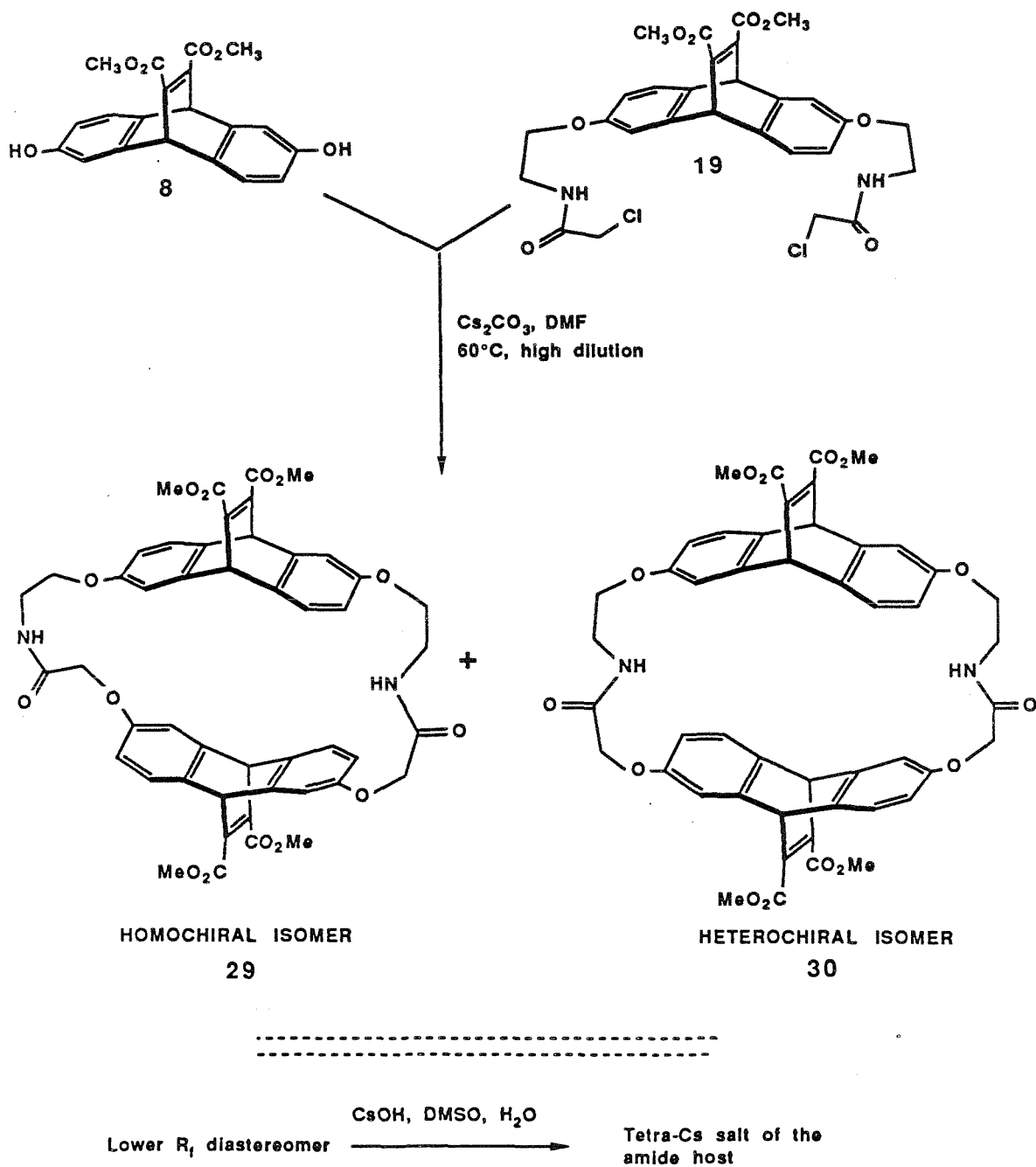
We chose to synthesize a macrocycle having amides in the linkers as a precursor to a macrobicyclic molecule. We reasoned that the amides would survive most of the proposed synthetic procedures and, when needed, they could be reduced to amines and then further elaborated.

Scheme 5.3 outlines the synthesis of the necessary building block, an  $\alpha$ -chloroamide, **19**; the coupling of this  $\alpha$ -chloroamide with our basic diphenol building block would afford a new series of macrocycles, the amide-linked macrocycles (Scheme 5.4).

Alkylation of the diphenol **8** with chloroacetonitrile in gently refluxing acetone with  $\text{Cs}_2\text{CO}_3$  as base led to dinitrile, **27**. The dinitrile could be reduced with  $\text{BH}_3\cdot\text{THF}$ <sup>8</sup> to the diamine, **28**, which was easily acylated with the *N*-hydroxysuccinimide ester<sup>7</sup> of chloroacetic acid to provide the bis  $\alpha$ -chloroamide. The only difficult step in this sequence is the borane reduction of the nitrile. The yield was low; while no evidence of reduction of the double bond was found, it was possible that this was the problem. However, on more



**SCHEME 5.3:** Synthesis of Chloroamide Building Block



**SCHEME 5.4:** Macrocyclization of Chloroamide and Diphenol to form the two Amide Macrocycles

than one occasion, one of the major products of the reaction mixture was mono-nitrile mono-amine. Despite the use of large excesses of borane, this problem could not be overcome. The reaction had to be conducted at as high a concentration as possible to achieve a reasonable reaction rate; however, this resulted in the formation of a polymer-like material (possibly a polymeric  $\text{BH}_3\cdot\text{NH}_2\text{-R}$  complex) before workup that would not dissolve upon the addition of more THF. Thus, slow diffusion of the  $\text{BH}_3\cdot\text{THF}$  into this polymeric material may be the reason for the low yield. Nevertheless, the product can be isolated in the workup.

Macrocyclization (Scheme 5.4) proceeded cleanly, with no difficulties. As before (Chapter 2), since both materials are racemic, two diastereomers, **29** and **30**, are produced. In this case, both the homochiral coupling product and the heterochiral coupling product have  $C_2$  symmetry. Their  $^1\text{H}$  and  $^{13}\text{C}$  NMR spectra (see the Experimental Section) confirm the reduced symmetry of these structures. Unfortunately, direct assignment of the stereoisomers is not possible in this case. Fortunately, in this case, these diastereomers are separable by conventional chromatography without the need to resort to HPLC.

The  $^1\text{H}$  NMR spectra (Figure 5.3) suggest that these two diastereomers have quite different conformations. While each pair of all of the simple aliphatic-linked macrocycles described earlier (see Chapter 2) had very similar NMR spectra, these amide-linked macrocycles are very different; the higher  $R_f$  diastereomer experiences significant shielding of some of its aromatic protons. The spectra of both diastereomers is complicated by the fact that these molecules are dynamic, and some broadening of the signals is observed. While it is tempting to assign relative configurations of these molecules based on these data and CPK models, the lack of any precedent in

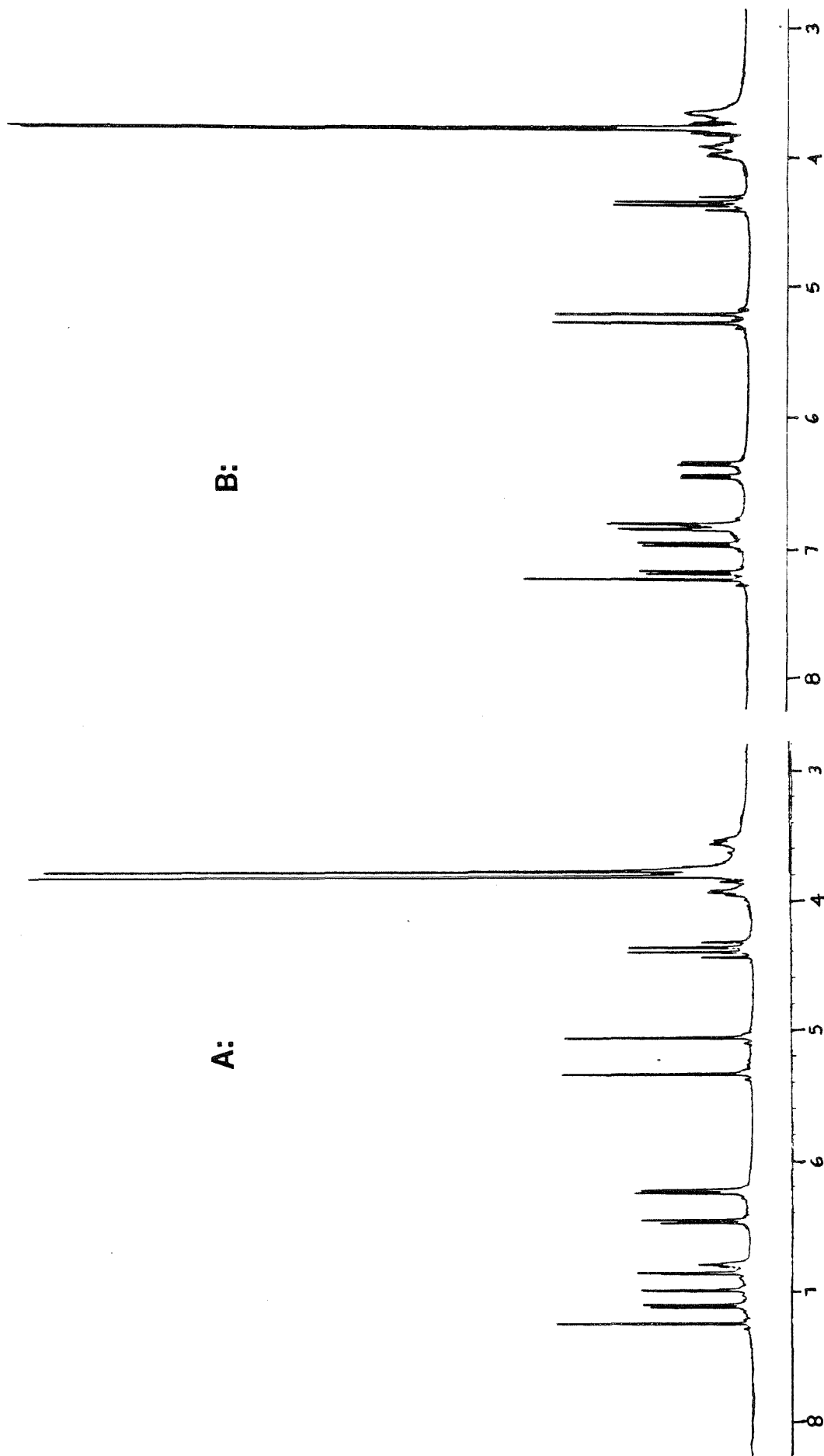


FIGURE 5.3: <sup>1</sup>H NMR spectra of amide diastereomers:

A= higher R<sub>f</sub> diastereomer, B= lower R<sub>f</sub> diastereomer

these systems or convincing conformational evidence on these types of amides requires that the question be left unanswered. The relative configurational assignment awaits the completion of the synthesis in the optically active series.<sup>9</sup>

Our standard hydrolysis conditions (CsOH (10 eq), THF or DMSO, H<sub>2</sub>O, 24 hrs) led to hydrolysis of the amides. Modification of the conditions (CsOH (5 eq), DMSO, H<sub>2</sub>O, 2.5 hours) led to clean hydrolysis of the esters without any cleavage of the amide linkers.<sup>10</sup> The lower R<sub>f</sub> diastereomer was hydrolyzed in this manner and used in subsequent studies. Since this was a new type of host structure, we performed some simple physical studies to determine some of its properties. The CMC of this host was determined by the NMR method.<sup>11</sup> The change in chemical shift of the protons of this host as a function of concentration indicates that the CMC is ~1 mM (see Figure 5.4). The sub-CMC <sup>1</sup>H NMR spectrum (D<sub>2</sub>O) of this molecule is quite different from the <sup>1</sup>H NMR spectrum in DMSO-d<sub>6</sub>, which is different from that of the tetraester precursor. All of these data argue for a highly solvent-dependent conformation of these amide-linked macrocycles.

We also were interested in this molecule's ability to bind a guest. The <sup>1</sup>H NMR spectrum of this amide-linked macrocycle (pH = 9, Cs<sub>2</sub>HPO<sub>4</sub> buffer) and adamantyltrimethylammonium iodide (ATMA) did not reveal any of the dramatic upfield shifts that we had observed with other hosts and ATMA. The small shifts could be analyzed nonetheless and the association constant, K<sub>a</sub>, was determined to be ~250 M<sup>-1</sup>. This association constant represents approximately an order of magnitude drop from the all hydrocarbon-linked macrocycles. While the reason for this drop is not clear at the present time, the response to a simple change in the linker hydrophobicity is quite dramatic.

## CMC Study of Amide Macrocycle

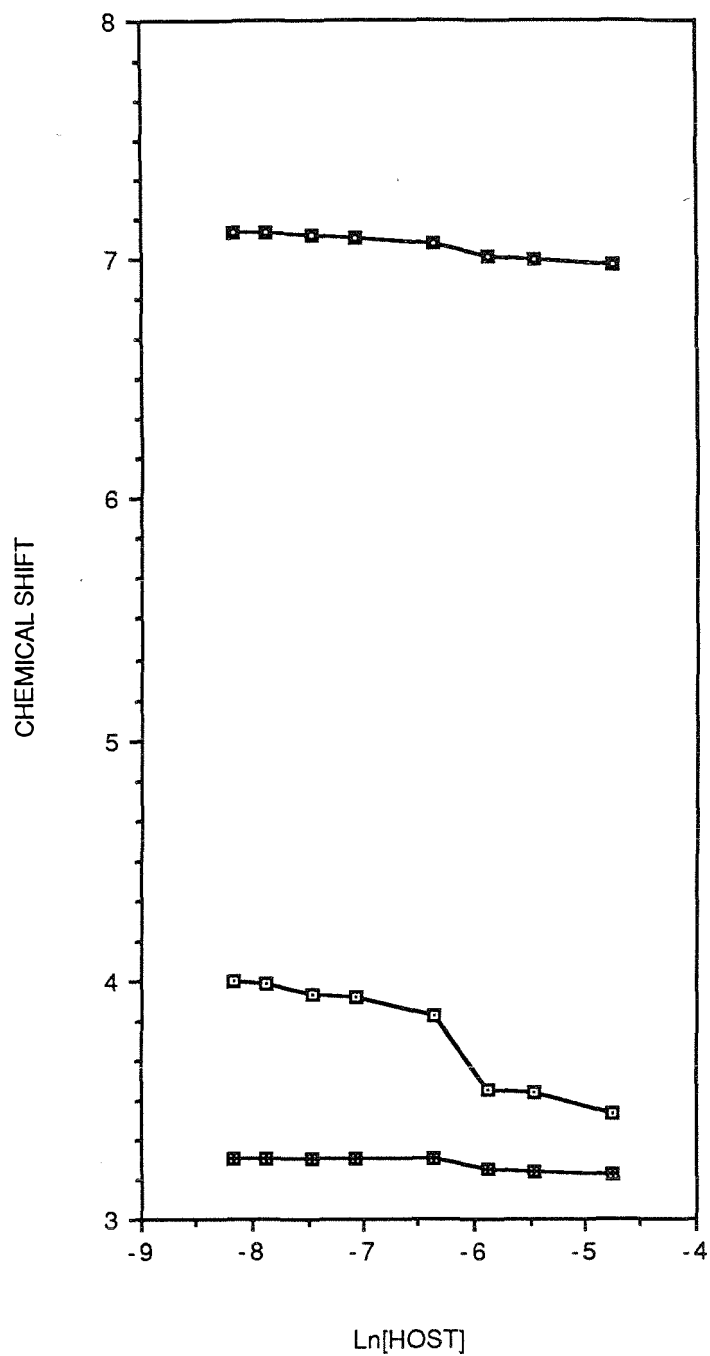


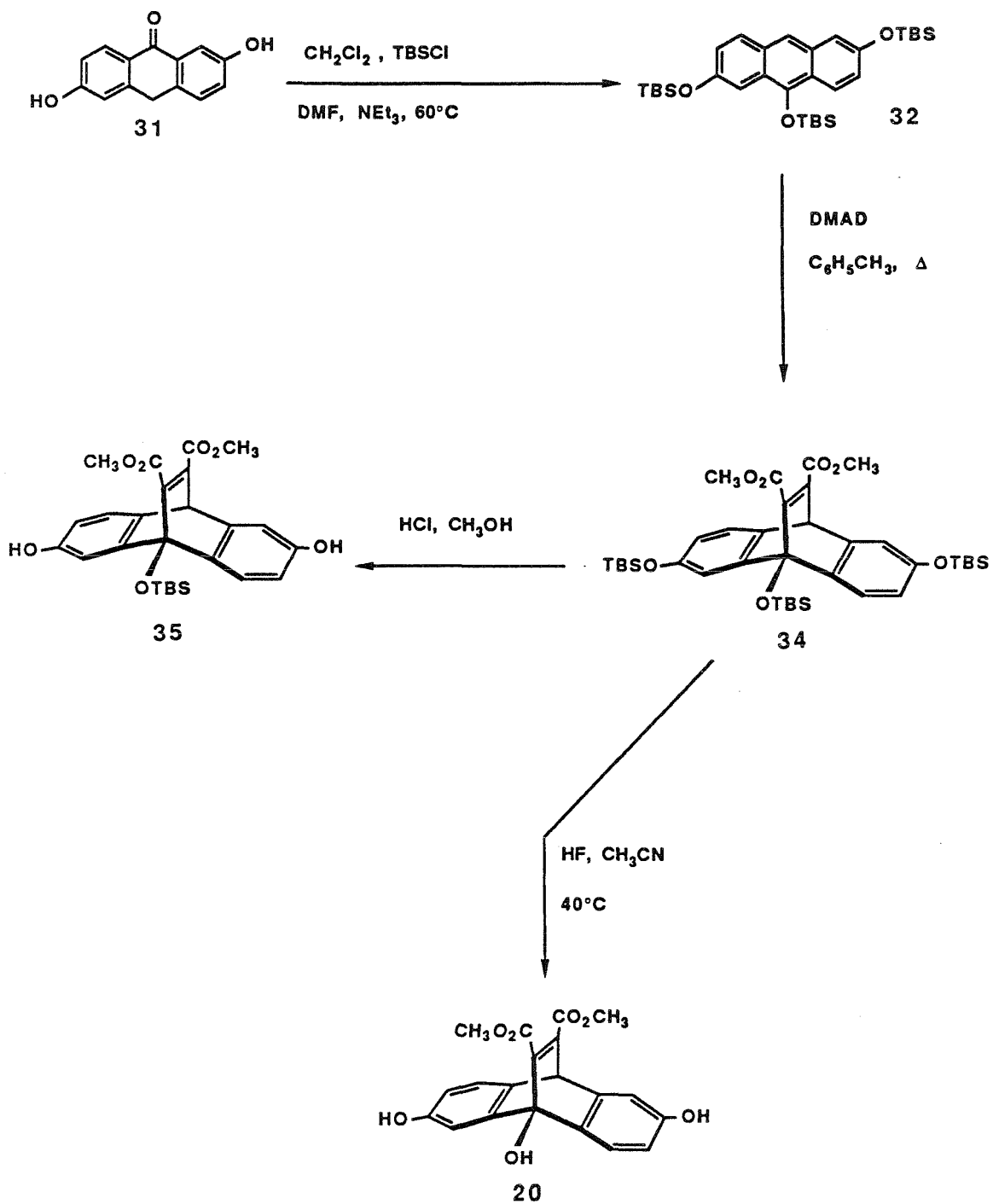
FIGURE 5.4: CMC Determination of macrocyclic amide

The further elaboration of these amide-linked macrocycles into macrobicycles would be straightforward. Reduction of the amides to amines and coupling with a bisfunctional tether would provide the requisite topography. This amine intermediate could be used to attach other functional groups with either catalytic or transport ability. This synthetic route is flexible enough to allow the introduction of a variety of groups for a number of specified purposes.

### Bridgehead Functionalization

The construction of a macrobicyclic framework where the third tether is between bridgeheads is synthetically more difficult. The synthesis of triol, **20** (Figure 5.1), proved simple enough; however, derivatization of the tertiary alcohol was not possible (*vide infra*).

Scheme 5.5 outlines the synthetic routes to **20**. 2,6-Dihydroxyanthrone, when treated with triethylamine in  $\text{CH}_2\text{Cl}_2$ , was isomerized to the 2,6,9-anthracenetriol. These oxygens could be protected as *tert*-butyldimethylsilyl ethers by adding *tert*-butyldimethylsilyl chloride to this reaction mixture. Thin layer chromatography evidence suggested that this isomerization could be prevented if DMF was used in place of  $\text{CH}_2\text{Cl}_2$  as solvent. 2,6,9-Tris-*tert*-butyldimethylsiloxyanthracene, **32**, underwent a smooth Diels-Alder reaction with dimethylacetylene dicarboxylate. If this Diels-Alder adduct was exposed to HCl in  $\text{CH}_3\text{OH}$ , only the phenol protecting groups were removed. The use of warm HF in  $\text{CH}_3\text{CN}$  removed all three of the protecting groups. Current results from this laboratory<sup>13</sup> indicate that boron trifluoride etherate might also be effective at removing all these silyl protecting groups. Attempts to derivatize the tertiary alcohol of **20** were completely unsuccessful. Acylation reactions and reactions with isocyanides were unsuccessful. The steric



SCHEME 5.5: Synthetic Route to Triol Building Block

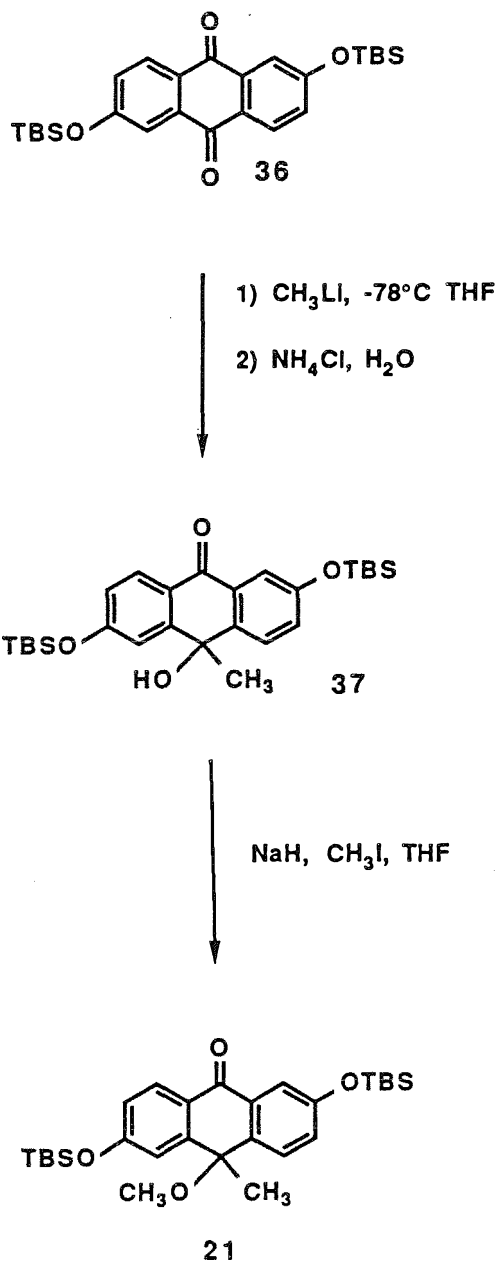
hindrance of this position may have contributed to the inability to derivatize this alcohol. These discouraging results prompted us to cease studies with this molecule.

This scheme to triol **20**, could also be attempted using triacetoxyanthracene as a starting material. However, upon attempted deacetylation with acid, only the phenolic acetates were removed. The bridgehead acetate was not easily removed. This would be a method to attach a specific group to the bridgehead position, provided the phenols could be regenerated (see Experimental Section for details).

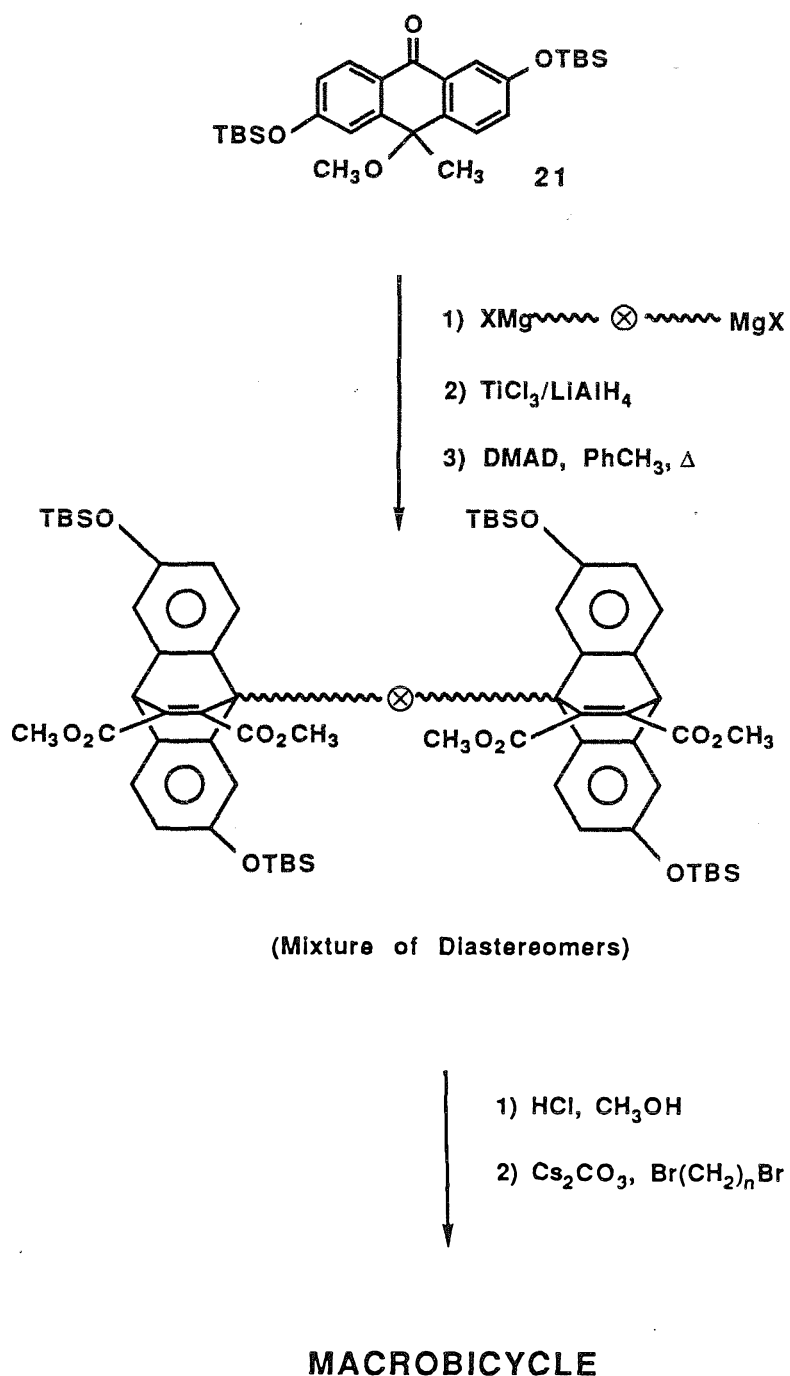
Other work from these laboratories<sup>14</sup> demonstrated the ability to add bridgehead substitution early on in the synthetic scheme. We adapted these results to synthesize the anthrone **21**. Scheme 5.6 shows our synthetic results. The bis-protected anthraflavic acid, **37**,<sup>14</sup> was allowed to react with  $\text{CH}_3\text{MgBr}$  at  $-78\text{ }^\circ\text{C}$  in THF to afford the tertiary alcohol. Careful examination of the reaction mixture indicated that small amounts of deprotection ( $<5\%$ ) had occurred. Nevertheless, good yields of the alcohol could be achieved. The use of MeLi at  $-78\text{ }^\circ\text{C}$  or at  $0\text{ }^\circ\text{C}$  led to deprotection as the major product of the reaction.

The alkylation of this tertiary alcohol proved difficult at best. The use of DMF as solvent led to deprotection, with isolation of phenyl methyl ether type products. The best yield was achieved using THF as solvent, NaH as base and dimethylsulfate as alkylating agent.

Both these steps proved to be more difficult than we had anticipated and the overall synthetic scheme (Scheme 5.7) was not pursued. Nevertheless, if the alkylation reaction could be improved, this method could prove to be a route to macrobicycles.



**SCHEME 5.6:** Synthetic Route to the Asymmetric Anthrone



**SCHEME 5.7:** Overall Synthetic Scheme for Macrobicyclic Synthesis, starting from the Asymmetric Anthrone

## EXPERIMENTAL SECTION

General:  $^1\text{H}$  NMR spectra were recorded on a Varian EM-390 spectrometer. Fourier transform NMR spectra ( $^1\text{H}$  and  $^{13}\text{C}$ ) were recorded on a JEOL FX-90Q, a Varian XL-200 or a JEOL GX-400 spectrometer. All coupling constants are in hertz. Mass spectra were performed by Regional MS Facilities (UCR and U Neb). All column chromatography was performed by the method of Still.<sup>15</sup>

**2,6-Dihydroxy-9,10-dihydro-9,10-(*N,N,N',N'*-tetramethyldicarboxamido)ethenoanthracene (18)**

To a suspension of acetylene dicarboxylic acid (58 mg, 0.51 mmol, 1.5 eq) in 5 mL of  $\text{CCl}_4$  was added  $\text{PCl}_5$  (223 mg, 1.02 mmol, 3.0 eq). 2,6-Diacetoxyanthracene was added and the reaction refluxed for 2 hours. A  $-10^\circ\text{C}$  condenser was used to efficiently cool the  $\text{CCl}_4$  vapors. Pure dimethyl amine (condensed from a cylinder  $\sim 6$  mL) was transferred into the cooled reaction vessel. The reaction was stirred at  $0^\circ\text{C}$  for 3 hours and at room temperature for 0.5 hour. The solvent was removed and the material pumped on overnight. Twenty milliliters of 1 N HCl was added and the material was continuously extracted with  $\text{Et}_2\text{O}$  (100 mL) for 24 hours. This procedure was called for since the product had some water solubility. The  $\text{Et}_2\text{O}$  was concentrated and  $\text{CHCl}_3$  was added. The product precipitated. The product was filtered giving 48 mg of a solid (38%).  $^1\text{H}$  NMR ( $\text{CD}_3\text{OD}$ ):  $\delta$  7.15 (d, 2H,  $J=7.8$ ), 6.84 (d, 2H,  $J=2.2$ ), 6.39 (dd, 2H,  $J=7.8, 2.2$ ), 5.04 (s, 2H), 2.91 (s, 6H), 2.71 (s, 6H).  $^{13}\text{C}$  NMR ( $\text{CD}_3\text{OD}$ ):  $\delta$  170.00, 155.62, 147.65, 146.65, 136.38, 124.58, 112.26, 111.29, 53.74, 38.82, 35.06. MS: (m/e) 378 ( $\text{M}^+$ ), 335, 235, 210, 72(100).

*Alternatively:*

To a solution of the TBS ether, **22**, (1.5g, 2.48 mmol) in 10 mL of THF was added 10 mL of a pH=5 NaF/HF buffer. The reaction was stirred for 3 days. Twenty-five milliliters of CH<sub>3</sub>OH was added and the reaction concentrated. Chloroform was added and the precipitated solid was filtered off (510 mg, 54%).

**2,6-Bis(tert-butyldimethylsiloxy)-9,10-dihydro-9,10-(*N,N,N',N'*-tetramethyldicarboxamido)ethenoanthracene (**22**)**

To a suspension of acetylene dicarboxylic acid (43 mg, 0.375 mmol, 1.5 eq) in 4 mL of dry CCl<sub>4</sub> was added PCl<sub>5</sub> (165 mg, 0.75 mmol, 3 eq). Argon was efficiently bubbled through the solution to remove the evolved HCl. An efficient condenser was used to catch the CCl<sub>4</sub> vapors. 2,6-Bis-*tert*-butyldimethylsiloxyanthracene **9** (110 mg, 0.25 mmol, 1 eq) was added and the solution refluxed for 13 hours. This solution was cannulated into 5 mL of aqueous dimethylamine and stirred for 0.5 hour. This solution was extracted with hexane (3×-10 mL each). The organic layer was dried over Na<sub>2</sub>SO<sub>4</sub>, filtered and concentrated. The product was isolated in ~65% yield via chromatography over SiO<sub>2</sub>, using the ethyl acetate as an eluant. <sup>1</sup>H NMR (CDCl<sub>3</sub>): δ7.10 (d, 2H, *J*=8.05), 6.79 (d, 2H, *J*=2.19), 6.38 (dd, 2H, *J*=8.05, 2.19), 4.96 (s, 2H), 2.86 (broad singlet, 6H), 2.56 (broad singlet, 6H), 0.89 (s, 18H), 0.085 (s, 6H), 0.082 (s, 6H). <sup>13</sup>C NMR (CDCl<sub>3</sub>): δ168.05, 152.43, 145.86, 143.44, 136.69, 123.41, 115.67, 115.08, 52.63, 38.12, 34.59, 25.75, 18.25, -4.19.

**2,6-Diacetoxyanthracene(23)**

To a salt-ice cooled ( $-10\text{ }^{\circ}\text{C}$ ) suspension of 2,6-dihydroxyanthracene, **7**, (1g, 4.8 mmol, 1eq) in 50 mL of  $\text{CH}_2\text{Cl}_2$  were added DMAP (58 mg, 0.48 mmol, 0.1 eq) and 1.9 mL (23.8 mmol, 5 eq) of pyridine. The acetic anhydride (2.3 mL, 23.8 mmol, 5 eq) was added via syringe over 8 minutes. The reaction was stirred at  $-10\text{ }^{\circ}\text{C}$  for 1.5 hours. Twenty milliliters of 1 N HCl was added. The reaction was extracted with  $\text{CH}_2\text{Cl}_2$  ( $2\times$ -25 mL). The  $\text{CH}_2\text{Cl}_2$  layer was dried over  $\text{MgSO}_4$  and concentrated. The solid residue was recrystallized from benzene to give 1.03 g (73% yield) of the product as an off-white solid.  $^1\text{H}$  NMR ( $\text{CDCl}_3$ ):  $\delta$ 8.36 (s, 2H), 7.97 (d, 2H,  $J=9$ ), 7.68 (d, 2H,  $J=2.2$ ), 7.22 (dd, 2H,  $J=9, 2.2$ ), 2.36 (s, 6H).

**2,6-Bis(tert-butyltrimethylsilyloxy)-9,10-dihydro-9,10-(1,2-bisdimethylaminomethyl)ethenoanthracene (24)**

To an ice-cooled solution of the bisamide, **22** (180 mg, 0.30 mmol, 1 eq) in 1 mL of freshly distilled anhydrous THF was added 6 mL of a 1M  $\text{B}_2\text{H}_6$  solution. The ice bath was removed and the reaction was refluxed for 1 hour. The reaction was cooled and water was added very slowly (VERY VIGOROUS REACTION:  $\text{H}_2$  EVOLUTION!). The solution was extracted with  $\text{Et}_2\text{O}$  ( $3\times$ -40 mL). The organic layers were combined, dried over  $\text{Na}_2\text{SO}_4$  and concentrated. The product (62 mg, 36% yield) was isolated as a viscous, colorless oil via chromatography over  $\text{SiO}_2$ , using 3:1  $\text{CH}_2\text{Cl}_2$ /Petroleum ether as an eluant.  $^1\text{H}$  NMR ( $\text{CDCl}_3$ ):  $\delta$ 7.09 (d, 2H,  $J=8.06$ ), 6.80 (d, 2H,  $J=2.2$ ), 6.41 (dd, 2H,  $J=8.06, 2.2$ ), 5.11 (s, 2H), 3.75 (s, 4H), 2.48 (s, 6H), 2.46 (s, 6H), 0.93 (s, 18H), 0.13 (s, 12H).  $^{13}\text{C}$  NMR ( $\text{CDCl}_3$ ): 152.55, 146.97, 145.83, 136.58, 123.56, 115.94, 115.15, 62.44, 55.87, 51.64, 51.59, 25.84, 18.37,  $-4.06$ ,  $-4.09$ .

**9,10-Dihydro-9,10-[1,2bis(trimethylammoniummethyl)]ethenoanthracene (26)**

To a solution of the diamine, **25** (26 mg, 0.0818 mmol, 1 eq) in 1 mL of  $\text{CHCl}_3$  was added 181 mg (1.23 mmol, 15 eq) of Meerwein's reagent with the aid of a dry box. The reaction was stirred for 12 hours. One milliliter of MeOH was added and the reaction was concentrated. The product could be isolated by precipitation from  $\text{Et}_2\text{O}$ .  $^1\text{H NMR}$  ( $\text{CDCl}_3$ ):  $\delta$  7.30 (m, 4H), 6.98 (m, 4H), 5.31 (s, 2H), 3.79 (s, 4H), 2.50 (s, 12H).

**2,6-Bis(1-cyanomethoxy)-9,10-dihydro-9,10-(1,2-dicarbomethoxy)ethenoanthracene (27)**

A 25-mL round-bottomed flask was charged with the diol **8** (200 mg, 0.568 mmol, 1 eq),  $\text{Cs}_2\text{CO}_3$  (1g, 2.841 mmol, 5 eq), chloroacetonitrile (426 mg, 360  $\mu\text{L}$ , 5.68 mmol, 10 eq) and 10 mL of acetone. The reaction was purged with argon and brought to a gentle reflux for 1 hour. The solids were filtered off and washed with  $\text{CH}_2\text{Cl}_2$ . The resulting solution was concentrated and the material chromatographed over  $\text{SiO}_2$ , using 15% Ethyl acetate/ $\text{C}_6\text{H}_6$  as an eluant. Yield 200 mg-oil (82%).  $^1\text{H NMR}$  ( $\text{CDCl}_3$ ):  $\delta$  7.2 (d, 2H,  $J=7$ ), 6.9 (d, 2H,  $J=2$ ), 6.55 (dd, 2H,  $J=7, 2$ ), 5.3 (s, 2H), 4.6 (s, 4H), 3.7 (s, 6H).  $^{13}\text{C NMR}$  ( $\text{CDCl}_3$ ) $\delta$ : 165.44, 154.53, 146.73, 145.95, 137.89, 124.50, 115.02, 112.28, 110.66, 53.93, 52.37, 51.52. MS: (m/e) 430 ( $\text{M}^+$ ), 371(100), 330, 291, 248, 220, 152, 59.

**2,6-Bis(2-aminoethoxy)-9,10-dihydro-9,10-(1,2-dicarbomethoxy)ethenoanthracene (28)**

To a solution of the dinitrile, **27** (200 mg, 0.456 mmol, 1 eq) in 500  $\mu\text{L}$  of distilled THF was added  $\text{BH}_3\cdot\text{THF}$  (2.3 mL of 1 M solution, 2.32 mmol, 5 eq,

15 H<sup>-</sup>). The solution was stirred for 4 hours at room temperature. Ten milliliters of acidic MeOH were added and the solution refluxed for 1 hour. KOH was added to bring the solution to pH  $\approx$  10.5-11. The aqueous suspension was extracted with CH<sub>2</sub>Cl<sub>2</sub> (3  $\times$  20 mL). The organic layer was dried over MgSO<sub>4</sub> and concentrated. <sup>1</sup>H NMR (CDCl<sub>3</sub>):  $\delta$  7.2 (d, 2H, *J* = 8), 6.95 (d, 2H, *J* = 2), 6.45 (dd, 2H, *J* = 8, 2), 5.3 (s, 2H), 3.97 (t, 4H, *J* = 8), 3.67 (s, 6H), 3.0 (t, 4H, *J* = 8), 1.68 (broad, 4H). <sup>13</sup>C NMR (CDCl<sub>3</sub>): 165.4, 156.4, 146.5, 145.5, 135.5, 123.9, 111.5, 109.7, 70.4, 52.4, 51.9, 41.6. This material was not purified but used as is for the next step.

### **2,6-Bis(2-( $\alpha$ -chloroacetyl-amido)ethoxy)-9,10-dihydro-9,10-(1,2-dicarbo-methoxy)ethenoanthracene (19)**

To the crude amine **28** (82 mg, 0.187 mmol) in CH<sub>2</sub>Cl<sub>2</sub> was added the chloroacetic acid NHS ester (75 mg, 0.393 mmol, 2.1 eq). The reaction was stirred at room temperature for 2 hours and then concentrated. The material was chromatographed over SiO<sub>2</sub>, using ethyl acetate as an eluant. The yield, from the nitrile, ranged from 15-40%. <sup>1</sup>H NMR (CDCl<sub>3</sub>):  $\delta$  7.18 (d, 2H, *J* = 8.06), 6.91 (d, 2H, *J* = 2.2 Hz), 6.91 (broad, 2H), 6.43 (dd, *J* = 8.06, 2.2), 5.27 (s, 2H), 3.97 (s, 4H), 3.93 (t, 4H, *J* = 5.00), 3.71 (s, 6H), 3.60 (q (d of t), 4H, *J* = 5.00). <sup>13</sup>C NMR (CDCl<sub>3</sub>):  $\delta$  166.03, 165.77, 156.35, 147.06, 145.95, 136.40, 124.31, 111.70, 110.14, 63.73, 52.37, 51.78, 42.56, 39.37. MS: (m/e) 590 (M<sup>+</sup>), 471, 412, 352, 292, 210, 120 (100).

### **Amide macrocycles (29, 30)**

To a solution of the diphenol **8** (75 mg, 0.214 mmol, 1 eq.) and the  $\alpha$ -chloroamide, **19** (126 mg, 0.214 mmol, 1 eq) in 25 mL of DMF was added the Cs<sub>2</sub>CO<sub>3</sub> (376 mg, 1.07 mmol, 5 eq). The solution was warmed to 60 °C for 108

hours. The DMF was removed with the aid of a vacuum pump. The residue was dissolved in 10 mL of CH<sub>2</sub>Cl<sub>2</sub>. The organic layer was extracted with water (3×-15 mL), dried over MgSO<sub>4</sub>, filtered and concentrated. The products were isolated by preparative (or column) chromatography (in 20% yield), using 10% CH<sub>3</sub>CN/EtOAc as an eluant. MS (on mixture): (m/e) 870 (M<sup>+</sup>), 811, 519, 459, 352, 292, 210, 85 (100).

#### Higher R<sub>f</sub> Diastereomer (R<sub>f</sub>=0.23)

<sup>1</sup>H NMR (CDCl<sub>3</sub>): δ7.10 (d, 2H, *J*=8.06), 6.98 (d, 2H, *J*=1.95), 6.78 (broad, 2H, NH), 6.46 (d, 2H, *J*=8.05), 6.23 (dd (unresolved), 4H (two sets)), 5.33 (s, 2H), 5.06 (s, 2H), 4.38 (AB pattern, 4H, *J*=15.9, Δ*v*=26.6), 3.93 (m, 4H), 3.81 (s, 6H), 3.77 (s, 6H), 3.55 (m, 4H). <sup>13</sup>C NMR (CDCl<sub>3</sub>): δ168.34, 165.41, 165.27, 155.92, 155.27, 146.40, 145.75, 145.39, 136.85, 135.86, 124.12, 123.99, 111.73, 111.63, 110.68, 109.71, 69.16, 66.92, 52.63, 52.54, 51.78, 51.63, 38.48.

#### Lower R<sub>f</sub> Diastereomer (R<sub>f</sub>=0.17)

<sup>1</sup>H NMR (CDCl<sub>3</sub>): δ7.18 (d, 2H, *J*=8.06), 6.97 (d, 2H, *J*=8.06), 6.85 (d, 2H, *J*=1.22), 6.81 (d, 2H, *J*=1.22), 6.84 (broad, 2H, NH), 6.45 (dd (poorly resolved), 2H, *J*=8.06, 1.22), 6.35 (dd (poorly resolved), 2H, *J*=8.06, 1.22), 5.27 (s, 2H), 5.21 (s, 2H), 4.36 (AB pattern, 4H, *J*=15.6, Δ*v*=22.1), 3.93 (m, 4H), 3.80 (s, 6H), 3.78 (s, 6H), 3.66 (m, 4H). <sup>13</sup>C NMR (CDCl<sub>3</sub>): δ168.09, 165.36, 165.20, 155.85, 155.35, 146.49, 146.36, 145.70, 145.52, 136.97, 135.91, 124.16, 123.95, 112.26, 111.17, 110.63, 110.22, 68.96, 66.93, 52.60, 52.54, 51.82, 51.59, 38.30.

**Amide macrocycle tetra-cesium salt (lower R<sub>f</sub> diastereomer)**

A 5-mL, round-bottomed flask was charged with the tetraester (12 mg, 0.014 mmol, 1 eq) and the CsOH (10 mg, 0.069 mmol, 5 eq). DMSO (600  $\mu$ L) and H<sub>2</sub>O (600  $\mu$ L) were added and the reaction stirred for 2.5 hours. The reaction mixture was frozen in dry ice and lyophilized. The solid was dissolved in the minimum amount of water and loaded onto a cation exchange column. Six fractions were collected with fractions 2 and 3 containing the product. Fractions 2 and 3 were lyophilized and dissolved in a pH=10, Cs<sub>2</sub>HPO<sub>4</sub>/D<sub>2</sub>O buffer.

<sup>1</sup>H NMR (D<sub>2</sub>O, borate buffer, rel. to external TSP):  $\delta$ 7.27 (d, 2H,  $J=8.05$ ), 7.10 (d, 2H,  $J=8.05$ ), 6.86 (d, 2H,  $J=2.44$ ), 6.57 (dd, 2H,  $J=8.05, 2.44$ ), 6.37 (dd, 2H,  $J=8.05, 2.44$ ), 6.22 (d, 2H,  $J=2.44$ ), 5.19 (s, 2H), 5.04 (s, 2H), 4.34 (d, 2H,  $J=15.87$ ,  $\Delta\nu=182$ , half of AB pattern), 4.17 (broad m, 4H), 3.88 (d, 2H,  $J=15.87$ ,  $\Delta\nu=182$ , half of AB pattern), 3.43 (broad m, 4H).

**2,6,9-Tris(*tert*-butyldimethylsiloxy)anthracene (32)**

To a solution of *tert*-butyldimethylsilylchloride (1.67 g, 11.05 mmol, 5 eq) and triethylamine (3 mL, 22.1 mmol, 10 eq) in 10 mL of DMF was added a 5 mL DMF solution of the anthrone, **6b**, (500 mg, 2.21 mmol, 1 eq) via an addition funnel. The reaction mixture was heated to 60 °C for 1.5 hours. The reaction was cooled and poured into a separatory funnel containing H<sub>2</sub>O/ether. The layers were separated. Five milliliters of Et<sub>2</sub>O was added to the aqueous layer and extracted. The organic layers were combined, dried over Na<sub>2</sub>SO<sub>4</sub> and concentrated. The material was chromatographed over SiO<sub>2</sub> using 3% Et<sub>2</sub>O/Petroleum ether as the eluant to give the product as a yellow solid (1.02 g, 81% yield). <sup>1</sup>H NMR (CDCl<sub>3</sub>):  $\delta$ 8.08 (d, 1H,  $J=9.28$ ), 7.84 (s,

1H), 7.77 (d, 1H,  $J=9.03$ ), 7.50 (d, 1H,  $J=2.19$ ), 7.20 (d, 1H,  $J=2.20$ ), 7.03 (m, 2H).

**2,6,9-Tris(*tert*-butyldimethylsiloxy)-9,10-dihydro-9,10-(1,2-dicarbomethoxy)ethenoanthracene (34)**

To a solution of the anthracene, **32** (1.02 g, 1.8 mmol, 1 eq) in 20 mL of freshly distilled benzene, was added 2.3 mL (18 mmol, 10 eq) of DMAD. The solution was refluxed for 5 days. The reaction time was 18 hours with xylene as solvent and 36 hours with toluene as solvent. The solution was cooled and concentrated under high vacuum. The material was chromatographed over SiO<sub>2</sub> using 20% Et<sub>2</sub>O/Petroleum ether as an eluant giving a quantitative yield of the product as a colorless oil. <sup>1</sup>H NMR (CDCl<sub>3</sub>): δ 7.38 (d, 1H,  $J=8.05$ ), 7.10 (d, 1H,  $J=7.81$ ), 7.10 (d, 1H,  $J=2.21$ ), 6.81 (d, 1H,  $J=2.21$ ), 6.45 (dd, 1H,  $J=8.05, 2.19$ ), 6.39 (dd, 1H,  $J=7.81, 2.20$ ), 3.76 (s, 3H), 3.70 (s, 3H), 1.09 (s, 9H), 0.93 (s, 18H), 0.43 (d, 6H), 0.15 (d, 6H), 0.11 (d, 6H).

**2,6,9-Trihydroxy-9,10-dihydro-9,10-(1,2-dicarbomethoxy)ethenoanthracene (20)**

A polyethylene bottle was charged with the tris silyl ether, **34**, and 30 mL of acetonitrile. Ten milliliters of 50% HF was added and the solution stirred with gentle warming to 45 °C. After 4 days the reaction was complete. The mixture was poured into 50 mL of saturated NaHCO<sub>3</sub>. The aqueous layer was extracted (3×-25 mL) with Et<sub>2</sub>O. The Et<sub>2</sub>O layer was dried over MgSO<sub>4</sub>, filtered and concentrated. The material was chromatographed over SiO<sub>2</sub> using Et<sub>2</sub>O as an eluant to give 400 mg of a white solid (61% yield). <sup>1</sup>H NMR (acetone d<sub>6</sub>): δ 8.27 (broad s, xch w/D<sub>2</sub>O, 2H, phenol), 8.24 (broad s, xch w/D<sub>2</sub>O, 1H, phenol), 7.36 (d, 1H,  $J=8.06$ ), 7.18 (d, 1H,  $J=7.81$ ), 7.13 (d, 1H,  $J=2.44$ ),

6.93 (d, 1H,  $J=2.44$ ), 6.49 (dd, 1H,  $J=8.06, 2.44$ ), 6.44 (dd, 1H,  $J=7.81, 2.44$ ), 6.11 (s, xch w/D<sub>2</sub>O, 1H, 3° alcohol), 5.42 (s, 1H), 3.71 (s, 3H), 3.70 (s, 3H).

### **2,6-Dihydroxy-9-tert-butyltrimethylsilyloxy-9,10-dihydro-9,10-(1,2-dicarbomethoxy)ethenoanthracene (35)**

The tris silylether, 34 (750 mg, 1.06 mmol) was dissolved in 10 mL of MeOH. Fifteen drops of concentrated HCl were added and the solution stirred for 18 hours. The solution was concentrated and chromatographed over SiO<sub>2</sub> using 1:1 ethyl acetate/Petroleum ether as an eluant to give the bisphenol. <sup>1</sup>H NMR (acetone-d<sub>6</sub>): δ8.41 (broad s, 2H, xch w/D<sub>2</sub>O, phenol), 7.44 (d, 1H,  $J=8.06$ ), 7.20 (m, 2H), 6.94 (d, 1H,  $J=2.44$ ), 6.53 (dd, 1H,  $J=8.06, 2.44$ ), 6.46 (dd, 1H,  $J=2.44, 8.06$ ), 5.41 (s, 1H), 3.74 (s, 3H), 3.71 (s, 3H), 1.12 (s, 9H), 0.48 (s, 3H), 0.47 (s, 3H).

### **2,6,9-Triacetoxyanthracene (33)**

A 25-mL Erlenmeyer flask was charged with the anthrone (750 mg, 3.31 mmol). Five milliliters of pyridine and 5 mL of acetic anhydride were added. A few crystals of DMAP were added. The solution was warmed for 15 minutes on a steam bath. Water was added and the flask was placed in the freezer. A precipitate formed; the solid was filtered and recrystallized from benzene to give 450 mg of the triacetate (40% yield). Ethanol was also an effective recrystallization solvent. <sup>1</sup>H NMR (CDCl<sub>3</sub>): δ8.30 (s, 1H), 7.95 (d, 1H,  $J=9.0$ ), 7.88 (d, 1H,  $J=9.0$ ), 7.70 (d, 1H,  $J=2.5$ ), 7.60 (d, 1H,  $J=2.5$ ), 7.20 (m, 2H), 2.6 (s, 3H), 2.40 (s, 6H).

**2,6,9-Triacetoxy-9,10-dihydro-9,10-(1,2-dicarbomethoxy)ethenoanthracene (33a)**

A 10-mL round-bottomed flask was charged with the anthracene triacetate (352 mg, 1 mmol, 1 eq), 5 mL of xylene and 123  $\mu$ L (142 mg, 10 mmol, 10 eq) of DMAD. The solution was refluxed for 8 days. Concentration of the solution followed by chromatography over SiO<sub>2</sub>, using 45% ethyl acetate/petroleum ether, gave the adduct. <sup>1</sup>H NMR (CDCl<sub>3</sub>):  $\delta$ 7.31 (d, 1H, *J* = 8.06), 7.25 (d, 1H, *J* = 8.3), 7.13 (d, 1H, *J* = 2.2), 7.08 (d, 1H, *J* = 2.0), 6.76 (m, 2H), 5.45 (s, 1H), 3.75 (s, 3H), 3.68 (s, 3H), 2.46 (s, 3H), 2.23 (s, 6H).

**2,6-Dihydroxy-9-acetoxy-9,10-dihydro-9,10-(1,2-dicarbomethoxy)-ethenoanthracene (33b)**

The triacetate, **33a** (10 mg, 0.0202 mmol) was dissolved in 2 mL of MeOH. A few drops of concentrated HCl were added and the solution was heated to reflux for 5 hours. Solid NaHCO<sub>3</sub> and MgSO<sub>4</sub> were added. The reaction was filtered and the solid washed with 25 mL of CH<sub>2</sub>Cl<sub>2</sub>. The product was isolated by chromatography of SiO<sub>2</sub> using 1:1 ethyl acetate/Petroleum ether as an eluant. <sup>1</sup>H NMR (CDCl<sub>3</sub>):  $\delta$ 7.10 (d, 1H, *J* = 7.82), 7.06 (d, 1H, *J* = 8.03), 6.83 (d, 1H, *J* = 2.24), 6.82 (d, 1H, *J* = 2.22), 6.40 (m 2H), 5.30 (s, 1H), 5.14 (broad singlet, xch w/D<sub>2</sub>O, 1H, phenol), 5.02 (broad singlet, xch w/D<sub>2</sub>O, 1H, phenol), 3.75 (s, 3H), 3.68 (s, 3H), 2.44 (s, 3H).

**2,6-Bis-(*tert*-butyldimethylsiloxy)-9-hydroxy-9-methylanthrone(37)**

To a -78 °C cooled solution in THF **36** (1 g, 2.13 mmol, 1 eq) was added MeMgBr (130  $\mu$ L of a 2.9 M solution, 0.377 mmol, 0.377 eq) slowly. The solution turned a red-maroon color. After 8 hours of stirring, the reaction was quenched with 50 mL of pH = 7 buffer. The solution was extracted (3  $\times$  -25mL)

each with Et<sub>2</sub>O. The organic layer was dried over Na<sub>2</sub>SO<sub>4</sub> and concentrated. The product (and recovered starting material) were isolated by chromatography over SiO<sub>2</sub>, using 15% Et<sub>2</sub>O/Petroleum ether as an eluant. The product (912 mg) was isolated in 88% yield (92% conversion). <sup>1</sup>H NMR (CDCl<sub>3</sub>): δ8.05 (d, 1H, *J*=8.85), 7.22 (d, 1H, *J*=8.54), 7.55 (d, 1H, *J*=2.74), 7.31 (d, 1H, *J*=2.44), 7.04 (dd, 1H, *J*=8.54, 2.74), 6.84 (dd, 1H, *J*=8.85, 2.44), 2.50 (s, 1H, xch w/D<sub>2</sub>O) 1.63 (s, 3H), 0.99 (s, 9H), 0.98 (s, 9H), 0.25 (s, 6H), 0.21 (s, 6H). <sup>13</sup>C NMR (CDCl<sub>3</sub>): δ181.70, 160.51, 155.07, 151.22, 141.32, 130.89, 129.45, 127.13, 125.58, 123.62, 120.00, 116.76, 116.44, 69.95, 36.96, 25.92, 25.88, 18.59, 18.50, -3.90, -3.91, -4.00.

#### **2,6-Bis-*tert*-butyldimethylsiloxy-9-methoxy-9-methylanthrone(21)**

A 50-mL, round-bottomed flask equipped with a stirrer and septum was oven-dried and cooled under N<sub>2</sub>. The alcohol, **37**, (22 mg, 0.413 mmol, 1eq) and dimethylsulfate (186 mg, 126 μL, 1.5 eq) were added. Ten milliliters of anhydrous, freshly distilled THF was added and the solution stirred. The NaH dispersion (30 mg dispersion) was added and the reaction stirred for 6 hours. One milliliter of pH=7 buffer was added and then enough 3N HCl to adjust the pH ≈ 7. The solution was extracted with CH<sub>2</sub>Cl<sub>2</sub> (3 × -25 mL each). The organic layer was dried over Na<sub>2</sub>SO<sub>4</sub> and concentrated. The product was isolated (91 mg, 44%) via chromatography over SiO<sub>2</sub>, using 10% Et<sub>2</sub>O/Petroleum ether as an eluant. <sup>1</sup>H NMR (CDCl<sub>3</sub>): δ8.25 (d, 1H, *J*=8), 7.75 (d, 1H, *J*=2.5), 7.65 (d, 1H, *J*=8), 7.17 (d, 1H, *J*=2.5), 7.15 (dd, 1H, *J*=8, 2.5), 6.95 (dd, 1H, *J*=8, 2.5), 2.90 (s, 3H), 1.70 (s, 3H), 1.10 (s, 18H), 0.40 (s, 6H), 0.35 (s, 6H).

## References for Chapter 5

1. For a review on the use of onium ions in host-guest chemistry see:  
Vögtle, F.; Löhr, H.-G.; Franke, J.; Worsch, D. *Angew. Chem., Int. Ed. Eng.* 1985, 24, 727-742.
2. Saggiomo, A. J. *J. Org. Chem.* 1957, 22, 1171-1175.
3. Maier, G.; Jung, W. A. *Chem. Ber.* 1982, 115, 804-807.
4. For the reduction of amides to amines using borane see:
  - (a) Brown, H. C.; Heim, P. *J. Am. Chem. Soc.* 1964, 86, 3566-3567.
  - (b) Brown, H. C.; Heim, P. *J. Org. Chem.* 1973, 38, 912-916.
  - (c) Kornet, M. J.; Thio, P. A.; Tan, S. I. *J. Org. Chem.* 1968, 33, 3637-3639.
5. For the reduction of amides to amines via amide activation see:
  - (a) Borch, R. F. *Tetrahedron Lett.* 1968, 1, 61-65.
  - (b) Kuehne, M.E.; Shannon, P. J. *J. Org. Chem.* 1977, 42, 2082-2087.
6. Masek, B. B. Ph.D. Thesis, California Institute of Technology, 1987.
7. Diederich, F.; Dick, K.; Griebel, D. *J. Am. Chem. Soc.* 1986, 108, 2273-2286.
8. Schürmann, G.; Diederich, F. *Tetrahedron Lett.* 1986, 27, 4249-4252.
9. Shepodd, T. J. unpublished results.
10.
  - (a) Gani, V.; Viout, P. *Tetrahedron* 1976, 32, 1669-1673.
  - (b) Gani, V.; Viout, P. *Tetrahedron* 1976, 32, 2883-2889.
  - (c) Biechler, S. S.; Taft, R. W., Jr. *J. Am. Chem. Soc.* 1957, 79, 4927-4935.
  - (d) Pavelich, W. A.; Taft, R. W., Jr. *J. Am. Chem. Soc.* 1957, 79, 4935-4940.

11. (a) Fendler, E. J.; Constien, V. G.; Fendler, J. H. *J. Phys. Chem.* **1975**, *79*, 917-926.  
(b) Mukerjee, P.; Mysels, K. J. *Natl. Stand. Ref. Data Ser., Natl. Bur. Stand.*, No. 36, **1971**.
12. Shepodd, T. J.; Petti, M.A.; Dougherty, D. A. *J. Am. Chem. Soc.* **1986**, *108*, 6085-6087.
13. Barrans, R. E. unpublished results.
14. Rider, M. M. S. Thesis, California Institute of Technology, 1985.
15. Still, W. C.; Kahn, M.; Mitra, A. *J. Org. Chem.* **1978**, *43*, 2923-2925.